

A silhouette of a bare tree stands in the foreground of a cracked, dry landscape. The ground is covered in numerous irregular, polygonal cracks, indicating severe drought. In the background, a sunset or sunrise is visible, with the sun low on the horizon, casting a warm, golden glow across the sky. The sky is filled with soft, wispy clouds, and the overall atmosphere is one of desolation and natural beauty.

Marjolein van Huijgevoort

Hydrological drought

Characterisation and representation in large-scale models

Hydrological drought
Characterisation and representation in large-scale
models

Marjolein van Huijgevoort

Thesis committee

Promotor

Prof. Dr R. Uijlenhoet
Professor of Hydrology and Quantitative Water Management
Wageningen University

Co-promotor

Dr H.A.J. van Lanen
Associate professor, Hydrology and Quantitative Water Management Group
Wageningen University

Other members

Prof. Dr M.F.P. Bierkens, Utrecht University
Prof. Dr W. Hazeleger, Wageningen University
Prof. Dr J. Seibert, University of Zurich
Dr K. Stahl, University of Freiburg

This research was conducted under the auspices of the Graduate School SENSE.

Hydrological drought

Characterisation and representation in large-scale models

Marjolein Hubertina Joanna van Huijgevoort

Thesis

submitted in fulfilment of the requirements for the degree of doctor
at Wageningen University
by the authority of the Rector Magnificus
Prof. Dr M.J. Kropff
in the presence of the
Thesis Committee appointed by the Academic Board
to be defended in public
on Friday 23 May 2014
at 4 p.m. in the Aula.

M.H.J. van Huijgevoort
Hydrological drought: Characterisation and representation in large-scale models
vi + 130 pages

PhD thesis, Wageningen University, Wageningen, NL (2014)
With references, with summaries in English and Dutch

ISBN 978-94-6173-941-4

Contents

1	Introduction	1
1.1	Setting the stage	3
1.2	Definitions of drought	5
1.3	Scientific background	5
1.3.1	Determination of drought	5
1.3.2	Propagation of drought	7
1.3.3	Modelling large-scale drought	7
1.3.4	Space-time development of historical drought	8
1.3.5	Influence of climate change on future drought	9
1.4	Research objective and questions	10
1.5	Outline	11
2	A generic method for hydrological drought identification	13
2.1	Introduction	15
2.2	Data	17
2.2.1	Discharge observations across climate regimes	17
2.2.2	Global simulated runoff data from large-scale models	17
2.3	A consistent method for hydrological drought identification at the global scale	19
2.3.1	Classical approach	19
2.3.2	Combining the characteristics of the TLM and CDPM	22
2.4	Illustration of the generic drought identification method	24
2.4.1	Drought identification for observed discharge data	24
2.4.2	Drought identification for simulated global runoff data	26
2.5	Discussion	29
2.6	Conclusions	30
3	Do large-scale models capture reported drought events?	33
3.1	Introduction	35
3.2	Large-scale models and forcing data	35
3.3	Drought analysis	36
3.4	Identification of major drought events	37
3.4.1	Drought in Europe	37
3.4.2	Drought in North America	38
3.4.3	Drought in Asia	38
3.4.4	Drought in regions related to ENSO	38
3.5	Discussion and conclusion	41
4	Global multi-model analysis of drought in historic runoff	43
4.1	Introduction	45
4.2	Large-scale models	46
4.3	Drought analysis	47
4.3.1	Temporal drought identification	47
4.3.2	Spatial drought identification	48
4.4	Results	48
4.4.1	Global drought characteristics	48
4.4.2	Temporal development of drought	49

4.4.3	Spatio-temporal development of two major historical drought events	53
4.5	Discussion	57
4.6	Conclusions	59
5	Changes in hydrological drought characteristics towards the future	61
5.1	Introduction	63
5.2	Data	64
5.2.1	Observed river discharge	64
5.2.2	Forcing data	64
5.2.3	Large-scale hydrological models	66
5.3	Low flow and drought identification	66
5.4	Results and discussion	68
5.4.1	Comparison of large-scale models and observations	68
5.4.2	Influence of climate change on low flows	71
5.4.3	Influence of climate change on hydrological drought characteristics	75
5.5	Conclusions	77
6	Influence of multi-year storage variation on hydrological drought	79
6.1	Introduction	81
6.2	Data	82
6.3	Methodology	83
6.3.1	Decomposition of discharge time series	83
6.3.2	Drought identification	84
6.4	Results and discussion	84
6.4.1	Decomposition of the discharge time series	84
6.4.2	Drought analysis	86
6.4.3	Link between discharge components and drought	87
6.5	Conclusions	89
7	Synthesis	91
7.1	Summary of results	93
7.2	Discussion	94
7.2.1	Drought versus water scarcity	94
7.2.2	Drought identification methods	95
7.2.3	Large-scale modelling	96
7.2.4	Drought and climate change	98
7.3	Outlook for large-scale drought analysis	100
A	Main characteristics of the large-scale models	103
	Bibliography	107
	Summary	119
	Samenvatting	121
	Dankwoord	123
	Acknowledgements	125
	List of publications	127

CHAPTER

1

Introduction



1.1 Setting the stage

Major natural hazards occur all over the world. Drought (Fig. 1.1) is one of the least understood natural hazards (Wilhite, 2000). This is partly due to the fact that drought develops slowly and imperceptibly and may therefore remain unnoticed for a long time (Tallaksen and Van Lanen, 2004). Drought can have large economic, social and environmental impacts (Fig. 1.2). The consequences and cost of drought are difficult to estimate due to the regionally extensive occurrence and the fact that drought affects many different sectors, which can not all be put in economic terms (Markandya et al., 2009). Published data on the economic costs of drought usually refer to one sector, one region and one year (EurAqua, 2004). Data for Europe from 2000 to 2006 show that each year on average 15% of the EU total area and 17% of the EU total population have suffered from the impact of drought (European Commission, 2006). The total cost of drought over the past 30 years amounts to €100 billion (European Commission, 2007). A severe drought occurred in Europe in 2003 and spread over a large part of western Europe. More than 30,000 people died from the associated heat wave. This drought was followed by severe events in 2004–2006 in the southwestern part of Europe (Iberian Peninsula, France and United Kingdom). In 2004–2005 a drought event over the Iberian Peninsula led to severely reduced cereal production and reduced hydroelectric power production due to low river flows (European Environment Agency, 2010). In the United States most damages in the period 1980–2011 were caused by tropical cyclones, but drought and associated heat waves had a huge impact as well (Smith and Katz, 2013). The US drought event in 2012 was one of the worst drought events in the United States in history with estimated crop losses alone worth \$18 billion (Schnoor, 2012). Deficits in precipitation in two rainy seasons in 2010–2012 led to a well-known drought event in the Horn of Africa (Dutra et al., 2013). This drought in combination with other factors such as increase in food prices, caused large food shortages and affected millions of people (Zarocostas, 2011). Drought events also occur in the wetter regions of the world, for example the Amazon region. The Amazon suffered from severe drought events in 2005 and 2010 with all associated impacts on the ecosystem (Zeng et al., 2008; Marengo et al., 2011; Lewis et al., 2011; Tomasella et al., 2011).

Direct effects linked to drought are among others loss of crops and reduction in drinking water supply (Tallaksen and Van Lanen, 2004). Declining water levels disrupt river navigation, the increased water temperatures linked to low water levels can be disastrous for fish, and lack of cooling water causes problems for electricity production (Wilhite, 2000; Tallaksen and Van Lanen, 2004;



Figure 1.1: Examples of areas in drought.

Van Vliet et al., 2012). Often it is difficult to separate direct impacts of drought from indirect impacts. Drought is usually associated with heat waves and forest fires. Although drought does not directly cause forest fires, dry conditions accelerate fires. Heat waves and drought are linked through feedbacks, where soil moisture drought plays an important role in enhancing heat waves (Seneviratne et al., 2006; Fischer et al., 2007). Moreover, drought is not only important in warm climates with already a low water availability, it can also have large impacts in cold climates (Tallaksen and Van Lanen, 2004; Van Loon, 2013). Winter drought can occur in snow-dominated climates, for example the 2006 winter drought in the Upper Rhine basin causing problems for inland water navigation (Pfister et al., 2006) and the extreme 2010 winter disaster in Mongolia causing great livestock mortality with all related impacts on livelihoods (Sternberg, 2010; Van Loon, 2013).

Climate change will affect the entire hydrological cycle. The projected changes are expected to cause an increase in the frequency and intensity of precipitation extremes (Meehl et al., 2007; Bates et al., 2008). It is also expected that the occurrence and severity of drought events will increase in the future in multiple regions across the world (e.g. Bates et al., 2008; Dai, 2011; Romm, 2011). In the 21st century, drought may intensify in parts of Europe, central North America, Central America and Mexico, northeastern Brazil and southern Africa (Seneviratne et al., 2012). However, the uncertainty in the predictions of drought development is large (e.g. Orłowsky and Seneviratne, 2013). The different future scenarios (climate forcing) and different hydrological model structures result in a large spread in the projected drought events (Orłowsky and Seneviratne, 2013; Prudhomme et al., 2014). Additionally, the employed drought identification method can have a large influence on the results as well (e.g. Trenberth et al., 2014).

Thorough knowledge of the space-time development of drought is necessary for an adequate assessment of drought impacts, drought management, and policy-making for food, energy and water security. Drought events can cover multiple river basins, several countries and large parts of continents. Since drought events usually occur at extensive spatial scales, it is important to investigate them at large scales. However, observations needed to study large-scale drought events are not available at the appropriate spatial and temporal scale. For drought analysis in general long time series of hydrological variables are required. Instead of observations, large-scale models forced with reanalysis datasets are increasingly being used to simulate time series of hydrological variables. From the model results large-scale drought events can be derived (e.g. Sheffield et al., 2004; Stahl et al., 2012; Gudmundsson et al., 2012a; Prudhomme et al., 2014). The gridded output of the large-scale models provides an opportunity to study the development of large-scale drought at a global scale or at a continental scale for both the past and the future.

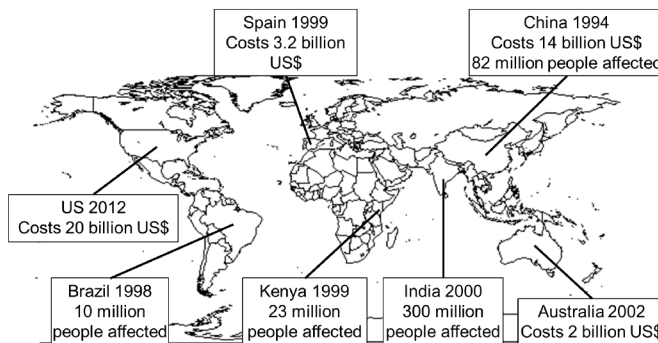


Figure 1.2: Examples of very severe drought events for the period 1994-2013 (data from EM-DAT: The OFDA/CRED International Disaster Database www.em-dat.net - Université Catholique de Louvain - Brussels - Belgium).

1.2 Definitions of drought

There are several different definitions of drought. In this thesis, I followed the definition proposed by Tallaksen and Van Lanen (2004):

“drought is a sustained and regionally extensive occurrence of below average natural water availability”.

Drought can be seen as a deviation from the long-term conditions of variables such as precipitation, soil moisture, groundwater and streamflow. Drought is usually caused by below average natural water availability due to climate variability, which results in low precipitation and/or high evaporation rates. In cold climates, snow accumulation or delayed snow melt can also cause drought conditions in winter (Van Loon and Van Lanen, 2012).

It is important to distinguish drought from aridity, water scarcity and desertification (Tallaksen and Van Lanen, 2004; Schmidt and Benítez-Sanz, 2013). Aridity is a permanent feature of a dry climate, whereas drought is a deviation from the long-term climate. Drought is a natural phenomenon, but water scarcity occurs when the shortage of water is caused by mankind using more water than naturally available. Human influence plays a role in water availability (Van Loon and Van Lanen, 2013; Wada et al., 2013a), but in this thesis only water shortages with natural causes were investigated. Desertification is a more or less permanent degradation of land in (semi-)arid and dry sub-humid areas (UNEP, 1994). Drought can contribute to desertification, but the main reasons are over-grazing, increased fire frequency, deforestation and/or overabstraction of groundwater.

Drought develops in the hydrological system from a deficit in precipitation to a deficit of soil water followed by a deficit of groundwater and river discharge. This development leads to different types of drought (Fig. 1.3). A meteorological drought is a lack of precipitation during a rather long period of time and over large areas. If this situation is prolonged and evapotranspiration is maintained, a soil moisture drought, or sometimes called agricultural drought, can occur. Subsequently, the groundwater recharge, groundwater storage and streamflow will diminish, which leads to a hydrological drought. Since groundwater is usually the last to react to a drought condition, hydrological drought events are often out of phase with meteorological and soil moisture drought events (Wilhite, 2000). This results in different drought dynamics for the different types of drought (Van Loon et al., 2012). In cold climates drought can also be caused by snow accumulation or delayed snow melt; these processes are linked to the temperature and not necessarily to the amount of precipitation. This is specified by Van Loon (2013) as precipitation control and temperature control on drought. These different causes are not identified in this thesis, because winter drought and summer drought are not explicitly separated. The main focus of this thesis will be on hydrological drought, although meteorological drought will be considered as well.

1.3 Scientific background

1.3.1 Determination of drought

Since drought is such a widespread phenomenon that differs for each climatic region, each physical catchment structure, and each component in the hydrological cycle, many different indices have been developed to characterise and quantify drought. There have been several attempts to classify and review the existing indices (Keyantash and Dracup, 2002; Niemeier, 2008; Wanders et al., 2010). Indices are usually categorized according to the different types of drought (meteorological drought, soil moisture drought or hydrological drought, Fig. 1.3), although some cover more than one type.

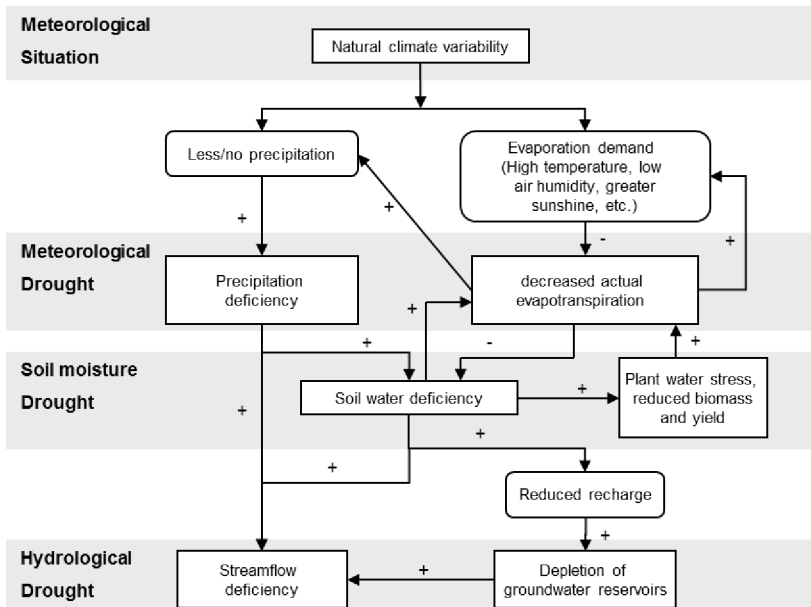


Figure 1.3: Different drought types and propagation of drought through the hydrological cycle (modified from Stahl, 2001). The plus (minus) signs indicate a positive (negative) effect.

One of the most widely used indices is the Standardised Precipitation Index (SPI) developed by McKee et al. (1993). This index is based on the probability of an observed precipitation amount occurring for a given prior time period (i.e., accumulated precipitation over the preceding month or several preceding months). Monthly precipitation data are fitted to a gamma probability distribution, which is then transformed to a normal distribution (Keyantash and Dracup, 2002; Wanders et al., 2010). The SPI is calculated from anomalies of the transformed data. The SPI is used, for example, by the National Integrated Drought Information System (NIDIS; www.drought.gov) to produce maps of global drought based on meteorological stations across the globe. Another well known index is the Palmer Drought Severity Index (PDSI; Palmer, 1965). The PDSI is based on the supply and demand concept of the soil water balance equation taking into consideration monthly mean precipitation and temperature as well as the locally available water content of the soil. This index has been applied widely, but it also has some limitations (Alley, 1984). For example, the method to derive the index does not take into account the effect of snow melt or frozen ground and the drought severity classes are designed arbitrarily. The PDSI is also sensitive to the method used to calculate the potential evaporation (Sheffield et al., 2012). Despite limitations, the PDSI is still widely applied (Lloyd-Hughes and Saunders, 2002; Dai et al., 2004; Burke and Brown, 2008; Dai, 2013; Sheffield et al., 2012) and attempts have been made to improve the index (Wells et al., 2004). Lloyd-Hughes and Saunders (2002) have compared the SPI and PDSI, concluding that SPI, when accumulated over 9 and 12 months, and PDSI give almost similar results.

For the quantification of hydrological drought, different methods have been developed. The threshold level method (TLM) is the most frequently applied method when determining the beginning and end of a drought and the associated deficit volume (Tallaksen and Van Lanen, 2004). Early development and application of this method includes the work of Yevjevich (1967), where it is called crossing theory. The threshold level method can be applied to each hydrological variable, whether it is a flux or state variable, although the deficit volume needs to be treated differently

(Tallaksen et al., 2009). A drought starts when the variable drops below a predefined threshold and ends when the threshold is exceeded again. Besides duration of a drought event, other drought characteristics such as deficit volume (accumulated difference between the variable value and the threshold value for each event) and drought frequency (number of drought events) can be determined as well. The threshold, if the method is applied to discharge, can be defined from, for example, a certain percentage of the flow duration curve, or the ecological minimum flow. The threshold level method was applied in this thesis and will be explained in detail in Chapter 2.

There are many different drought indices and each index usually is developed for specific purposes and certain regions. Therefore, each index is most suitable for those purposes and regions. For example, in dry areas the number of consecutive dry days (CDD, consecutive days without precipitation; Deni and Jemain, 2009) may be a good index, while in wet areas SPI would be more useful. This leads to difficulties when performing drought analysis at a global scale and towards the future as well, because environmental conditions may change in a certain region. Multiple indices would have to be used, or results will be less reliable in some areas. The lack of a worldwide applicable drought index calls for development of a hydrological drought index suitable at a global scale.

1.3.2 Propagation of drought

Meteorological drought may develop into hydrological drought (Fig.1.3), but how to quantify this is still fairly unknown (e.g. Wong et al., 2013). Not every meteorological drought event becomes a hydrological drought event and under some conditions a major hydrological drought event develops as a response to a series of minor meteorological drought events (Van Loon and Van Lanen, 2012). Besides depending on the lack of precipitation, this propagation also depends on the climate and river basin characteristics (Peters et al., 2003; Van Loon and Van Lanen, 2012). Important characteristics that play a role in drought propagation are soil type, land use, hydrogeological conditions, lakes and stream network (Van Lanen et al., 2004; Van Loon and Van Lanen, 2012). The main factors controlling the propagation and occurrence of drought are the differences in hydrological stores (Tallaksen et al., 2009; Van Lanen et al., 2013). Drought events occur more frequently and are of shorter duration in catchments with a considerable contribution of quickly-responding components (e.g., overland flow, shallow saturated subsurface flow, groundwater flow in delta areas) than in slowly-responding (e.g., baseflow) catchments (Van Lanen et al., 2004, 2013). These stores might not be well represented by large-scale models with a resolution of 0.5° by 0.5° , especially not for smaller catchments (Van Loon et al., 2012; Gudmundsson et al., 2012a; Stahl et al., 2012).

1.3.3 Modelling large-scale drought

For drought analysis, long time series of hydrological variables are essential. These time series of observations with sufficient spatial coverage are not available at a global scale (McGlynn et al., 2013), thus modelled time series have to be used. For analysis at a global scale, gridded time series can be derived as direct output from General Circulation Models (GCMs) or from more detailed Land Surface Models (LSMs) and Global Hydrological Models (GHMs), that can use GCM output as forcing data for hydrological simulations. GCMs are based on the physical laws of the atmosphere and oceans, and each GCM incorporates processes in different ways. LSMs are generally based on the energy balance at the land surface, while GHMs are intended to simulate the terrestrial water fluxes with simple conceptual hydrological models (Harding et al., 2011). LSMs are usually off-line versions of the land surface schemes used in GCMs. All these large-scale models have different parameterizations of the physical processes and different ways of modelling these processes and feedback mechanisms between various components of the system. Therefore, every model gives different output. To account for uncertainty in model structures, model ensembles are constructed to include most of these differences. However, even when several models are used,

some processes might still be missing and alternative parameterizations of implemented processes may share common systematic biases (Meehl et al., 2007). Covey et al. (2003) used 18 GCMs from the Coupled Model Intercomparison Project (CMIP) to simulate present-day climate. They compared these simulations with global observation sets. Global statistics indicated that the difference between a typical model simulation and a baseline set of observations is not much greater than the difference between different reanalysis datasets of observations (ERA15 and NCEP). Other model intercomparison projects that focused more on hydrology are WaterMIP (Water Model Intercomparison Project) and ISI-MIP (Inter-Sectoral Impact Model Intercomparison Project, Warszawski et al., 2014). Within WaterMIP results from eleven GHMs and LSMs were compared and a large spread was found (Haddeland et al., 2011). Within ISI-MIP multiple large-scale models were used to investigate the impact of climate change on water resources and other sectors (e.g. Davie et al., 2013; Wada et al., 2013b; Haddeland et al., 2014; Schewe et al., 2014). All model intercomparison projects found that the choice of the model is an important factor, whether for identifying future change or for studying historical behaviour. Therefore, the use of a multi-model ensemble is recommended.

The European project Water and Global Change (WATCH) was aimed at bringing together climate and water scientists to extend our knowledge on the current and future water cycle (Harding et al., 2011). WATCH was the main contributor to WaterMIP. Within the WATCH project, results of multiple large-scale models (LSMs and GHMs) forced with the same input data were made available for analysis of extremes. This dataset was used in this thesis and made it possible to perform global drought studies with a multi-model ensemble.

1.3.4 Space-time development of historical drought

The space-time development, distribution and occurrence of drought in the past century have been studied at different spatial scales, e.g., catchment (Hisdal and Tallaksen, 2003; Vicente-Serrano and López-Moreno, 2005; Peters et al., 2006; Tallaksen et al., 2006, 2009; Van Loon and Van Lanen, 2012; Yan et al., 2013; Fundel et al., 2013), regional (Soulé, 1993; Hisdal et al., 2001; Sheffield et al., 2004; Andreadis et al., 2005; Andreadis and Lettenmaier, 2006; Shukla and Wood, 2008; Bordi et al., 2009; Wang et al., 2009; Prudhomme et al., 2011; Gudmundsson et al., 2012b; Stahl et al., 2012) and global scale (Dai et al., 2004; Fleig et al., 2006; Sheffield and Wood, 2007, 2008a; Dai et al., 2009; Sheffield et al., 2009; Corzo Perez et al., 2011).

Most of the drought studies at larger scales have focused on soil moisture or meteorological drought, less is known about the development of hydrological drought. Sheffield et al. (2009, 2012) investigated soil moisture drought globally and trends therein. They used a single large-scale model, VIC, rather than a multi-model ensemble to simulate soil moisture. The same model was earlier used by Andreadis et al. (2005) to study soil moisture drought over the continental US. A multi-model analysis of soil moisture drought over the US was carried out by Wang et al. (2009). Soil moisture drought events in China were studied by Wang et al. (2011) using several large-scale models.

Some studies at the global and regional scale have investigated drought in streamflow (Hisdal et al., 2001; Peel et al., 2005; Fleig et al., 2006; Dai et al., 2009). However, they analysed streamflow drought events in a selected set of rivers spread over the world instead of hydrological drought at the continuous global scale. Shukla and Wood (2008) did analyse hydrological drought at the continuous spatial scale for the US, but only used time series from a single model, i.e., the VIC model. In a global study, Corzo Perez et al. (2011) investigated results of hydrological drought identification methods with the global hydrological model WaterGAP. Several studies that focused on hydrological drought for Europe have used results of the large-scale models of the WATCH project, e.g., Prudhomme et al. (2011), Gudmundsson et al. (2012a), Gudmundsson et al. (2012b), and Stahl et al. (2012). They all found large differences between the models, however, they also concluded that an ensemble mean could provide information about hydrological drought across Europe.

A spatio-temporal characterisation of historical hydrological drought (e.g., runoff, streamflow), however, from a multi-model ensemble at a global scale has been lacking so far.

1.3.5 Influence of climate change on future drought

The Intergovernmental Panel on Climate Change (IPCC) defines climate change as follows:

“Climate change refers to a change in the state of the climate that can be identified (e.g., by using statistical tests) by changes in the mean and/or the variability of its properties, and that persists for an extended period, typically decades or longer. Climate change may be due to natural internal processes or external forcings, or to persistent anthropogenic changes in the composition of the atmosphere or in land use” (IPCC, 2012).

Unlike other definitions, this one takes into account natural processes as well as anthropogenic influences. This change in climate can have large consequences for drought occurrence. Drought events are expected to increase in the future in multiple regions of the world (Seneviratne et al., 2012).

Several studies have investigated the expected changes in soil moisture drought in the future (e.g. Vidal et al., 2012; Dai, 2013; Orlowsky and Seneviratne, 2013). Vidal et al. (2012) found that all characteristics of soil moisture or agricultural drought events in France increase in the 21st century. Severe drought conditions in the 21st century over large parts of the globe were determined with the PDSI by Dai (2013). A large range in soil moisture drought projections at a global scale was found by Orlowsky and Seneviratne (2013), but increased drought was consistent in several regions, namely the Mediterranean, South Africa and Central America/Mexico.

Besides studies on soil moisture drought, many studies have investigated the effect of climate change on the total discharge regimes at the global scale (e.g. Arnell, 1999b; Nijssen et al., 2001a; Manabe et al., 2004; Milly et al., 2005; Nohara et al., 2006; Sperna Weiland et al., 2012), sometimes including low flows. Expected changes are an increase in the annual discharge in cold climates and a shift of the snow melt peak in these areas (e.g. Sperna Weiland et al., 2012). Less is known about changes in hydrological drought events (drought in groundwater and surface water). Hirabayashi et al. (2008) have studied the changes in number of drought days at the global scale by taking the annual drought days from discharge data. Significant increases in drought were found for many regions across the globe (Hirabayashi et al., 2008). For Europe, Feyen and Dankers (2009) investigated changes in streamflow drought by deriving low flows and drought deficits. They concluded that in many rivers, with the exception of rivers in the most northern and northeastern parts of Europe, low flow conditions and flow deficit volumes are projected to become more severe in the frost-free season. This study on changes in streamflow drought in Europe was expanded by Forzieri et al. (2014). They also concluded that streamflow drought in many parts of Europe are projected to become more severe and persistent, except in the northern and northeastern parts of Europe.

Several studies investigated the impact of climate change on water resources using multiple large-scale models within ISI-MIP (e.g. Schewe et al., 2014; Haddeland et al., 2014; Prudhomme et al., 2014). From these studies, Prudhomme et al. (2014) specifically focused on hydrological drought at the global scale, in their case drought in runoff. They found a likely increase in spatial extent of drought at the end of the 21st century. In the Caribbean, South America, Western and Central Europe, Central Africa, Australia and New Zealand, and the Western Indian Ocean, drought duration and spatial extent of drought were very likely to increase (Prudhomme et al., 2014). Knowledge on hydrological drought events is important for water resources and needed for adequate planning and assessment of drought impacts in the future.

For historical drought studies the use of a multi-model ensemble was recommended because of the different model structures. For the same reasons it is important to include multiple hydrological models in studies about future changes as well. Many scenario studies employ only one GHM

in combination with one or an ensemble of GCMs that provide forcing data (e.g. Sperna Weiland et al., 2012; Arnell and Gosling, 2013). Hagemann et al. (2013) found large differences in the projected changes in runoff between several GHMs. Prudhomme et al. (2014) also used an ensemble of GHMs to assess changes in drought and concluded that uncertainty in projected changes in drought caused by GHMs is larger than that of GCMs. An ensemble of GHMs should be applied in climate change studies to get an overview of all uncertainties.

1.4 Research objective and questions

At the start of this research project, multi-model studies at the global scale for hydrological drought were missing both for the historic and future climate. To understand the space-time development of large-scale hydrological drought events and the relations between different types of drought, more research considering multiple models was needed. This knowledge was expected to lead to improved drought prediction and can be used to safeguard global water availability in the future.

The main objective of this research was to investigate the space-time development of large-scale hydrological drought for historic and future drought events through a multi-model analysis. To reach the main objective, the research was carried out in three different steps with each their own research questions.

1. Multi-model hydrological drought analysis at a global scale for the 20th century.

- How can we better characterise the space-time development of large-scale drought?
- How do hydrological drought events develop in space and time as a response to (a series of) meteorological drought event(s) at a global scale?

Most drought research focused on either single models or on individual variables (often precipitation or soil moisture) and has been mainly carried out for the catchment scale and continental scale. As a result less is known about the development and propagation of hydrological drought at the global scale and about appropriate metrics to characterise this development and propagation. Methodologies for this characterisation involved the use of indices that are often only valid for certain environmental conditions and not suitable for the global scale (Sect. 1.3.1). For a reliable description of space-time development of large-scale drought, existing methodologies (e.g., threshold level method) have been evaluated and extended.

2. Multi-model hydrological drought analysis at a global scale for the 21st century.

- What is the impact of projected climate change on large-scale drought?

Large-scale models run with several scenarios for the future climate make it possible to determine changes in hydrological drought characteristics. Many studies have indicated that drought in precipitation and soil moisture is likely to increase in the future (Sect. 1.3.5). For drought in discharge the changes are less certain. A multi-model analysis across the globe focused on hydrological drought was applied for multiple river basins.

3. Representation of drought by large-scale models.

- How well do large-scale models represent historical drought?
- Can we assess the plausibility in spatio-temporal characteristics of simulated large-scale drought by considering model ensembles, and by comparing with previous drought studies?
- Which processes that influence hydrological drought development are missing or insufficiently represented in the large-scale models?

Research has so far mainly focused on the occurrence and extent of meteorological or soil moisture drought instead of hydrological drought. Large-scale models (LSMs, GHMs) have been used for drought research at larger scales (Sect. 1.3.3). Most studies in the past have only used one single LSM or GHM (Sect. 1.3.4), however, results are dependent on the model used for the simulation of time series of soil moisture, runoff and other hydrological variables. The results of a multi-model ensemble were evaluated specifically for simulation of extremes to explore model structure uncertainty. The identification of shortcomings in large-scale models, like missing or inadequately described processes that are important for drought analysis (Sect. 1.3.2), will provide a way forward for global drought studies.

1.5 Outline

This thesis is organised as follows (Fig. 1.4). In Chapter 2, the methodology used to identify drought is explained. This methodology was developed for drought analysis at a global scale and combined two existing methodologies. Large-scale model results of five LSMs from the second part of the 20th century and observed discharge data were used for the development and illustration of the method.

Results from the drought analysis for the second part of the 20th century using ten large-scale models (GHMs and LSMs, Fig. 1.4) are given in Chapter 3. Here, drought events derived from simulated runoff were compared with known drought events from literature.

The identified drought events from the large-scale models (Fig. 1.4) are described in more detail in Chapter 4. Temporal and spatial development of drought events across the globe was investigated for meteorological and hydrological drought. The propagation from meteorological drought to drought in runoff was included as well.

Chapter 5 gives the results of a multi-model analysis of changes in drought characteristics in the future (Fig. 1.4). Model output of five large-scale models and observed discharge data have been used in the analysis. Observed data were employed to evaluate model performance for simulating low flows, leading to a selection of models for future analysis. By comparing drought characteristics between a control and future period, changes were identified.

Drought development within catchments was studied in more detail in Chapter 6 (Fig. 1.4). The influence of multi-year variation in storage on drought characteristics was investigated. For this analysis, observed data of discharge, groundwater and precipitation were used.

A synthesis of the research is given in Chapter 7. Main conclusions from the previous chapters and answers to the research questions are provided. Recommendations for the way forward in drought research are included as well.

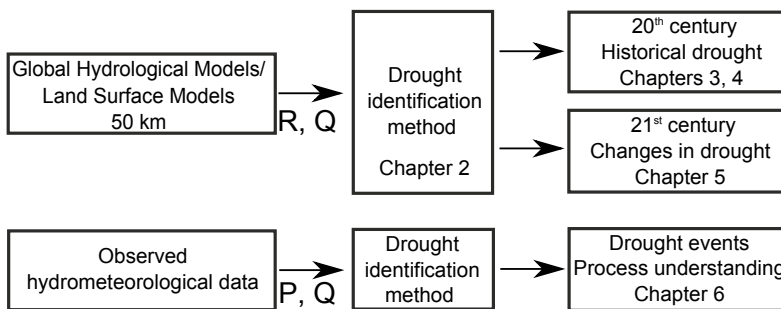


Figure 1.4: Overview of the different chapters in this thesis.



A generic method for hydrological drought identification

Abstract

The identification of hydrological drought at the global scale has received considerable attention during the last decade. However, climate-induced variation in runoff across the world makes such analyses rather complicated. This especially holds for the drier regions of the world (both cold and warm), where for a considerable period of time, zero runoff can be observed. In this chapter, we present a method that enables to identify drought at the global scale across climate regimes in a consistent manner. The method combines the characteristics of the classical variable threshold level method that is best applicable in regions with non-zero runoff most of the time, and the consecutive dry days (period) method that is better suited for areas where zero runoff occurs. The newly presented method allows a drought in periods with runoff to continue in the following period without runoff. The method is demonstrated by identifying drought events from discharge observations of selected rivers situated within different climate regimes, as well as from simulated runoff data at the global scale obtained from an ensemble of five different land surface models. The identified drought events obtained by the new approach are compared to those resulting from application of the variable threshold level method or the consecutive dry period method separately. Results show that, in general, for drier regions, the threshold level method overestimates drought duration, because zero runoff periods are included in a drought, according to the definition used within this method. The consecutive dry period method underestimates drought occurrence, since it cannot identify drought events for periods with runoff. The developed method especially shows its relevance in transitional areas across the world, because in wetter regions, results are identical to the classical threshold level method. By combining both methods, the new method is able to identify single drought events that occur during positive and zero runoff periods, leading to a more realistic global drought characterisation, especially within drier environments.

2.1 Introduction

Climate variability causes drought to occur on all continents under all climatic conditions. One of the most costly climate-related natural hazards is drought. The impacts are immense, for example, the European Commission (2007) estimated the total cost of drought at €100 billion for Europe alone over the past 3 decades. Over the United States, the estimated damage is \$6–8 billion per year on average (Dai, 2011). Observations show that some regions of the world (e.g., southern Europe and West Africa) have experienced more frequent, more intense or longer drought events, although in other regions the opposite happened. In the 21st century drought is expected to intensify in some areas in Europe, Central and Northern America and Southern Africa (Seneviratne et al., 2012). Drought is one of the most imperative natural hazards that needs better understanding, e.g., for global food security, but which receives too little attention (Romm, 2011). One of the reasons mentioned by Seneviratne et al. (2012) that the outcome of drought research is presented with maximally medium confidence, is lack of clarity concerning the definition of drought.

Drought is characterised by a temporal, sustained and spatially-extensive occurrence of below-average natural water availability. It affects all components of the water cycle; it propagates from a lack of precipitation or snow melt (meteorological drought), into the soil (soil moisture drought) and then into the aquifers, streams, lakes and reservoirs (hydrological drought), which again can have an impact on local atmospheric conditions (Koster et al., 2004). This leads to socio-economic drought (impact on economic goods and services) and ecological drought (ecosystem services) (e.g. Wilhite, 2000; Tallaksen and Van Lanen, 2004). Since drought is such a complex phenomenon, characterising it requires multiple climatological and hydrological parameters (Mishra and Singh, 2010). Additionally, Kallis (2008) argues that interdisciplinary analyses of drought as a natural hazard are needed to determine its actual impact. As a final step, policy and management options need to be identified to reduce drought vulnerability, and hence the risk of future drought (e.g. Kampragou et al., 2011). For a complete and comprehensive assessment of drought events from the hazard to the drought management measures, the nature of each individual drought component has to be understood (Dracup et al., 1980), which calls for a step-wise approach. This chapter contributes to the first step of understanding and determining the natural hazard by developing a new methodology to identify drought. For the first time, to the authors' knowledge, a methodology is proposed that allows identification of a drought event that starts in a period with non-zero runoff and continues in the period afterwards with generally no runoff in a single robust metric. Such a metric is essential, for instance, to intercompare large-scale models that have to handle very different climate conditions in one run.

Global drought studies need drought identification tools that are robust, meaning that these should be applicable to all climate regions, irrespective of the dryness of the climate. Regions with periods with and without runoff are typical for transition areas in the world, in particular from the hot and dry (hyper-arid) to the wetter climates (semi-arid) or from the extremely cold (polar frost) to the warmer climates (polar tundra). An adequate hydrological drought analysis of transition areas is extremely important because of the already low water availability in normal situations (e.g. Tallaksen and Van Lanen, 2004). Especially within these transitional regions, hydrological anomalies can have a dominant effect on the local climate (Koster and Suarez, 2001; Koster et al., 2004; Anyah et al., 2008), potentially intensifying the hydrological anomaly (e.g., the duration of the drought). Transition zones are also very vulnerable to climate change (e.g. Wetherald and Manabe, 2002), making projections of drought events using adequate identification tools essential. Dry areas across the world have been increasing in the last decades and will continue to increase in the future (Dai, 2011; Romm, 2011), implying that transition regions likely will move. This means that regions with zero flow will partly occur in other places, which calls for a generic method for drought analysis that can handle this non-stationary aspect of periods with and without runoff. When using different methods depending on regions, hydrological regimes in these regions might change in the future (change of periods with runoff to no-runoff periods, or the other way around),

meaning that results from different methods have to be compared for one specific period. This can be avoided by using one single all-encompassing method.

A suite of identification tools has been developed to address different drought phenomena. The Standardised Precipitation Index (SPI) and the Palmer Drought Severity Index (PDSI) (e.g. Dai, 2011) are best known, and widely used for large-scale studies on meteorological and soil moisture drought because of their generic applicability. The threshold level method (TLM) is another frequently-applied tool for studies at the global scale and the continental scale. For example, Sheffield and Wood (2007) used the TLM for large-scale soil moisture drought studies, and Corzo Perez et al. (2011) for drought in runoff at the global and continental scale. All these drought identification tools, however, do not operate well when drought in fluxes (e.g., runoff) has to be investigated in environments where fluxes are zero for significant periods of time. Typically dry regions (either hot or cold) are excluded (e.g. Corzo Perez et al., 2011), or rather high percentiles are chosen as threshold. For example, Fleig et al. (2006) used a river flow that is exceeded 20% of the time for a Spanish river basin, which is not in line with the concept that drought should be uncommon.

Studies in regions where precipitation is absent for longer periods introduced the consecutive dry days (CDD) approach as a means to investigate variability of the length of the dry period (e.g. Vincent and Mekis, 2006; Griffiths and Bradley, 2007; Deni and Jemain, 2009; Im et al., 2011). In this thesis we refer to this approach as consecutive dry period method (CDPM), because it can also be applied to data with other temporal resolutions, for example monthly. So far this approach has hardly been used for ephemeral or intermittent rivers to the authors' knowledge. Van Lanen and Tallaksen (2008) made a first attempt in two European river basins. In addition to the TLM, they identified drought events in an at-site hydrological drought analysis using the durations of subsequent months with zero flow. Nevertheless, the TLM and CDD approaches were still applied separately instead of combined. For drought events in runoff, one method that enables drought analysis for the whole globe is still missing. For instance, for the determination of synchronicity of drought at the global scale, comparison between regions is needed. This can only be achieved with a similar method across the globe.

When performing a multi-model analysis at large scales, runoff in a region might be simulated differently by each model, in particular some models will simulate runoff and others will not for a certain region. In case different drought identification methods would be applied to each simulation, model comparison will be very difficult.

The aim of this chapter is: (i) to develop a generic drought identification method, allowing an integrated large-scale drought analysis in environments with and without permanent fluxes, and (ii) to demonstrate and discuss the developed identification method with observed river flow from basins for different climates, and with simulated global runoff from an ensemble of land surface models. The generic drought identification method combines the threshold level method and the consecutive dry period method and allows a single drought event to continue in periods with and without runoff. In this manner, new information is gained compared to applying both methods separately. The presented method is primarily meant for natural conditions and large-scale studies, since human influences (e.g., storage dams) significantly alter flow regimes and these effects require different approaches for drought analysis.

This chapter starts with the main characteristics of the selected river basins and the land surface models (Sect. 2.2). The next section elaborates step by step the drought identification approach through a description of the TLM and the CDPM, and how these eventually are integrated into a novel methodology (Sect. 2.3). Next the methodology is illustrated by showing drought events in discharge of the selected rivers, which were derived from the TLM and the CDPM separately and from the new integrated methodology. Differences in area in drought and the average drought duration at the continental scale are used to reveal differences between the methods, as described in Sect. 2.4. The results are discussed in Sect. 2.5. Eventually, the conclusions are presented (Sect. 2.6).

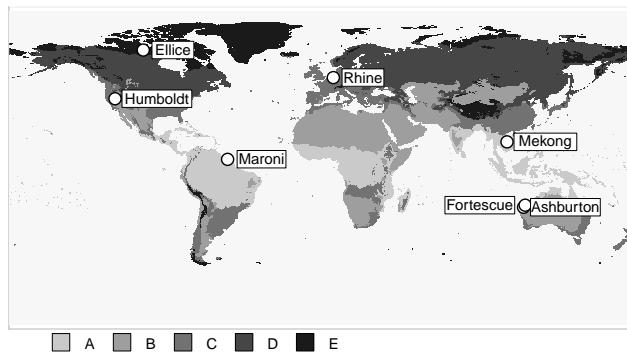


Figure 2.1: Locations of the discharge gauges of the selected rivers within the 5 major climate types.

2.2 Data

2.2.1 Discharge observations across climate regimes

Observed daily discharge data of seven rivers, which provide a wide range of runoff regimes, were used to illustrate the new method for hydrological drought identification. Each river is located in a different climate region (based on the Köppen-Geiger classification of the WATCH forcing data, see Wanders et al., 2010) and represents one major climate type. These five major climate types, as defined by the Köppen-Geiger classification, are the equatorial (A), arid (B), warm temperature (C), snow (D), and polar climates (E). These major climate types are subdivided into subtypes based on precipitation regime and air temperature (Wanders et al., 2010; Peel et al., 2007). The seven rivers selected are the Rhine (Europe, C-climate), Mekong (Asia, A-climate), Maroni (South-America, A-climate), Ashburton (Australia, B-climate), Fortescue (Australia, B-climate), Humboldt (North-America, C-climate) and Ellice (North-America, E-climate) rivers. Discharge data were made available by the Global Runoff Data Centre (GRDC, 2013). Figure 2.1 gives the approximate locations of the discharge gauges of these rivers. For all rivers, their mean daily discharge regime, as well as the spread between the 10th and 90th percentile values are shown in Fig. 2.2.

Data availability as well as climatology vary for the selected rivers. The river Rhine (data 1950 to 2007) is situated mainly in a Cfb-climate and can be classified as a perennial river. The Maroni river (data 1952 to 1995) is also a perennial river, but flows through a region with an A-climate. The Mekong (data 1968 to 1993) and Humboldt (data 1946 to 2008) rivers are perennial rivers as well. The Ellice river, the Fortescue river and the Ashburton river are ephemeral rivers, but situated in completely different climates. The Ellice river (data 1971 to 1996) lies in the ET-climate region and is dry in winter due to snow accumulation and temperatures below 0 °C. The Ashburton river (data 1973 to 2005) and Fortescue river (data 1969 to 1999) drain areas mainly in the BWh-climate and are dry for most of the time, caused by a lack of precipitation and high evapotranspiration. Although for drought analysis long time series are needed, in this chapter some shorter discharge series were used, because these are only meant for illustration. The discharge series were considered to be representative for the different climates.

2.2.2 Global simulated runoff data from large-scale models

To determine drought at a global scale, generally large-scale model output is used (e.g. Sheffield and Wood, 2007). Within the EC-FP6 project WATCH (Water and Global CHange), several large-scale models have been run at the global scale with the same model set-up and forcing data, described in detail by Haddeland et al. (2011).

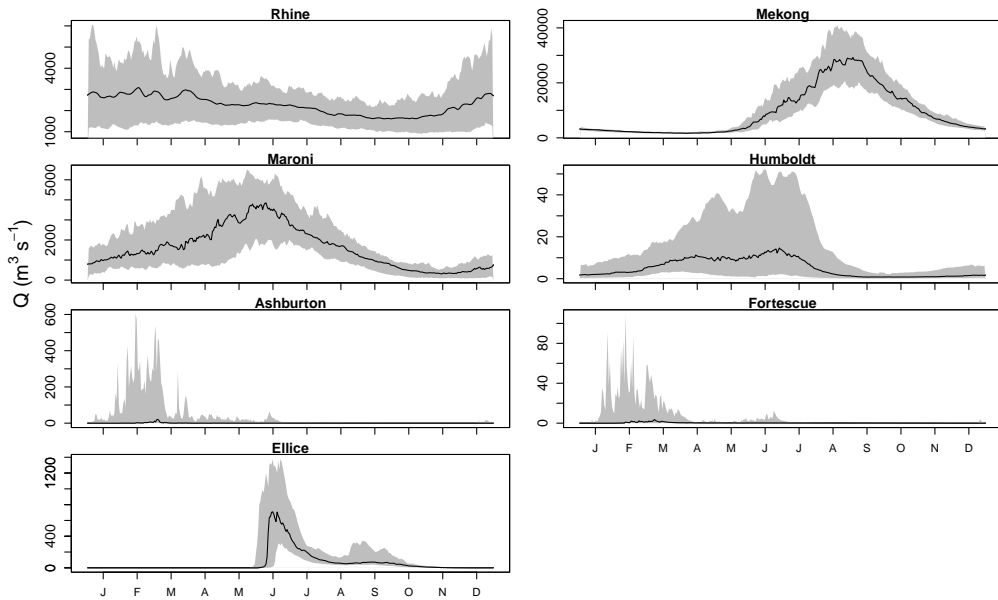


Figure 2.2: Yearly regimes of the selected rivers based on median daily discharge (black line) and the spread between the 10th and 90th percentile values (grey zone).

The meteorological forcing data for the models were the WATCH forcing data (WFD) developed by Weedon et al. (2011). The WFD consist of gridded time series of meteorological variables at a resolution of $0.5^\circ \times 0.5^\circ$ on a subdaily basis for the period 1958–2001. In this chapter, the ensemble median of results of five Land Surface Models (LSMs) (following the division in subgroups as proposed by Haddeland et al., 2011) was used: H08, HTESSEL, JULES, MATSIRO, Orchidee. Some model properties are given in Appendix A. All models classified as LSMs by Haddeland et al. (2011) solve both the water and energy balance. The snow scheme of all models is based on the energy balance approach. They use the land mask defined by CRU (Climate Research Unit, www.cru.uea.ac.uk), resulting in a resolution of $0.5^\circ \times 0.5^\circ$ for land points only.

In large-scale climate and hydrological studies the use of a multi-model ensemble instead of single models is quite common and even advocated for simulated river flows (e.g. Stahl et al., 2012). Several studies have shown that the ensemble mean or median is often closer to the observations than either of the individual models (Gao and Dirmeyer, 2006; Guo et al., 2007; Tallaksen et al., 2011). Because this chapter focuses on regions with zero runoff, we have chosen to use the ensemble median instead of the mean. By taking the ensemble median, one model with anomalous values has less influence. Some examples of time series of the ensemble median of total runoff for single grid cells, randomly chosen in different climate regions, as well as the range of the LSMs are given in Fig. 2.3.

The focus of this chapter is on hydrological drought identification. Therefore, the simulated time series of total runoff (sum of surface and subsurface runoff) were taken. Model output was available at a daily time step for the period 1963–2001 (the first five years, 1958–1963, of the WFD have been used as spin-up period). However, it was decided to aggregate these data into monthly values, since drought events generally tend to last a considerable period of time ranging from multiple months up to a few years (Tallaksen and Van Lanen, 2004; Sheffield et al., 2009) and the daily output values from the models were very dynamic. We do not intend to analyse the quality of the LSMs by comparing their simulations to observed runoff data. Such an analysis lies outside

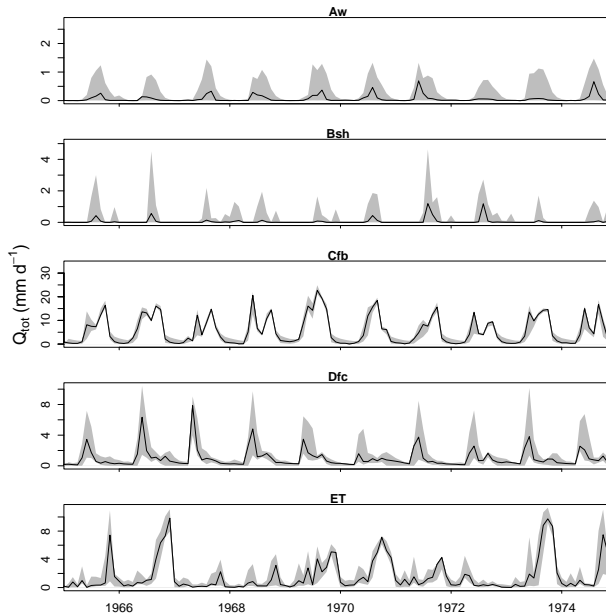


Figure 2.3: Time series of total runoff. Ensemble median (black line) and the range of the models (grey zone) for several, randomly chosen, single grid cells in different climate regions.

the scope of this chapter. Here, we only wish to present the capabilities of the newly developed hydrological drought identification method to be able to identify drought across different climate regimes.

2.3 A consistent method for hydrological drought identification at the global scale

2.3.1 Classical approach

Variable threshold level method

In temperate regions where runoff values are usually larger than zero, the most widely used method to estimate hydrological drought is the threshold level method (TLM) (Yevjevich, 1967; Hisdal et al., 2004; Fleig et al., 2006; Tallaksen et al., 2009). Advantages of the TLM over other drought identification methods like SPI and PDSI are: (i) no a-priori knowledge of probability distributions is required, and (ii) it directly produces drought characteristics (e.g., frequency, duration, severity), if the threshold is set by drought-impacted sectors. According to the TLM as applied in this chapter, a drought is observed once the variable of interest X (e.g., streamflow, runoff, recharge) is equal to or drops below a predefined threshold. This threshold can either be defined from its empirical percentile statistics, generally taken as the 20th percentile of the hydrological variable of interest, also known as the 80th exceedance percentile (Tallaksen et al., 2009), or by fitting some kind of statistical function through the data (normal, gamma, beta, etc.) from which probabilities can be estimated, e.g., the 20% of the cumulative probability function (e.g. McKee et al., 1993; Sheffield and Wood, 2007; Jaranilla-Sanchez et al., 2011). The benefit of applying the latter approach is that it leads to more robust statistics especially in case only a limited time

series is available. However, a drawback of this method is that especially for extreme situations (both during extreme dry and wet conditions) this distribution does not fit the entire range of observations. Therefore, in case long time series are available, calculating percentile statistics is expected to lead to more robust results.

The TLM can be implemented using either a fixed or variable (seasonal, monthly, or daily) threshold (Hisdal et al., 2004). In this chapter it was decided to apply the variable threshold making use of the percentile information. This was done, since at a global scale, in many regions the runoff response is influenced through seasonal climate variability. The variable threshold level method was implemented as follows:

1. Based on all data X observed for a given period of interest (e.g., day, month) calculate the different percentile statistics or quantiles ($\overline{X}_{P,T}$, where $P = 5, 10, 15, \dots, 95\%$ and T being the variable period of interest). At the daily time scale, in order to improve the robustness of the percentile statistics as well as to decrease the impact of inter-daily variations, all data observed M days centred around the day of interest (e.g., 5, 10, 15 days) are used to estimate the different percentile statistics.
2. Convert each of the data values X into their corresponding percentile value P_T .
3. Define a threshold $P_{threshold,T}$ according to a given percentile statistic (e.g., 20th percentile). In case the calculated percentile value is equal to or smaller than this threshold ($P_T \leq P_{threshold,T}$), a drought is assumed to occur. In this chapter, drought is defined when the variable is equal to or smaller than the threshold value. This was chosen to make sure that when using for example the 20th percentile as threshold, the time series will be in drought 20% of the time.

A graphical implementation of the variable TLM used to identify drought is presented in Fig. 2.4 for a time series of monthly runoff data. Since this data series shows considerable seasonal variability, thresholds were defined for each month separately. Here, the 20th percentile for a given month ($P_{20,T}$, where $T = 1, 2, \dots, 12$) was used as a threshold, which is given by the dashed line in Fig. 2.4 (top). During months for which the percentile value of runoff is below or similar to this threshold, a drought occurs. These months are identified by the black dots in Fig. 2.4 (bottom).

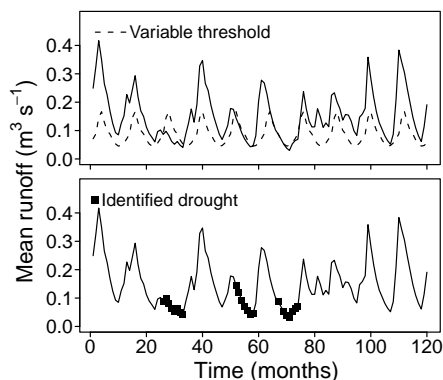


Figure 2.4: Example of the variable threshold level method (TLM) to identify drought for monthly runoff data. Based on the runoff time series (black line), for each individual month m a threshold $Q_{threshold}$ (dashed line) is calculated (here taken as the 20th percentile). Months with runoff $Q \leq Q_{threshold}$ are in a drought (black dots).

Consecutive dry period method

The TLM specifically focuses on positive hydrological data values. In case zero values in the hydrological data values are observed, according to our definition presented in the previous section, these periods are assumed to correspond to a drought. For many dry environments this leads to unrealistic results. A different approach has been taken in a number of studies dealing with meteorological drought (e.g. Vincent and Mekis, 2006; Groisman and Knight, 2008; Deni and Jemain, 2009), focusing specifically on periods with zero or limited precipitation. Since precipitation forms the main input to many hydrological and water supply systems, the general idea behind this method is that during long periods without precipitation the occurrence of drought can be triggered. As such, the statistical dynamics of consecutive periods without precipitation within a region can be used as a proxy for drought occurrence. Since this can be done at various time steps (day, month etc.), the method is now referred to as consecutive dry period method (CDPM). In regions where intermittent runoff occurs, this CDPM can be implemented to identify hydrological drought as well.

The CDPM was implemented as follows:

1. Identify within the hydrological data series all time steps with a zero value.
2. For each of these identified time steps, calculate its consecutive dry period number N_{dry} . Once a dry period is followed by a positive value, the consecutive series is “broken”. The next time step containing a zero value after such a wet period will then start again with $N_{dry} = 1$.
3. Based on the series with consecutive dry period numbers, the percentile statistics can be calculated (N_P , where $P = 5, 10, 15, \dots, 95\%$). As such, based on the time series it is possible to relate each consecutive period number N_{dry} to a given percentile statistic.
4. A drought is then identified using a given exceedance threshold, generally defined by a given percentile value $N_{threshold}$ (e.g., 80th percentile). In case the consecutive number of a given time step surpasses this threshold value ($N_{dry} > N_{threshold}$), the region is assumed to experience a drought.

A hypothetical example for runoff data is presented in Fig. 2.5. For this time series, a considerable number of months with zero runoff is observed. For each of these months, the consecutive dry period number N_{dry} is calculated as given by the grey line in Fig. 2.5 (top). Months with a

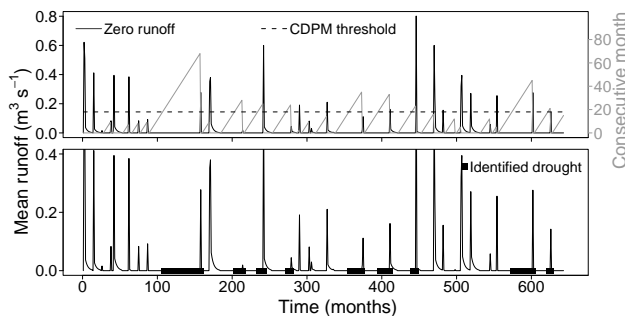


Figure 2.5: Example of the consecutive dry period method (CDPM) to identify a hydrological drought for runoff data. Based on the monthly runoff data (black line), for months with zero runoff its consecutive dry period number is calculated (grey line). Based on the CDPM series a given fixed exceedance threshold can be set (dashed line). Drought is identified for those months which exhibit a CDPM value larger than the threshold (black dots).

consecutive dry period number larger than the defined percentile threshold ($N_{dry} > N_{threshold}$) are in drought. The final result of this procedure is presented in Fig. 2.5 (bottom), where months in drought are shown by the black dots.

2.3.2 Combining the characteristics of the TLM and CDPM

The previous sections presented the specific details behind the TLM and the CDPM to identify hydrological drought. In case each method is used separately, they either fail to identify drought correctly within drier environments (TLM) where runoff becomes zero, or are not applicable within temperate environments (CDPM) where runoff is always positive. However, by developing a procedure which is able to use the benefits of both techniques, a robust hydrological drought identification method can be obtained.

This combined method was implemented according to the following procedure:

1. For each time series of a hydrological variable for each period of interest (e.g., day, month) a number of percentile statistics are calculated ($P = 5, 10, 15, \dots, 95$).
2. In case less than 5 percent of the time series contains a value of zero ($\bar{X}_5 > 0$), the variable TLM is followed as presented in Sect. 2.3.1. For situations where this does not hold, the variable TLM has to be combined with the CDPM.
3. For the time series with $\bar{X}_5 = 0$, for each time step with $X = 0$ its consecutive dry number N_{dry} is calculated, from which again the different percentile statistics can be obtained (N_P , where $P = 5, 10, 15, \dots, 95$). Notice that, contrary to the variable TLM implementation, the

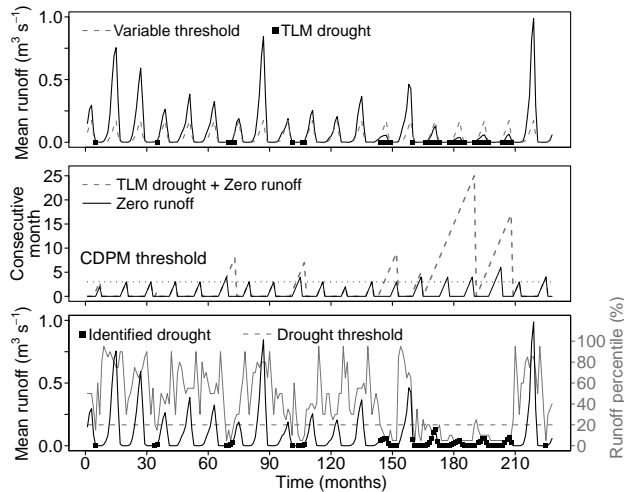


Figure 2.6: Combined drought identification method using characteristics of both the variable TLM (Fig. 2.4) and the fixed CDPM (Fig. 2.5). The runoff series in the upper panel (black line) contains multiple periods with zero runoff. Within the first step, monthly varying runoff thresholds $Q_{threshold}$ are calculated (dashed line). Months for which $Q > 0$, $Q_{threshold} > 0$ and $Q \leq Q_{threshold}$ are assumed to be in a drought according to the TLM (black dots). For months with $Q = 0$, the CDPM series (black line in middle panel) is used to obtain a given CDPM fixed threshold (dotted line in middle panel). Next, the CDPM series is combined with TLM drought series to obtain the consecutive period of being either in a drought or zero (dashed grey line in middle panel). Based on this series, dry months which exceed the CDPM threshold are also assumed to be in a drought. Bottom panel presents the final result, with the months in a drought indicated as black dots.

CDPM statistics are estimated as a fixed concept based on the entire time series for time steps with zero value observations without considering seasonality. This approach was chosen, because in areas with many short periods of zero runoff (e.g., every winter period during 2 to 3 months) a variable approach would give too many short drought events.

4. All positive data values ($X > 0$) are then transformed into their corresponding percentile statistic. In case the calculated percentile value is smaller than or equal to the defined threshold $P_{T,threshold}$ (e.g., the 20th percentile), a drought is assumed to occur.
5. Periods of positive runoff which experience a drought are combined with the zero runoff observations to obtain a new series. This series defines the consecutive number $N_{dry,drought}$ for all time steps which are either zero or in a drought.
6. Next, the corresponding percentile statistics are estimated for each time step with zero runoff. This is done by comparing $N_{dry,drought}$ of the combined series (step 5) to the statistics obtained from the consecutive zero runoff series only (step 3). If a time series has both zero and positive runoff in the given period of interest, both methods contribute to the transformation to percentile statistics. It should be noted that the maximum percentile value for a zero runoff time step can never exceed the value $100 - F_{wet}$, where F_{wet} is the fraction of positive runoff values observed at the given period of interest. Therefore, the percentile fractions as calculated according to the CDPM for dry periods are scaled. For example, if a monthly threshold is used, not all months January in the entire time series have the same characteristics. In some years, runoff might be positive, while in other years a no-flow situation occurs. In this case, both the TLM and CDPM contribute to determining the percentile values. If runoff occurs in 60% of the time series, percentiles derived from CDPM are rescaled to the lowest 40 (i.e., $100 - F_{wet}$) percentiles. In other words, the 50th percentile derived from the CDPM part of the method will become the 20th percentile of all months January.
7. The final result of this combined drought identification procedure is a continuous series of estimated percentiles for both wet (high percentile values) and dry (low percentile values) conditions. All time steps which contain a percentile value below or equal to a defined threshold $P_{threshold}$ (here the 20th percentile) are assumed to correspond to a drought.

This procedure enables one to associate each time step with a given percentile value. By using the consecutive number of the combined series of zero or in a drought, the method tries to ensure that a hydrological drought observed for positive runoff data according to the variable TLM, is generally followed by a drought according to the CDPM. A graphical example of the combined method to identify hydrological drought is presented in Fig. 2.6 for part of a time series which contains intermittent runoff data. Such a time series is generally observed within a cold arid environment, where in the winter period as the result of below zero temperatures and the occurrence of snow, zero runoff values are observed. The first step is to calculate the variable threshold percentile (dashed line in Fig. 2.6, top). Next, for all periods with zero runoff, its consecutive dry number is estimated (black line in Fig. 2.6, middle), from which the CDPM drought threshold can be estimated (dotted line in Fig. 2.6, middle). A drought is observed for positive runoff values smaller than or equal to the variable threshold. These months in drought are then combined with the consecutive dry period series, to obtain a consecutive period series for which the observation is zero or in a drought (dashed grey line in Fig. 2.6, middle). Months for which the combined consecutive dry period is larger than the CDPM threshold are assumed to experience a drought as well. The final result of this procedure is presented in Fig. 2.6 (bottom), where each month defined to be in drought either with positive or zero runoff data is presented by the black dot. Figure 2.6 (bottom) also gives the corresponding runoff percentile statistic for each month.

2.4 Illustration of the generic drought identification method

2.4.1 Drought identification for observed discharge data

Drought events were determined from observations for seven different rivers, which have a different hydrological regime and climate, as described in Sect. 2.2.1. Results of the different drought analysis methods (Sect. 2.3) were compared. For the perennial rivers Maroni, Rhine, Mekong and Humboldt, the CDPM does not yield any additional information, in other words the results for the TLM and the combined method are the same. Figure 2.7 gives the drought events identified by the two methods (TLM and combined method) for a representative period of 5 yr. As was expected the two methods determine the same drought events in this period. Since the aim of this chapter is to present a robust drought identification method for studies covering the whole globe or continents with very different climate conditions as well as under changing climatic conditions, results of the perennial rivers are also shown here. This illustrates the ability of the combined method to identify drought events in the completely different climates of both rivers.

For the other three rivers, however, the situation is different. The Ellice river, and Fortescue

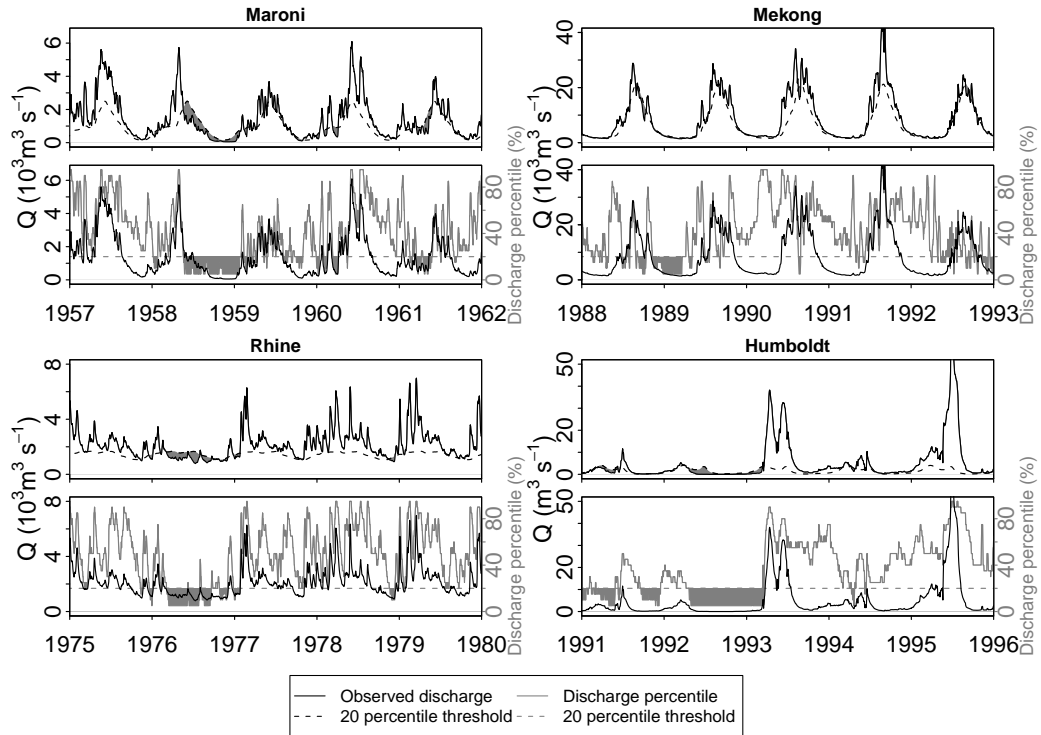


Figure 2.7: Drought events (indicated in grey) identified by the different methods for the Maroni and Rhine rivers (left) and the Mekong and Humboldt rivers (right). Left upper panel: TLM for Maroni river; second panel: combined method for Maroni river; third panel: TLM for Rhine river; fourth panel: combined method Rhine river. Right upper panel: TLM for Mekong river; second panel: combined method for Mekong river; third panel: TLM for Humboldt river; fourth panel: combined method Humboldt river. In all panels the observed discharges are given (black line) and the threshold values (here the 20th percentile, dashed lines). From the observed discharge, percentile values for each day are calculated (grey line).

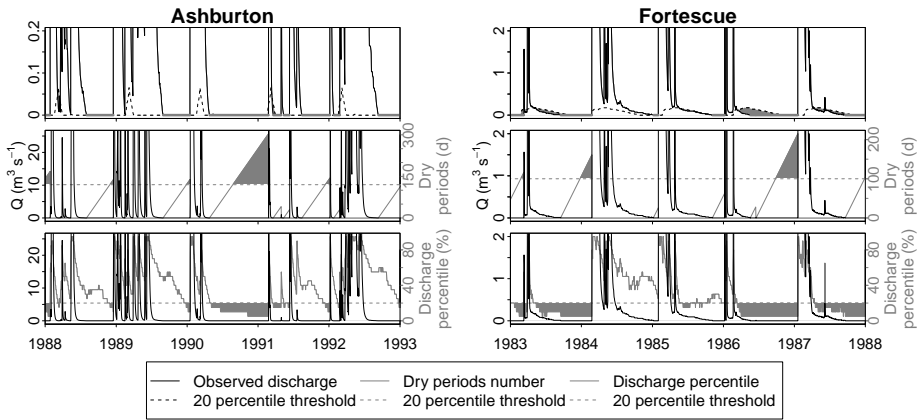


Figure 2.8: Drought events (indicated in grey) identified by the different methods for the Ashburton river (left) and the Fortescue river (right). The upper panels give the TLM, discharge values are shown as solid black line, the dashed line is the calculated threshold (20th percentile). Please note only the low flow values are given on y-axis. The middle panels give drought events calculated with the CDPM, where the consecutive dry periods are indicated by the grey line and drought events are identified if periods exceed the threshold (dashed grey line). When combining these methods, the discharge is converted to percentile values (lowest panels, grey solid line). If the percentile value drops below or equals the 20% (dashed grey) line, the month is in drought.

and Ashburton rivers have periods with zero discharge, which are caused by different processes (e.g., snow versus lack of precipitation, Sect. 2.2). For these three rivers, all three methods were applied to identify drought events. Results of these drought analyses are shown in Figs. 2.8 and 2.9. In these rivers, the TLM determines drought events in the period when discharge is larger than zero and all periods with zero flow are classified as drought (Figs. 2.8 and 2.9). This is due to the methodology used here that drought occurs when discharge is lower or equal to the threshold. This leads to a relatively large number of drought events and a long average duration for the TLM (Table 2.1). When the CDPM is used, by definition no drought events are determined in the periods with discharge, so all drought events occur at the end of long zero flow periods. This leads to a relatively small number of drought events and shorter average durations than with the TLM. Because the Ashburton and Fortescue river show a similar behaviour, we will only focus on the Ellice river and the Ashburton river for the rest of this chapter.

By combining both methods, drought events both in the periods with runoff as well as in zero flow periods can be determined. This sometimes increases the duration of a drought event compared to the CDPM (Fig. 2.8), but also includes more shorter events compared to both methods separately. In Fig. 2.10 the cumulative distributions of the durations of drought for the Ellice and Ashburton rivers are given. This gives the frequency at which a drought with a certain duration is equalled or exceeded, i.e., it indicates whether there are many short or many long drought events. From Fig. 2.10 and Table 2.1 it can be concluded that the combined method determines shorter drought events, leading to a short average duration. The TLM yields for both rivers the drought events with the longest duration (Fig. 2.10). The cumulative distribution of drought durations determined with the CDPM is rather steep for both rivers (Fig. 2.10), with no drought events shorter than 6 days, but also the shortest maximum drought duration. For the Ashburton river, the maximum durations determined with the TLM and with the combined method are the same. This is a drought event that already started before a zero discharge period, which caused the entire zero discharge period to be determined as drought by both methods. For the Ellice river, there is a large difference in maximum durations for the TLM and combined method. This implies that the

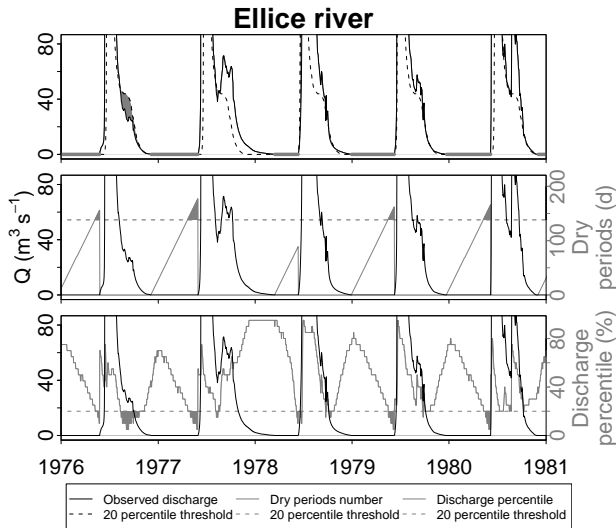


Figure 2.9: Drought events (indicated in grey) identified by the different methods for the Ellice river. The upper panel gives the TLM, discharge values are shown as solid black line, the dashed line is the calculated threshold (20th percentile). The middle panel gives drought events calculated with the CDPM, where the consecutive dry periods are indicated by the grey line and drought events are identified if periods exceed the threshold (dashed grey line). When combining these methods, the discharge is converted to percentile values (lowest panel, grey solid line). If the percentile value drops below or equals the 20% (dashed grey) line, the month is in drought.

largest drought of the TLM was a zero runoff period only, without preceding drought days. Such drought events will be shorter or excluded in the combined method, because they are determined with the CDPM part of the method.

2.4.2 Drought identification for simulated global runoff data

Besides on river basin scale observations, the drought analysis methods were also tested at the global scale using the ensemble median results of five different LSMs. At the global scale, the TLM identifies drought events in all continents, while the CDPM only gives results in cells where zero runoff periods occur. These cells are shown in Fig. 2.11. A small part of the world is simulated without runoff during the entire time series. These cells were excluded from all analyses (black area in Fig. 2.11). The CDPM mainly determines drought events in Africa and Australia, since the other continents have no or only a small area of cells with zero runoff periods. Therefore, to compare the three methods, results of the continents Africa, Australia and, to illustrate regions with continuous runoff, Europe are given (Fig. 2.12).

According to the TLM, a large fraction of Africa was in drought from 1982 until 2001. This is due to the employed methodology, which classifies all zero runoff periods as drought events, and thus gives a large area in drought in Africa. The CDPM only shows a small fraction of Africa in drought, since it is only relevant for part of the continent. However, both methods identify the 1980s as dry years, which corresponds with literature (Dai et al., 2004; Sheffield et al., 2009), and show an increase in drought in the 1980s and 1990s as compared to the 1960s and 1970s. By combining the methods, the erroneous drought events identified by the TLM due to the recurring zero runoff periods, and the lack of drought events in regions with runoff when using the CDPM, can be avoided. Therefore the combined method gives a much smaller area in drought in Africa

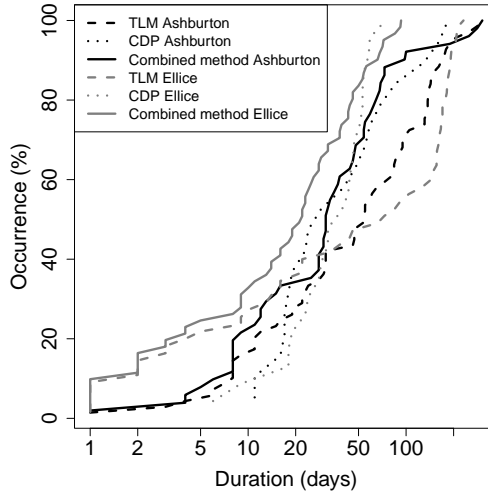


Figure 2.10: Cumulative distribution of the duration of drought events determined with all three methods for Ellice river (grey) and Ashburton river (black). Dashed lines give the drought durations determined with the TLM, dotted lines show the durations from the CDPM and the solid lines are durations calculated with the combined method.

Table 2.1: Drought characteristics for the different rivers identified with the drought analysis methods

River	Period	Method	Number of droughts	Duration (days)		
				avg	min	max
Rhine	1950–2007	combined	242	17.4	1	137
Maroni	1952–1995	combined	170	13.8	1	145
Mekong	1968–1993	combined	128	12.7	1	150
Humboldt	1946–2008	combined	196	23.5	1	340
Ashburton	1973–2005	TLM	69	75.9	1	304
		CDPM	19	53.6	11	184
		combined	51	51.5	1	304
Fortescue	1969–1999	TLM	76	39.6	1	315
		CDPM	7	50.7	16	115
		combined	69	35.1	1	315
Ellice	1971–1996	TLM	55	90.7	1	231
		CDPM	23	37.3	6	74
		combined	61	27.0	1	93

than the TLM, but larger than the CDPM. The historic drought years in the 1980s are still reflected and trends seem to be similar for all methods.

In Australia, differences between the methods are less extreme, but similar observations can be made. The TLM gives the largest area in drought, the CDPM gives only very low fractions in drought and the combined method filters out the extremes of the TLM. In the years 1963–1968, Australia experienced a severe multi-year drought (BoM, 1997), which is captured by all methods, but most clearly by the combined method, which shows higher fractions in drought in this period.

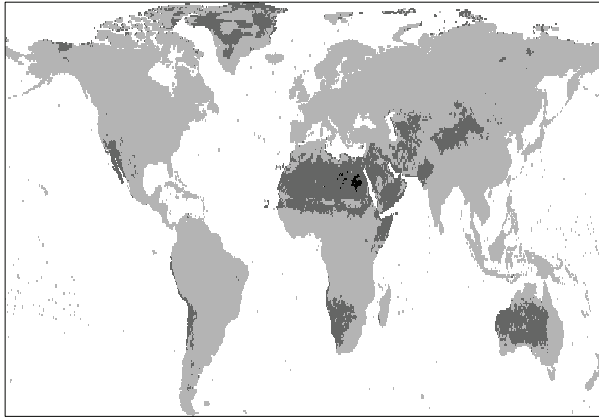


Figure 2.11: Location of the grid cells (dark grey colour) in which periods with zero runoff occur according to the ensemble median of five LSMs and where the CDPM can be applied. The black cells indicate the area without runoff during the entire time series (hyper-arid cells), which have been excluded from the analysis.

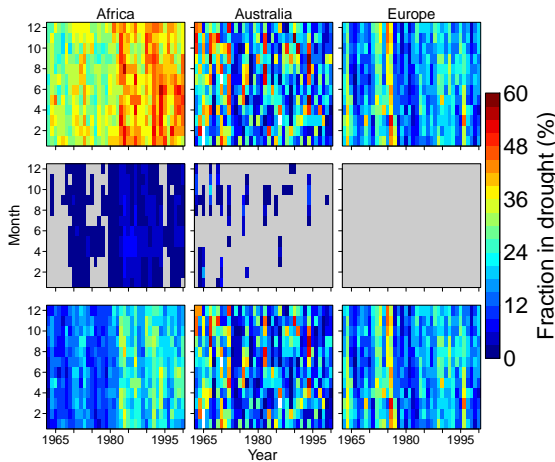


Figure 2.12: Fraction of the area in drought (%) for 3 continents (Africa, Australia and Europe) as identified with the different methods from the ensemble median of 5 LSMs. Top row: TLM; middle row: CDPM; bottom row: combined method.

The results of the drought analyses with all three methods for Europe are given to illustrate the method in a climate without zero runoff periods. Obviously, in such a climate, the CDPM does not give any drought, which means that the combined method gives the same results as the TLM. This is also visible in Fig. 2.12. The largest fraction in drought is identified in 1975–1976, which is a well-known drought event in Europe (Stahl, 2001; Zaidman et al., 2002).

For each grid cell, drought characteristics, such as the number of drought events and drought duration, can be calculated from the time series with drought events. Figure 2.13 shows the average duration of drought events (in months) determined with all three methods for each grid cell in Africa. Africa is chosen as illustration, because a relatively large area of the continent consists

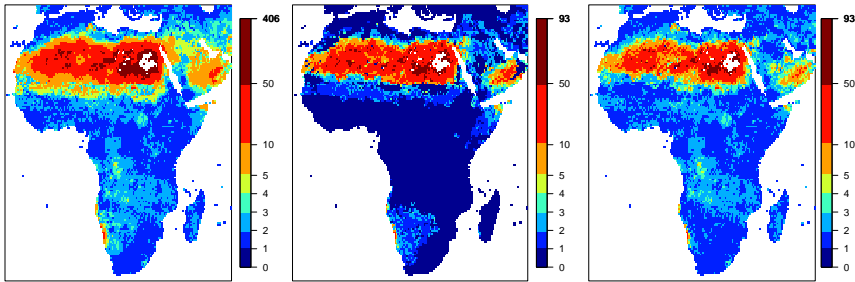


Figure 2.13: Average durations of drought events in months for each grid cell in Africa as identified with all three methods from the ensemble median of 5 LSMs. Left: TLM; middle: CDPM; right: combined method.

of drier regions and the differences between the methods are thus expected to be largest here. The maximum average drought duration differs substantially between the TLM and combined method. The area with a long average drought duration is largest with the TLM and smallest with the combined method.

2.5 Discussion

The newly-developed method is suitable for global studies, which have to cope with drought analysis of regions with a wide variety of flow types in a single analysis, i.e., perennial, intermittent and ephemeral flow. The method allows characterisation of drought events that continue from periods with runoff into periods without runoff and vice versa. This means the method especially shows its relevance for the transitional areas, because beyond these regions, results are identical to the widely-applied threshold level method or hydrological analysis is meaningless because flow is negligible. Since these areas are expected to increase in future (Romm, 2011), this method can be a valuable addition to existing drought identification tools.

The new method uses one uniform threshold level for the TLM across the world, which overcomes the selection of different percentiles in different climates, which makes a global comparison difficult. For example, Fleig et al. (2006) used in their global study of drought in streamflow very high threshold values, e.g., Q_{50} – Q_{80} for intermittent streams, to avoid threshold values of zero, whereas for perennial rivers substantially lower thresholds were applied. Hisdal et al. (2004) recommend thresholds between Q_{30} and Q_5 for the latter category of rivers. Periods with a zero threshold are still excluded in the studies using only TLM. In this study, we have used one uniform threshold for the variable TLM, the 20th percentile value. The new method is flexible and other threshold levels can be chosen depending on the purpose of the analysis.

In the new methodology presented, a drought occurs when the runoff value is equal to or below the threshold. This leads to overestimation of the number of drought events and duration by using the TLM only in the areas with zero runoff (Figs. 2.10, 2.12 and 2.13). In Africa, the TLM yields some cells with very long average durations (up to 406 months), whereas the combined method results in shorter drought events in each cell leading to a maximum average duration of 93 months (Fig. 2.13). These cells with an average drought duration of 93 months only have one long drought in the entire time series, since per definition 20% of the time series is in drought and the length of the total time series is 468 months. The TLM can give longer durations, because higher threshold percentiles (e.g., Q_{30} or Q_{40}) could still be zero and all zero runoff periods are completely classified as drought. Other studies, e.g., Tallaksen et al. (2009), only classify a period as in drought when the runoff is below the threshold. In this case, the TLM would underestimate

the number and duration of drought events compared to the new method, since periods with zero runoff are never considered as a drought when the Q_{20} is equal to zero (or very high threshold levels are needed). So regardless of the choice for a certain methodology in the TLM, the combined method will lead to more realistic results by including both the periods with and without runoff.

By including all periods, the combined method considers the entire time series, leading to more minor drought events. To reduce this number, pooling of drought events can be done in the same way as after the traditional threshold level method (Tallaksen et al., 1997; Fleig et al., 2006). Several metrics can be used to make a selection from the identified drought events, e.g., based on duration or severity. However, due to zero runoff periods, not all drought characteristics can always be identified. For example, the deficit volume simply cannot be determined from the periods with zero runoff, whereas in other periods this is possible. Depending on the purpose of a drought analysis study, spatial coverage of drought can be investigated using a cluster algorithm (Andreadis et al., 2005; Corzo Perez et al., 2011) after the identification of drought with the combined method (Sect. 4.3.2).

In this chapter, we used the ensemble median of five LSMs to illustrate the new method. Haddeland et al. (2011) found in their multi-model analysis, which included 11 different large-scale models (both GHMs and LSMs), that in general the models overestimate runoff in semi-arid and arid basins. They also found a very large spread in runoff between the models in these areas. The LSMs gave lower runoff values than the GHMs and were closer to observations (Haddeland et al., 2011), which was the reason to use LSMs only in this chapter. Global or continental hydrological analyses extensively use output of large-scale models (e.g. Andreadis et al., 2005; Dirmeyer et al., 2006; Sheffield et al., 2009; Corzo Perez et al., 2011; Haddeland et al., 2011; Prudhomme et al., 2011; Stahl et al., 2011, 2012). As large-scale models have difficulties capturing all hydrological processes, infinitesimal runoff values that may occur in model results, can be set to zero using a minimum threshold, depending on the purpose of the study. The number of grid cells that experience zero runoff periods can be different for each individual model. Some models tend to have very long recession periods, leading to extremely small, but non-zero runoff. For example, in the ET-climate, the ensemble median now has runoff almost everywhere, while in observations of the Ellice river long zero runoff periods occur. When these periods with small values are considered to be zero runoff periods, the area in which the combined method is beneficial, will substantially increase.

Since in this chapter, model results are only used as illustration of the method, they have not been validated against observations. Further drought analyses with large-scale models will require additional validation, in which limitations in measuring very low flows (e.g. Rees et al., 2004) should be taken into account.

2.6 Conclusions

This chapter presented a novel method to identify hydrological drought across different climate regimes. The method integrates the variable TLM, which is well-known from hydrological drought analysis (e.g. Sheffield and Wood, 2007; Fleig et al., 2006; Corzo Perez et al., 2011), and the CDPM, which has historically mostly been used to assess meteorological drought (e.g. Vincent and Mekis, 2006; Griffiths and Bradley, 2007; Deni and Jemain, 2009; Im et al., 2011). The developed method was demonstrated by identifying drought from discharge observations of selected rivers situated in different climate regions and from the simulated runoff of five land surface models. Based on the findings in this chapter, the following conclusions can be drawn:

1. The new hydrological drought identification method is able to define drought across the globe in a consistent manner.
2. Compared to the classical variable threshold level method, the new combined method is much better able to define drought in the transition areas of the world (from the hot and

dry (hyper-arid) to the wetter climates (semi-arid) or from the extremely cold (polar frost) to the warmer climates (polar tundra)). The threshold level method either overestimates the drought events in these regions by identifying all zero runoff periods as drought, or underestimates them by excluding these periods.

3. The combined method can be applied to both areas with and without runoff, whereas the CDPM is only applicable in areas with zero runoff and thus in a limited part of the world.

Overall, the combination of the TLM and the CDPM leads to a more robust drought identification method. As such, the combined method is able to identify drought within different climate regions, which enables one to perform global drought analysis in a consistent, more reliable manner. In Chapters 3 and 4, we will implement this method at the global scale for runoff data as simulated by 10 different hydrological and land surface models.



Do large-scale models capture reported drought events?

Abstract

Large-scale hydrological models are used to determine drought at a global scale. However, it is important to know how well these large-scale models can reproduce major drought events in the past before projections can be made. This chapter presents a comparison between a multi-model ensemble and reported drought events in literature to assess the performance of large-scale models. Major drought events in the selected period (1963–2000) were reproduced by the model ensemble median, although the duration and spatial extent differed substantially from reported events. The major drought events are caused by precipitation deficits linked to oscillations in climatic patterns, such as ENSO. This implies that major drought events were simulated if these were included in the forcing data. Spatial extent and duration of simulated drought events differed from extent and duration of reported ones due to a fast runoff response in some models.

Adapted from Van Huijgevoort, M.H.J., H.A.J. van Lanen, A.J. Teuling, R. Uijlenhoet, 2014: Do large-scale models capture reported drought events? In: *Hydrology in a Changing World: Environmental and Human Dimensions*, Proceedings of FRIEND-Water 2014 (IAHS Publ. 363, 66–71).

3.1 Introduction

Drought is one of the natural hazards with the most impact. In the future, impacts of drought are expected to increase in large parts of the world due to climate change (Romm, 2011). To investigate the impacts of drought, long time series are needed for several hydro-meteorological variables, which are usually not available at the global scale. To overcome this lack of data, large-scale models are used to estimate the values of hydro-meteorological variables, e.g., soil moisture, runoff. However, before these large-scale model results are used for projections, it is important to know how well they reproduce major drought events in the past. Although some studies have been reported, they either mainly focused on mean discharge (e.g. Haddeland et al., 2011), or focused on drought using a single model (e.g. Sheffield et al., 2009), or focused on drought at the regional scale rather than the global scale (e.g. Wang et al., 2009; Prudhomme et al., 2011; Wang et al., 2011; Gudmundsson et al., 2012b; Stahl et al., 2012).

The lack of observed time series at a global scale makes it difficult to evaluate large-scale model results. Direct comparison between observed discharges and gridded runoff values from the models is not recommended. Therefore in this chapter, a qualitative comparison has been made between a multi-model ensemble and reported drought events in literature during the second part of the 20th century to assess the performance of large-scale models for drought analysis.

3.2 Large-scale models and forcing data

Through the project WATCH (WATER and Global CHange, www.eu-watch.org) results from different large-scale models using the same forcing data were made available. The multi-model analysis in this chapter comprises ten models: H08, HTESSEL, JULES, Orchidee, MATSIRO, WaterGAP, MPI-HM, LPJml, GWAVA and Mac-PDM. A condensed overview with characteristics of each model, after Haddeland et al. (2011), is presented in Appendix A. The model ensemble median was derived to represent the overall hydrological behaviour rather than focusing on individual models. This chapter does not intend to evaluate individual models.

The use of an ensemble mean is quite common when analysing large-scale model output, for both soil moisture and runoff (e.g. Haddeland et al., 2011; Gudmundsson et al., 2012a; Stahl et al., 2012), and is often found to be closer to the observations than results of individual models (Gao and Dirmeyer, 2006; Guo et al., 2007). Tallaksen et al. (2011) found that the ensemble median performed better in comparison against observations than the ensemble mean. Wang et al. (2011) also use an ensemble median to exclude the effect of outliers. In this chapter, we have chosen to use the multi-model ensemble median rather than the ensemble mean, to reduce the effect of zero runoff periods in dry regions. In these cases, the ensemble median gives a more robust result compared to the ensemble mean. A minimum threshold of $10^{-6} \text{ kg m}^{-2} \text{ s}^{-1}$ was used to avoid infinitesimally small values of runoff, which may occur in the model output. All values below this threshold have been set to zero.

All models had the same simulation setup and forcing data as described in detail in Haddeland et al. (2011) and Gudmundsson et al. (2012a), but the employed time step, meteorological variables and model structure differ between the models (Appendix A). They used the land mask defined by CRU (Climate Research Unit), at a resolution of $0.5^\circ \times 0.5^\circ$. Only land points (67 420 grid cells in total) were considered by the models. Model forcing was provided by the WATCH forcing data (WFD) developed by Weedon et al. (2011). The WFD consist of gridded time series of meteorological variables (e.g., rainfall, snowfall, temperature, wind speed) both on a subdaily and daily basis for 1958–2001 with a resolution of $0.5^\circ \times 0.5^\circ$. The WFD originate from modification (bias-correction and downscaling) of the ECMWF ERA-40 re-analysis data (Uppala et al., 2005). The different weather variables were elevation-corrected and bias-corrected using CRU data. Precipitation data were bias-corrected using monthly GPCP precipitation totals (Schneider et al., 2008)

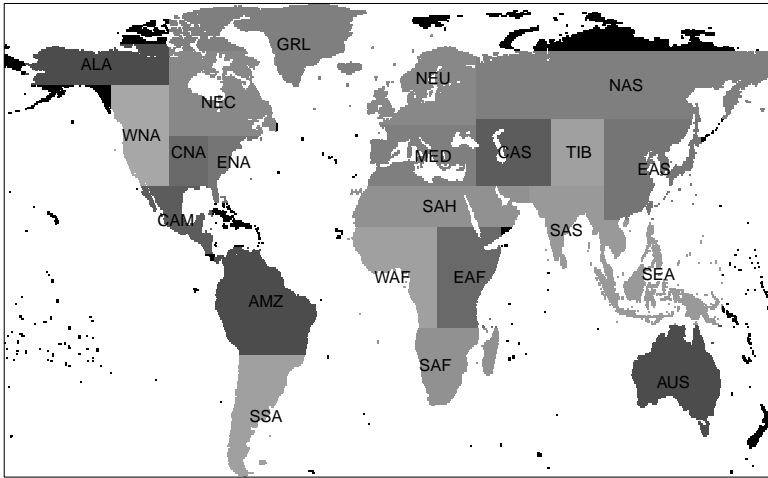


Figure 3.1: Location of regions (see Table 3.1) across the globe as derived from Giorgi and Francisco (2000) and as adapted by Sheffield and Wood (2007).

and gauge-catch corrections were applied separately for rainfall and snowfall. More information can be found in Weedon et al. (2011).

As our study focused on hydrological drought at the global scale, we have used time series of natural total runoff (sum of surface runoff and subsurface runoff, i.e., all water discharged from a single grid cell). Total runoff was chosen, because this is most relevant for water resources. All models provide output on a daily time step for the period 1963–2001, following 5 years of model spin up. The simulated daily data are often highly fluctuating, while hydrological drought events develop over months and years. Therefore, the daily data have been aggregated to monthly time scales for analysis. The ensemble median was calculated from the monthly total runoff time series of all models.

3.3 Drought analysis

Drought events have been derived with the combined drought identification method (Van Huijgevoort et al., 2012), which combines the characteristics of the threshold level method (Yevjevich, 1967) and the consecutive dry period method (Vincent and Mekis, 2006). This method allows a drought in periods with runoff to continue in a following period without runoff and thus provides a robust drought indicator for all climates. The threshold used in this study is the 20th percentile (Q_{20}), which is defined as the value that is equalled or exceeded 80% of the time. A detailed description of the method is given in Chapter 2.

Time series of area in drought were calculated for several regions (Fig. 3.1), the regions are defined by Giorgi and Francisco (2000) and adapted by Sheffield and Wood (2007). An overview with abbreviations and full names of the regions is given in Table 3.1. The abbreviations will be used to indicate the regions in this chapter and Chapter 4. Since most models do not include a glacier scheme (Haddeland et al., 2011), the results for Greenland were excluded from further analysis. The Sahara region was also not considered because the drought analysis was very difficult there, even with the combined method, due to small runoff during the entire period (average annual runoff values of less than 1 mm per year). For each region, drought events were divided into short events of 2 to 6 months and long events of 7 months or longer to find the most extreme drought

Table 3.1: Full names and abbreviations of the regions (see Fig. 3.1) used in this study (Giorgi and Francisco, 2000)

Abbreviation	Region
ALA	Alaska
GRL	Greenland
NEC	Northeastern Canada
WNA	Western North America
CNA	Central North America
ENA	Eastern North America
CAM	Central America
AMZ	Amazon
SSA	Southern South America
NEU	Northern Europe
NAS	Northern Asia
MED	Mediterranean
CAS	Central Asia
TIB	Tibetan Plateau
EAS	East Asia
SAS	Southern Asia
SEA	Southeast Asia
AUS	Australia
SAH	Sahara
WAF	Western Africa
EAF	Eastern Africa
SAF	Southern Africa

events as simulated by the model ensemble median and to remove short drought events (duration of 1 month). The variability in the percentages of area in drought across the regions is a function of scale, since the regions have different areas. Occurrence of drought events in each region was compared with literature as a qualitative assessment of the results. Additional information about the main literature sources used is given in Table 3.2. For the investigation of synchronicity of drought events across the different regions, the largest spatial events with duration longer than 6 months (the top 10% of the events to investigate a representative number of events) have been selected. The percentages of area in drought for each region (this includes drought events with all durations again) at the time of these most severe events were determined.

3.4 Identification of major drought events

3.4.1 Drought in Europe

In the period 1975–1977, drought events occurred in the NEU region. During 1976, around 30% of NEU was in drought for longer than 6 months according to the ensemble median (Fig. 3.2). This drought event in Europe is well-known and described in the literature (e.g. Zaidman and Rees, 2000; Stahl, 2001). Other events were found from the ensemble median, both in short and long duration drought events in 1964, around 1990 and 1995–1996. These drought events are also listed by Bradford (2000) and Stahl (2001). The drought in 1989 and the beginning of 1990 spread over large areas of Europe and also affected the MED region (Bradford, 2000). That region showed a large increase in area in drought from 1989 until the mid-1990s (Fig. 3.2).

Table 3.2: Overview of main literature sources used for comparison

Authors	Year	Drought type	Data
Dai et al.	2004	Meteorological	Observed data
Sheffield and Wood	2007	Soil moisture	Model data
Sheffield et al.	2009	Soil moisture	Model data
Sheffield and Wood	2011	Soil moisture and hydrological	Observed and model data
Stahl	2001	Hydrological	Observed data
Vicente-Serrano et al.	2011	Meteorological	Reanalysis data
Wang et al.	2011	Soil moisture	Model data
Wu et al.	2011	Soil moisture	Model data
Zaidman et al.	2002	Hydrological	Observed data

3.4.2 Drought in North America

In North America, several drought events occurred that covered large areas and were most extreme in multiple regions in this study. In 1976, a long duration drought event (Fig. 3.2) occurred in three regions (NEC, WNA, and CNA). This winter drought was one of the most extensive drought events in the period 1950–2000 (Sheffield et al., 2009). Another extreme event was found in the regions WNA, CNA, and ENA in 1988 (Figs 3.2 and 3.3). This was a major drought in the US and Canada (Trenberth and Branstator, 1992; Sheffield and Wood, 2011). In the ALA region, the timing of the high percentages of area in drought longer than 6 months and the overall pattern agreed with time series of soil moisture drought reported by Sheffield and Wood (2007). The lack of extreme drought events in the CAM region (hardly any higher percentages of area with long duration drought events) was also consistent with findings of Sheffield et al. (2004), although the large area in drought in 2000 was different.

3.4.3 Drought in Asia

Drought events in China have been investigated in several studies (e.g. Wang et al., 2011; Wu et al., 2011). They found an increase in area in drought in China since the 1990s. In this study, the TIB region showed a high percentage of area in drought with short durations around 1997 and the EAS region in 1999 (Fig. 3.2), but a clear increase in area in drought or duration of drought events has not been found. Drying according to literature has been mostly limited to north and northeast China, which cannot be identified by the large regions used in the current study. Other extreme events have been simulated. For example, the event ranked as most severe in east China by Wu et al. (2011) and as severe by Wang et al. (2011) in 1978–79, has been identified in the current study in the long duration drought events in EAS. In the 1970s and towards the end of the 1990s most of the CAS region experienced short duration drought events. This is consistent with soil moisture drought time series found by Sheffield and Wood (2007) for this region. The NAS region exhibited events with a long duration in 1975–1977 in the ensemble median, corresponding with a drought mentioned by (Sheffield and Wood, 2011) in Russia in 1975, which caused severe crop failures. However, other years with known crop failures were not reproduced in the model time series.

3.4.4 Drought in regions related to ENSO

Since drought events often affect large areas, single events typically occur in several regions at the same time (Fig. 3.3). For example, teleconnections may exist for multiple regions affected by the El Niño-Southern Oscillation (ENSO). ENSO has a large influence on the occurrence of drought at large scales in both precipitation (e.g. Ropelewski and Halpert, 1987) and streamflow (e.g. Chiew and McMahon, 2002). This overview provides information on whether extreme events occurred simultaneously in different regions. Although there were several drought events that covered

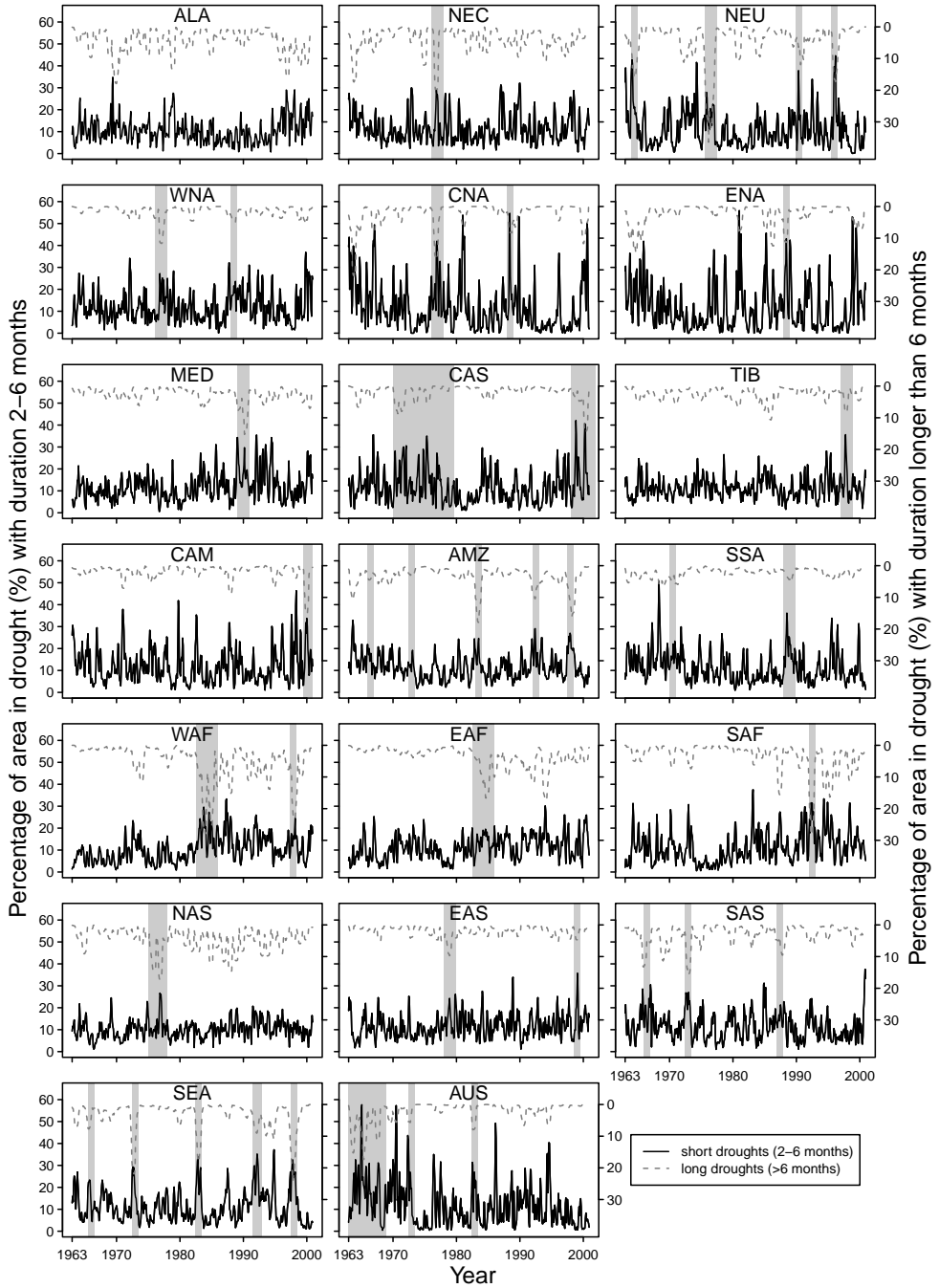


Figure 3.2: Fraction in drought of the ensemble median for different drought duration classes. Drought events discussed here are indicated in grey.

multiple regions (Fig. 3.3), the model outcome did not reveal any clear synchronicity pattern, besides the pattern related to ENSO. Drought events linked to ENSO were most clearly identified in strong El Niño years (the warm phase of ENSO): 1966, 1972, 1983, 1992, 1998 (e.g. Smith and Sardeshmukh, 2000; Wolter and Timlin, 2011; NCEP, 2012). In these years, the regions mainly affected were AUS, SEA, AMZ, and SAS (Fig. 3.3), which is consistent with the regions under influence of ENSO mentioned by Vicente-Serrano et al. (2011). When including the dates with the highest percentage in drought for all drought durations (not shown here), SAF was also affected in these years. Drought events in these El Niño years were caused by lack of precipitation and strongly linked to the timing of the meteorological drought events. The influence of ENSO was very strong in 1997–1998, leading to very low water levels in the Amazon region and large forest fires in Indonesia (Bell and Halpert, 1998; Tomasella et al., 2011). Drought events mentioned by Sheffield and Wood (2011) as the most widespread and damaging in SAS occurred in the years 1966, 1972 and 1987, which were all identified as extreme events by the ensemble median of this study (Fig. 3.3). In the AUS region almost no large spatial drought events of long duration could be identified from the ensemble median in the period with available model data. The most extreme events for both duration classes (Fig. 3.2) were found in 1963–1968, corresponding with literature (BoM, 1997). The model ensemble median showed long drought events with large percentages of area in drought in WAF and EAF in the mid-1980s (Figs. 3.2 and 3.3). In the 1980s large parts of Africa suffered from drought, including the well-known drought in the Sahel in 1983–1984 (Dai et al., 2004; Sheffield et al., 2009; Dai, 2011). This event was caused by very low rainfall in the Sahel following a major El Niño event (Dai et al., 2004). Overall, it can be concluded that the model ensemble median reproduced major drought events linked to El Niño rather well.

La Niña years (the cold phase of ENSO) have also been linked to drought events in some regions, but these events generally tend to be less widespread (Ropelewski and Halpert, 1987). Southern USA and northern Mexico (CNA and WNA regions), southern Russia and eastern Europe (NAS, CAS and NEU regions) and parts of the SSA region have been identified by Vicente-Serrano et al. (2011) as areas with drought events influenced by La Niña. Strong La Niña years were 1971, 1974, 1976, 1989, 2000 (e.g. Smith and Sardeshmukh, 2000; Wolter and Timlin, 2011; NCEP, 2012). Some drought events in these years were found in the model outcome in the regions mentioned (e.g., the NAS region in 1976 and the CAM region in 2000, Fig. 3.2). In the SSA region, years with extreme events mainly corresponded to La Niña years (1970, 1989), but the highest per-

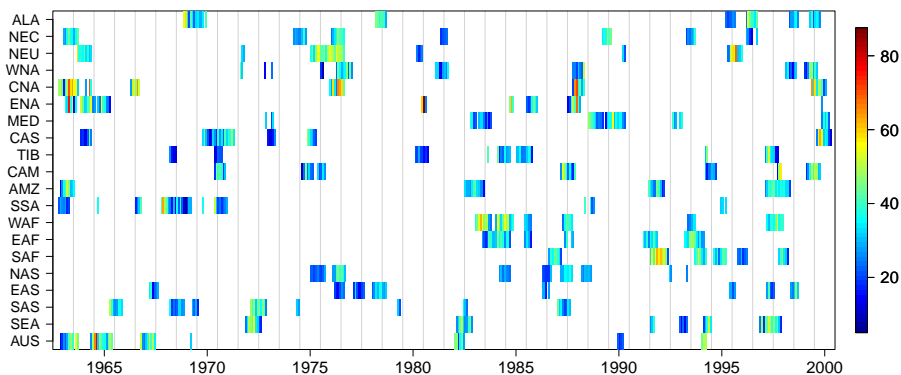


Figure 3.3: Total fraction in drought per region for large spatial events (top 10% of events with a duration longer than 6 months).

centages of area in drought in the long duration class in this region were relatively low and peaks were almost non-existent. Overall, the connection between drought events and La Niña is not as strong as for El Niño. This can be explained by the relatively small areas that are affected by La Niña, as compared to the size of the regions used in this study.

3.5 Discussion and conclusion

The major drought events in the second part of the 20th century were reproduced by the model ensemble median, although the duration and spatial extent differed substantially from reported events. The major drought events are caused by precipitation deficits linked to oscillations in climatic patterns, like ENSO. When comparing the runoff of the models with the precipitation forcing, a fast reaction of some models was observed (Van Huijgevoort et al., 2013). This implies that the models simulate major drought events if these are included in the forcing data. When compared to other model studies (e.g. Sheffield and Wood, 2007), differences in the forcing data could account for some of the differences in spatial extent and duration of drought events that were found in the model results in this study. In the same way, similarities could be caused by the use of the same forcing data. Another reason for the differences could be the drought identification method and the variables used. The outcome of a drought analysis is in most cases dependent on the definition used and this should be considered for an adequate intercomparison of the outcome from different studies. Due to the lack of observed data and the limited number of independent drought studies for runoff or streamflow at the global scale, we compared drought events in runoff (hydrological drought) with drought events in other variables (soil moisture) and with results from single model studies. This has influenced the comparison, however, major drought events are expected to propagate through the hydrological cycle, so they should be identifiable in the different variables although with somewhat different characteristics. Overall, the large-scale models are able to capture extreme drought events.



Global multi-model analysis of drought in historic runoff

Abstract

During the past decades large-scale models have been developed to simulate global and continental terrestrial water cycles. It is an open question whether these models are suitable to capture hydrological drought, in terms of runoff, on the global scale. A multi-model ensemble analysis was carried out to evaluate if ten of such large-scale models agree on major drought events during the second half of the 20th century. Time series of monthly precipitation, monthly total runoff from ten global hydrological models, and their ensemble median have been used to identify drought. Temporal development of area in drought for various regions across the globe was investigated. Model spread was largest in regions with low runoff and smallest in regions with high runoff. In vast regions, correlation between runoff drought derived from the models and meteorological drought was found to be low. This indicated that models add information to the signal derived from precipitation and that runoff drought cannot directly be determined from precipitation data alone in global drought analyses with a constant aggregation period. Furthermore, duration and spatial extent of major drought events differed between models. Some models showed a fast runoff response to rainfall, which led to deviations from reported drought events in slowly responding hydrological systems. By using an ensemble of models, this fast runoff response was partly overcome and delay in drought propagating from meteorological drought to drought in runoff was included. Finally, an ensemble of models also allows to consider uncertainty associated with individual model structures.

Adapted from Van Huijgevoort, M.H.J., P. Hazenberg, H.A.J. van Lanen, A.J. Teuling, D.B. Clark, S. Folwell, S.N. Gosling, N. Hanasaki, J. Heinke, S. Koirala, T. Stacke, F. Voss, J. Sheffield, R. Uijlenhoet, 2013: Global multimodel analysis of drought in runoff for the second half of the twentieth century. *Journal of Hydrometeorology*, 14, 1535–1552, doi:10.1175/JHM-D-12-0186.1.

4.1 Introduction

Drought is a natural hazard that occurs at the land surface all over the world and can have large economic, social and environmental impact (Wilhite, 2000). Drought is defined as a period of below-average natural water availability due to low precipitation and/or high evaporation rates. It is characterised as a deviation from normal conditions of the physical system (climate and hydrology), which is reflected in variables such as precipitation, soil moisture, groundwater, and streamflow (Tallaksen and Van Lanen, 2004; Wilhite, 2000). Dry areas worldwide have been expanding in recent decades and are expected to continue to do so in the near future (Dai, 2011; Romm, 2011; Fraser et al., 2013), also leading to more severe impacts of drought events. In the 21st century drought may intensify in parts of Europe, central North America, Central America and Mexico, northeast Brazil and southern Africa (Seneviratne et al., 2012). To reduce impacts of drought, thorough knowledge regarding its space-time development both for the current and future climates is essential.

Long time series of hydro-meteorological variables are needed for drought analysis. At the global scale, observed time series are usually not available. Instead, large-scale models can be used to simulate global and continental terrestrial water cycles. In principle, results from large-scale models offer possibilities for hydrological drought analyses (drought in runoff), although certain limitations are expected, depending on the model and data used. For example, any given model is unlikely to be able to accurately simulate runoff for all regions of the globe, the models used in this study are typically run at 0.5 degree resolution, and model performance/ability is somewhat contingent upon the quality of the input data that is used for calibrating, validating, or forcing the model.

To reduce the influence caused by a single model structure, multi-model drought analyses provide a promising way forward. Recently, results of eleven global models were used in an intercomparison project (WaterMIP). Haddeland et al. (2011) investigated whether land surface models and global hydrological models showed consistent differences in their simulations of the water cycle by looking at the hydrological regimes (e.g., mean monthly values) compared to observations and global statistics. They concluded that “the models gave a large range in global and regional water flux and storage terms”. No clear differences were found between the two groups of models. Due to uncertainty caused by the differences between model results, Haddeland et al. (2011) recommend using multiple models instead of a single model realisation when studying climate change impacts. However, it has not yet been determined whether multi-model analyses provide suitable data for the analysis of global hydrological extremes, such as drought.

Sheffield et al. (2009) used a single large-scale model, VIC, to simulate soil moisture globally. From simulated series, they calculated soil moisture drought characteristics and investigated the spatial extent of soil moisture drought events over the globe. Andreadis et al. (2005) also employed the VIC model to simulate time series of soil moisture and runoff and studied associated drought over the continental US, which was extended to a multi-model analysis by Wang et al. (2009). Wang et al. (2011) examined large-scale soil moisture drought events and trends for China using a similar set of models. In a global study, Corzo Perez et al. (2011) investigated results of hydrological drought approaches with the global hydrological model WaterGAP. A spatio-temporal characterisation of global hydrological drought (e.g., runoff, streamflow), however, from a multi-model ensemble is lacking.

Multi-model studies have been carried out for Europe by Prudhomme et al. (2011), Gudmundsson et al. (2012a), Gudmundsson et al. (2012b), and Stahl et al. (2012). Prudhomme et al. (2011) assessed the ability of three, global, gridded hydrological models to simulate large-scale high and low flow events in a comparison with catalogues of historical drought events and high flows derived from discharge observations across Europe. According to Prudhomme et al. (2011) there was a reasonable similarity between observed and simulated drought whilst it was recommended that differences between the various model outputs and observations should be taken into account in

further studies. They also concluded that “model behaviour and the ability to reproduce hydrological processes may be very different in different climate regimes”. Gudmundsson et al. (2012a) and Gudmundsson et al. (2012b) compared an ensemble of nine large-scale hydrological models to observed discharge for small catchments in Europe to quantify the uncertainty in model simulations. One of their main conclusions was that, despite the large spread in model performance, “the ensemble mean is a pragmatic and reliable estimator of spatially-aggregated time series of annual low, mean and high flows across Europe” (Gudmundsson et al., 2012a). The main objective of Stahl et al. (2012) was to assess the accuracy of a multi-model ensemble of eight large-scale models by comparing modelled trends against trends in observed streamflow in Europe. Results showed that individual models disagreed regarding magnitudes and even trend direction in several areas (Stahl et al., 2012). They also found that variability in the simulated trends was high and encouraged multi-model approaches and similar studies for other continents.

Another issue concerning the analysis of hydrological drought at a global scale is the lack of reliable, observed data to test model results (see also Chapter 3). At the global scale, validation against hydrological observations (river flow) is difficult, because: (i) only a limited number of measurements exist, (ii) observed river flow at gauging stations cannot be compared directly to gridded runoff (i.e., natural large basins and a routing approach needed). Instead, this chapter looks for agreement between members of an ensemble of models as an indication that results are plausible and compares drought in model results with meteorological drought to identify information added by the large-scale models, which is expected to occur because of the non-linear transformation of meteorological drought in the subsurface.

The aim of this chapter is to investigate whether large-scale models are able to reproduce hydrological drought (runoff), to identify the variability among models in different climate zones, and to analyse the differences between meteorological and hydrological drought. This was done by a global, multi-model analysis of drought based on monthly aggregated runoff data from ten different models, the ensemble median of these models and global precipitation data. Patterns and occurrence of drought characteristics corresponding to the ensemble median are investigated, while taking into account the variability among individual models. Differences between precipitation drought events and runoff drought events derived from the ensemble median are identified. This study aims to contribute to our knowledge on the potential of large-scale models to capture extreme hydrological drought events, both in space and in time.

4.2 Large-scale models

For the identification of hydrological drought, model results from 10 different large-scale models were used from the European project WATCH (Water and Global Change, www.eu-watch.org). The multi-model analysis in this chapter comprises the following models: GWAVA, H08, HTESSEL, JULES, LPJml, Mac-PDM, MATSIRO, MPI-HM, Orchidee and WaterGAP. Associated model references can be found in Haddeland et al. (2011) and Appendix A. All models were run at the same $0.5^\circ \times 0.5^\circ$ resolution with the same forcing data, the WATCH Forcing Data (WFD). More information about the WFD, set-up of the models and model structure can be found in Sect. 3.2, Appendix A and Haddeland et al. (2011).

As our study focused on hydrological drought at the global scale, we have used time series of natural total runoff (sum of surface runoff and subsurface runoff, i.e., all water discharged from a single grid cell). Time series of daily total runoff were aggregated to monthly total runoff time series that were used to analyse hydrological drought for the period 1963–2000 following 5 years of model spin up. Since this chapter does not intend to evaluate individual models, the ensemble median runoff, calculated from the monthly runoff time series of all models, was used for the drought analysis. Precipitation (rainfall and snowfall) data from the WFD were used for identification of meteorological drought.

4.3 Drought analysis

4.3.1 Temporal drought identification

To derive drought from time series of total runoff and precipitation for each grid cell, we follow the combined drought identification method, as presented by Van Huijgevoort et al. (2012). This method combines the characteristics of the threshold level method (TLM, Yevjevich, 1967; Hisdal et al., 2004) and the consecutive dry period method (CDPM, Vincent and Mekis, 2006; Groisman and Knight, 2008; Deni and Jemain, 2009). This combination led to a robust drought indicator for all climates (including regions with frequent periods of zero runoff). The method allows a drought in periods with runoff/precipitation to continue in a following period without runoff/precipitation. For detailed information the reader is referred to Van Huijgevoort et al. (2012) and Chapter 2.

The 20th percentile (Q_{20}) was used as the threshold in this study. The Q_{20} is defined as the value that is equaled or exceeded 80% of the time. This means anomalies are identified in each grid cell regardless of the magnitude of runoff/precipitation. The Q_{20} value was selected in order to be consistent with other global and large-scale studies (e.g. Corzo Perez et al., 2011; Sheffield et al., 2009; Andreadis et al., 2005). Since this is a rather high threshold value, less extreme events are also identified compared to, for example, a threshold of Q_5 .

Meteorological drought events have been identified from the monthly precipitation data (1-month data) and for time series with a backward moving average of a different number of months (3, 6 and 9 month data). From the hydrological drought analysis, drought characteristics, such as the number of drought events and their average duration, were derived for each model and the ensemble median at the grid cell scale. Since the focus of this chapter is not to compare individual models, but to assess the potential of using a model ensemble for drought analysis, we use the following relative measure of variability between the model results, the inter-model spread:

$$\text{spread} = (C_{85} - C_{15})/C_{50} \quad (4.1)$$

where C are the values of a certain drought characteristic from all models for a grid cell. By taking the 85th and 15th percentiles, the most extreme values in each grid cell (i.e., two most extreme models) were omitted. The spread was calculated for each identified drought characteristic for each grid cell. The spread does not include the absolute values of the runoff and hence a complementary diagnostic is required to analyse impacts on local water resources directly. The drought characteristics and spread were visualised in a bivariate colour map with the methodology introduced by Teuling et al. (2011), which enables plotting of two variables on the same map using a two-dimensional colour scale.

In addition to mapping global drought characteristics, time series of area in drought for certain regions were also examined. The regions, which are defined by Giorgi and Francisco (2000) and adapted by Sheffield and Wood (2007), were used to explore model results in more detail at a regional scale (Fig. 3.1). An overview with full names of the regions and abbreviations is given in Table 3.1. The abbreviations will be used in the next sections. For these time series of the area in drought the model variability is shown by the model range. The model range was calculated from all individual model results by excluding the models with the minimum and maximum percentages of area in drought for each region at each time step. Synchronicity in drought between these regions was evaluated with a hierarchical cluster analysis by complete linkage based on the Euclidean distance matrix for time series of the percentages of area in drought derived from the model ensemble median (Hastie et al., 2001). To emphasize the larger drought events in the cluster analysis, percentages below 20% were set to zero in the time series used for the cluster analysis.

4.3.2 Spatial drought identification

Simulated drought events generally encompass large regions. Therefore, a method is needed that is able to allocate individual half-degree grid cells to a given drought cluster. Andreadis et al. (2005) applied a recursion-based approach to link neighbouring cells, which are identified to be in drought, into a cluster. Even though this method is easy to implement, recursion-based approaches are generally computationally inefficient and time-consuming. A more efficient approach to connect individual cells that experience hydrological drought into a cluster of cells, is to apply a component labeling algorithm (Rosenfeld, 1970; Suzuki et al., 2003; Chang et al., 2004). In this chapter, we used a contour tracing technique (Chang et al., 2004; Wagenknecht, 2007) to identify the outer boundaries of a given cluster. Next, cells belonging to the inner regions of a drought cluster are found by applying a connected component labelling approach (Suzuki et al., 2003; He et al., 2009; Wu et al., 2009). The combination of these two techniques results in a double-pass segmentation algorithm, which is generally assumed to be computationally efficient (He et al., 2009).

To focus only on major spatial drought events, an areal threshold was implemented (Andreadis et al., 2005; Tallaksen et al., 2009; Sheffield et al., 2009). The areal threshold for a spatial cluster was set to 25 grid cells (approximately 77 275 km² around 0° latitude, 62 500 km² around 36° latitude and 26 100 km² around 70° latitude).

4.4 Results

4.4.1 Global drought characteristics

For each grid cell, drought characteristics (total number of drought events and average drought duration) have been derived from the runoff time series over the period 1963–2000. In Fig. 4.1 the mean runoff and values of the drought characteristics from the ensemble median and spread (Eq. 4.1) are illustrated. Regions with the highest spread in mean runoff were the very dry regions (e.g., Sahara) and Greenland (Fig. 4.1a). The smallest spread occurred in tropical regions (e.g., Amazon, southeast Asia), which had high mean runoff values. In most parts of Europe, northern Asia and the eastern US, the spread was small as well. Since most models do not include a glacier scheme (Haddeland et al., 2011), the results for Greenland were excluded from further analysis.

Even though considerable differences in runoff values existed (Fig. 4.1a), the overall patterns of the various drought characteristics were consistent among the models. The largest spread between models in the number of drought events (Fig. 4.1b) occurred in the (very) dry regions (e.g., Sahara) of the globe. In other regions, the spread was relatively small. For example, all models agreed on a relatively large number of drought events in regions with high runoff (e.g., Amazon), because in these areas runoff exhibits a large variability and therefore often crosses the threshold. Areas with low runoff generally tend to have a smaller number of drought events (e.g., areas adjacent to the Sahara). Striking is the large number of drought events in vast parts of Australia, which was not expected, since runoff was low in these areas as well. This may be caused by the fast reaction of runoff to precipitation in most models in this region. Australia received rainfall, albeit small amounts, more regularly compared to other dry areas, for example the Sahara and surroundings. These small rainfall amounts led to runoff due to the fast reaction and thus ended hydrological drought events immediately, which decreased drought duration and increased the number of drought events. The same process occurred in other semi-arid regions, for example, areas in southwestern US.

The employed definition of drought (Sect. 4.3.1) implies a negative correlation between the number of drought events and their average duration. This leads to short durations in areas with large runoff variability, and long durations when only a few drought events occur (Fig. 4.1c). Due to this negative correlation, the pattern in the model spread of the average drought duration was similar to the pattern in spread for the number of drought events.

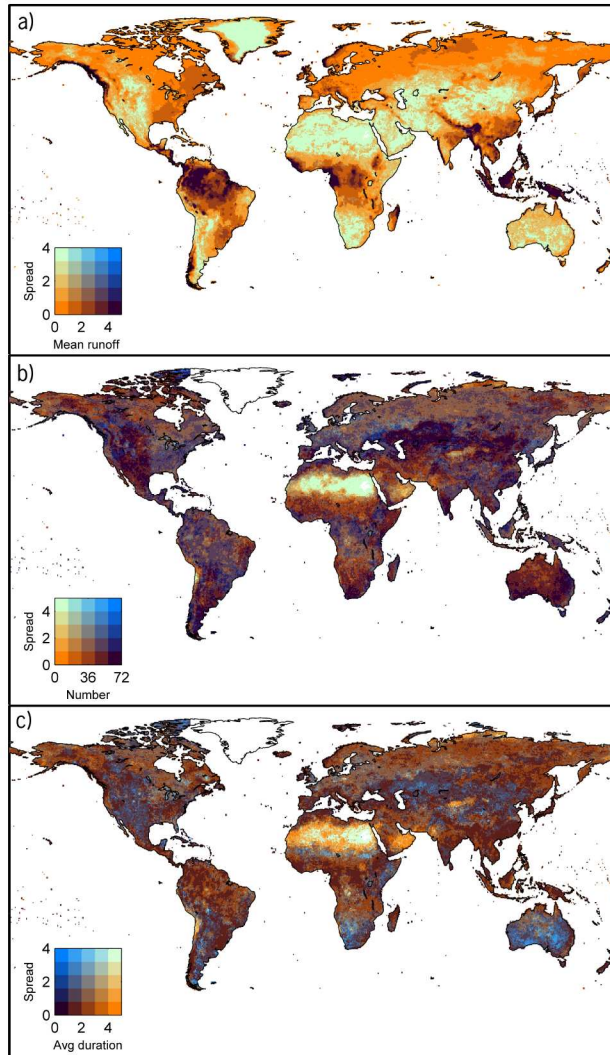


Figure 4.1: Drought characteristics and fractional spread in model results (Eq. 4.1) for each grid cell: a) mean runoff (mm day^{-1}), b) number of drought events, c) average duration (months).

4.4.2 Temporal development of drought

Relation between meteorological and runoff drought

In the rest of the chapter, the Sahara region, in addition to Greenland, was not considered because there the models showed large differences and the drought analysis was very difficult, even with the combined method, due to small runoff during the entire period (average annual runoff values of less than 1 mm per year). Within each of the remaining regions (Table 3.1), the percentage area in drought for each month (Fig. 4.2) was calculated from the models, from the ensemble median and the precipitation data (3-month data). For each month, the model range was determined by excluding the models with the minimum and maximum percentages. The models showed rather

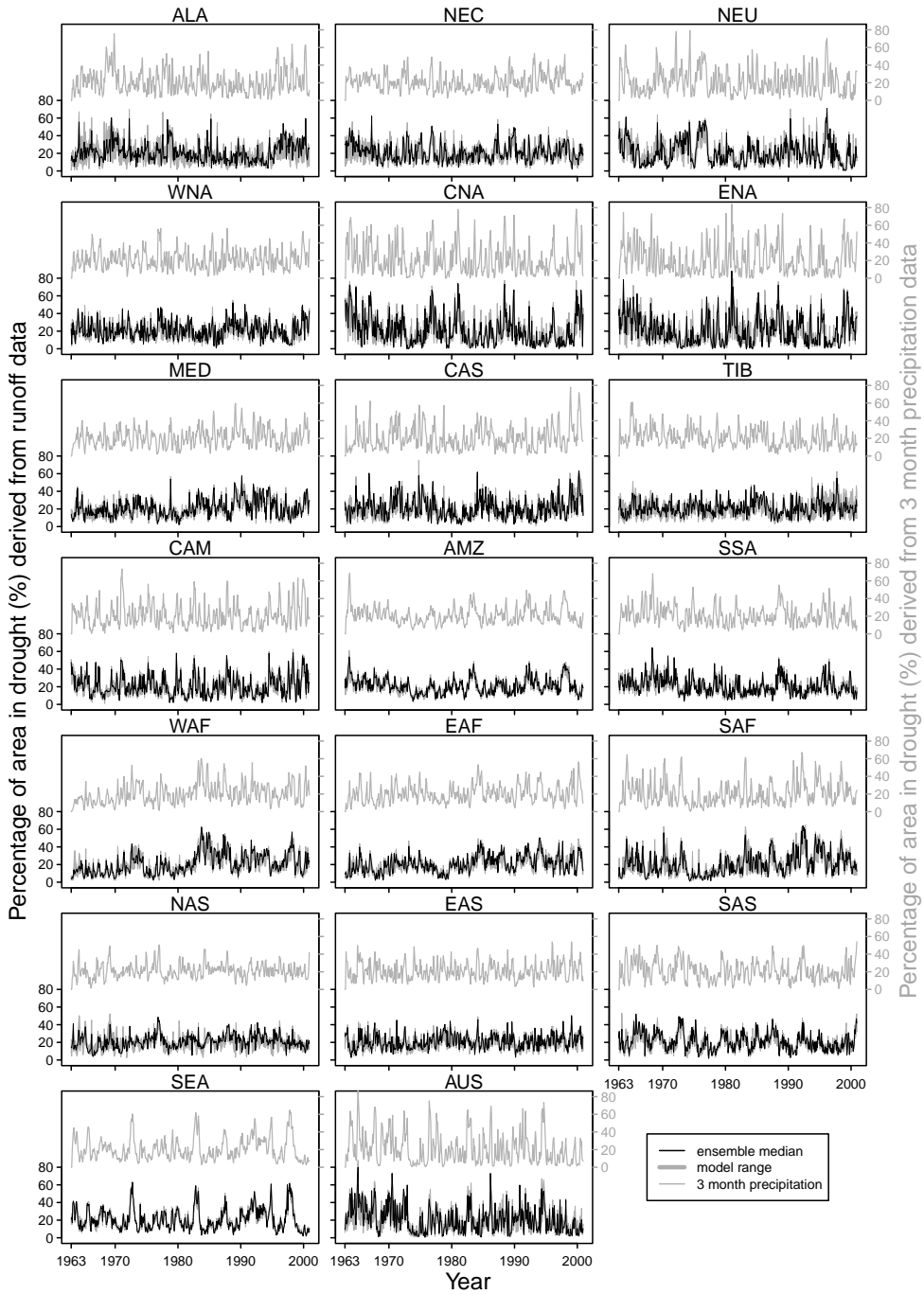


Figure 4.2: Fraction in drought for each region derived from precipitation (3-month data), from runoff for the ensemble median and the range of the models.

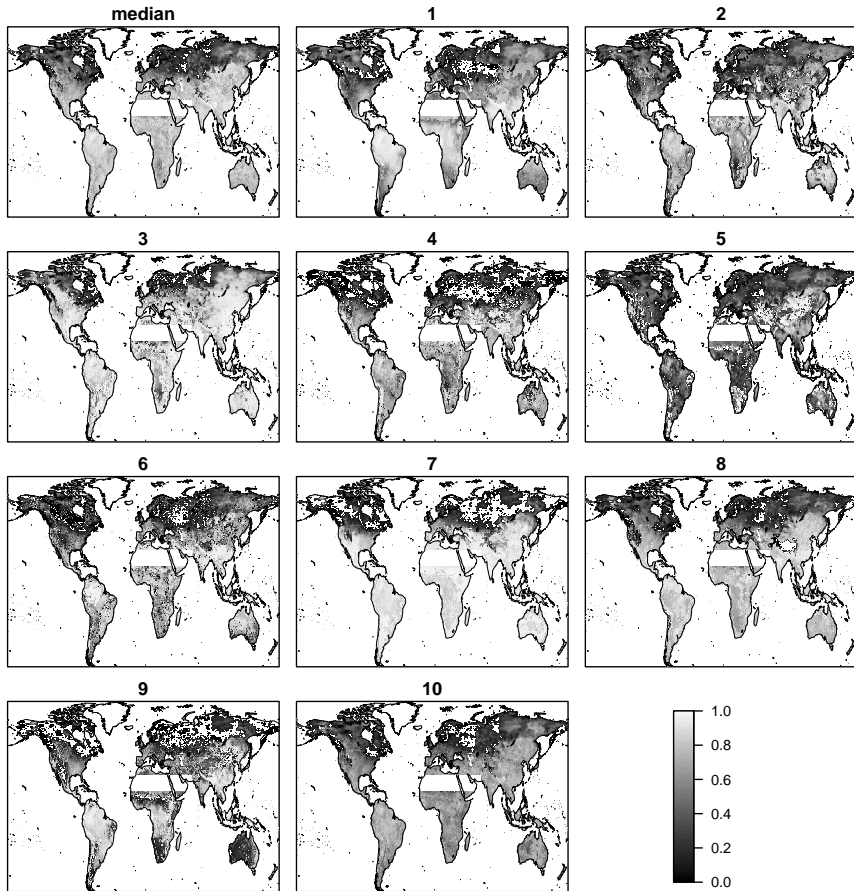


Figure 4.3: Correlation between runoff and precipitation (1-month data) in each grid cell for the ensemble median and the individual models (1-10). Greenland and the Sahara region are excluded due to small runoff during the entire period in these areas. Only correlations significantly different from zero at the 95% level using a standard two-sided test are shown and negative significant correlation values, in this case caused by a continuous snow cover of several months, have been set to zero.

small differences in many regions, i.e., a small range. Exceptions were the regions ALA, NEU, CNA, ENA, SAF, and AUS, for which the overall range between the models was largest. The differences in range across the regions were consistent with the patterns in spread of the drought characteristics and mean runoff (Sect. 4.4.1). Regions with a large runoff variability (e.g., SEA, and AMZ regions) had a small inter-model range in drought percentage. Drought events in these regions are very much controlled by the fast runoff response of almost all models to precipitation. The drought events in both precipitation and runoff occur almost simultaneously in these regions. This fast reaction of the models to precipitation is also shown in Fig. 4.3, which gives the correlation between monthly precipitation and total runoff time series in each grid cell for all models. Negative correlation values occurring in cold regions, caused by a continuous snow cover of several months, have been set to zero (Fig. 4.3). Some models reacted faster to precipitation in large parts of the world than others, especially in the southern hemisphere we found large differ-

ences. In general, correlations for all models were lowest in snow-dominated regions, as would be expected. The ensemble median showed relatively high correlations in the southern hemisphere, regions around the equator and southern Asia.

To analyse the differences between meteorological drought and runoff drought, correlations between the meteorological drought (time series of percentiles) and runoff drought in the ensemble median (time series of percentiles) were calculated for each grid cell as well (Fig. 4.4). The meteorological drought events were determined for precipitation aggregated over different periods of 1, 3, 6 and 9 months (Sect. 4.3.1). The correlations showed a clear spatial pattern across the globe, which was similar for the different aggregation periods. Regions with high runoff values showed high correlations, colder and drier regions gave low correlations. This indicates that the large-scale models add information to the signal derived from the precipitation and that runoff drought cannot directly be determined from precipitation data in global drought analyses when a constant aggregation period is used.

Synchronicity of drought events at the global scale

Since drought events often affect large areas, a single event can occur in several regions simultaneously (Sect. 3.4.4). Teleconnections may exist for multiple regions, for example, in regions influenced by the El Niño-Southern Oscillation (ENSO) phenomenon (Ropelewski and Halpert, 1987). ENSO has a large influence on the occurrence of drought at large scales in both precipitation (e.g. Ropelewski and Halpert, 1987) and streamflow (e.g. Chiew and McMahon, 2002). For the investigation of synchronicity of drought events across the different regions caused by large-scale climate drivers, two different measures were used. Firstly, a hierarchical cluster analysis was applied to identify similarities between the regions. Secondly, the correlations between the time series of the percentage of area in drought for all regions have been determined (Table 4.1). The median runoff results showed a larger synchronicity between regions influenced by the ENSO phenomenon and neighbouring areas, whereas for other regions no clear pattern was found. Neighbouring regions often showed higher correlations (Table 4.1): for example, the region CNA with WNA (0.33) and ENA (0.44), and the WAF region with EAF (0.50). The cluster analysis also showed similarities in several neighbouring regions, for example, regions in Africa, North America and Asia. However, there were some unexpected positions of regions in the tree resulting from the cluster analysis (Fig. 4.5), for example, the WNA, CAM and ALA regions. This could be caused by the choices made for the cluster analysis, like the 20% minimum for the percentage of area in drought per region or the use of Euclidean distance (Sect. 4.3.1). The relatively low correlations and similarities between the regions could also cause difficulties in determining homogeneous clusters.

Table 4.1: Correlation between the time series of percentage of area in drought from the ensemble median for the different regions

	ALA	NEC	NEU	WNA	CNA	ENA	MED	CAS	TIB	CAM	AMZ	SSA	WAF	EAF	SAF	NAS	EAS	SAS	SEA
NEC	0.05																		
NEU	0.03	0.15																	
WNA	0.03	0.11	0.04																
CNA	0.01	0.18	0.13	0.33															
ENA	0.01	0.06	-0.08	0.04	0.44														
MED	-0.15	0.01	-0.09	0.04	-0.15	-0.02													
CAS	0.10	-0.11	-0.01	0.02	0.03	0.06	0.02												
TIB	0.05	-0.14	-0.08	-0.16	-0.15	0.04	-0.10	0.29											
CAM	0.05	-0.08	0.03	0.11	0.13	-0.12	-0.12	0.14	0.03										
AMZ	-0.01	0.16	0.00	-0.14	0.00	0.10	-0.12	-0.22	-0.09	-0.02									
SSA	0.06	0.09	0.02	0.09	0.13	0.03	-0.02	0.00	-0.06	-0.02	-0.13								
WAF	-0.16	-0.02	-0.09	-0.11	-0.33	-0.11	0.24	0.04	0.09	-0.07	0.12	-0.32							
EAF	-0.11	-0.07	-0.07	-0.03	-0.19	0.00	0.24	0.22	0.15	0.08	-0.10	-0.21	0.50						
SAF	-0.06	0.05	-0.08	0.01	-0.15	0.02	0.17	-0.06	-0.05	-0.09	0.27	-0.16	0.26	0.17					
NAS	-0.16	0.12	0.25	0.14	-0.04	-0.01	-0.02	-0.07	0.00	0.03	-0.05	-0.05	0.12	0.17	0.03				
EAS	0.10	-0.06	-0.08	-0.05	0.01	0.01	-0.21	0.03	0.20	0.02	-0.10	-0.06	-0.08	-0.02	-0.13	-0.01			
SAS	-0.05	0.03	-0.10	-0.09	-0.08	0.08	-0.15	-0.02	0.02	0.06	0.10	-0.10	-0.02	0.03	0.08	0.06	0.04		
SEA	-0.16	0.08	-0.04	-0.19	-0.15	-0.08	-0.07	-0.27	0.05	0.00	0.41	-0.24	0.16	-0.08	0.13	0.05	0.01	0.23	
AUS	-0.01	0.06	0.06	-0.04	0.07	0.05	-0.11	-0.09	-0.06	0.00	0.21	0.03	-0.10	-0.10	0.06	-0.04	-0.10	0.12	0.23

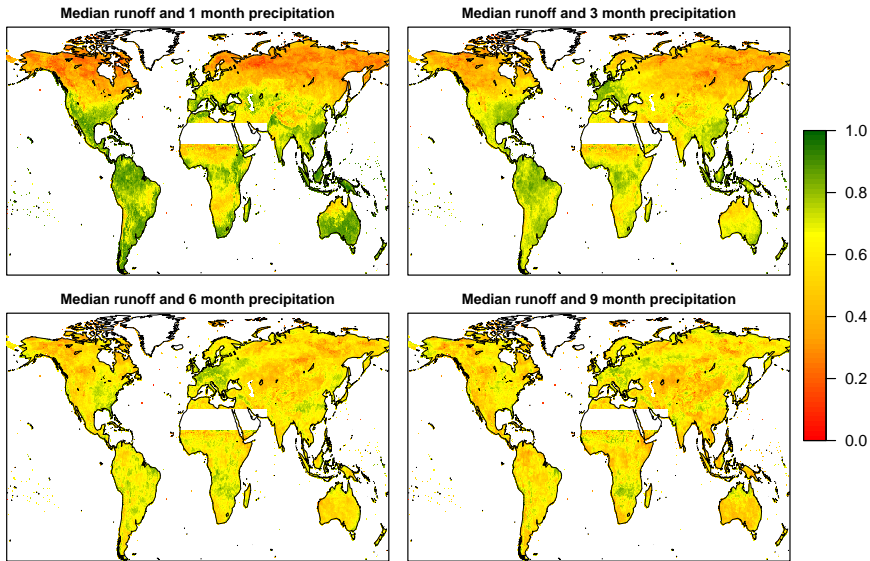


Figure 4.4: Correspondence between meteorological drought and runoff drought expressed as the correlation between percentiles determined from the modelled ensemble median runoff and percentiles derived from precipitation data with different aggregation periods (1, 3, 6 and 9 months) in each grid cell. Only correlations significantly different from zero at the 95% level using a standard two-sided test are shown. Greenland and the Sahara region are excluded due to small runoff during the entire period in these areas.

Drought events linked to ENSO were most clearly identified in strong El Niño years (the warm phase of ENSO): 1966, 1972, 1983, 1992, 1998 (e.g. Smith and Sardeshmukh, 2000; Wolter and Timlin, 2011; NCEP, 2012). In these years, the regions mainly affected were AUS, SEA, AMZ, SAS and SAF (Sect. 3.4.4 and Fig. 4.2), which is consistent with the regions influenced by ENSO as identified by Vicente-Serrano et al. (2011). These regions showed relatively high correlations in the percentage of area in drought (Table 4.1), for example SEA with AMZ region (0.41). Drought events in these El Niño years were caused by lack of precipitation and strongly linked to the timing of the meteorological drought (Fig. 4.2). The same regions, except SAF, also showed similarities in the cluster analysis (Fig. 4.5). Regions affected by La Niña, southern USA and northern Mexico (CNA and WNA region), southern Russia and eastern Europe (NAS, NEU and CAS regions) and parts of the SSA region, often showed negative correlations with the regions affected by El Niño (Table 4.1), as was expected, e.g., SSA with SEA (-0.24). Overall, the connection between drought events and La Niña, and synchronicity between the regions, were not as strong as for El Niño. This can be explained by the relatively small size of the areas that are affected by La Niña, as compared to the size of the regions used in this study (Fig. 3.1).

4.4.3 Spatio-temporal development of two major historical drought events

Two examples of severe drought events have been selected to analyse the spatio-temporal evolution of drought in runoff and precipitation, namely, the mid 1980s drought in Africa and the 1976 drought in Europe. The spatial extent was investigated at the continental scale, since these drought events were observed across different regions in Africa and Europe (Sect. 4.4.2).

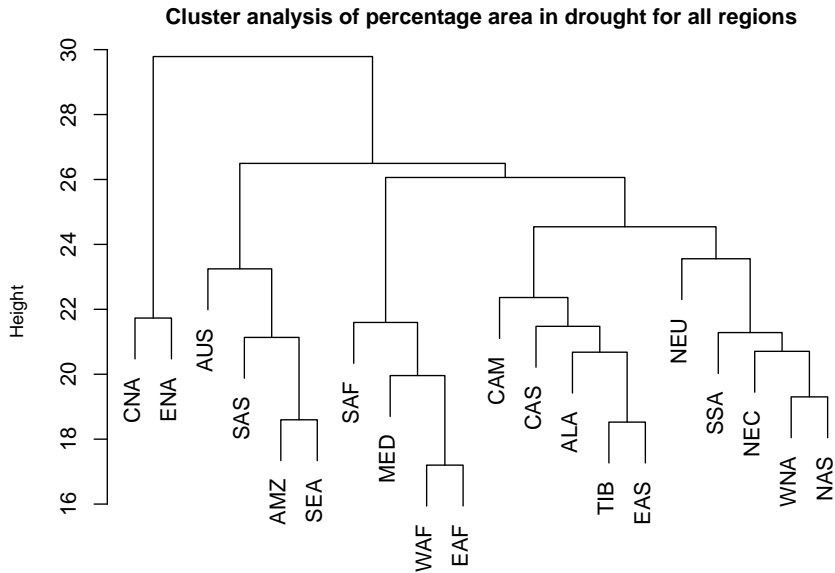


Figure 4.5: Hierarchical cluster analysis by complete linkage of time series percentages area in drought (minimum area taken as 20%) derived from the modelled ensemble median runoff, using Euclidean distance matrix, for all regions across the globe. Height is a measure of the dissimilarity between the time series based on the Euclidean distance and is expressed as percentage of area in drought per time step.

1980s drought event in the Sahel

Figure 4.6a-d show the spatial distributions of the drought in Africa for three different months, derived from the precipitation data (1-month and 3-month data), from the runoff of each model and from the ensemble median. The precipitation deficit causing the drought event was clearly identified in the precipitation data both for the monthly (Fig. 4.6a) and 3 monthly data (Fig. 4.6b), although the spatial extent differed. The spatial extent of the runoff drought event identified by the ensemble median (Fig. 4.6d) largely resembled the extents found in the precipitation, but disparities were found that indicated the difference between meteorological and hydrological drought caused by the models. All models identified drought somewhere in Africa for all three months, however, the spatial extent differed considerably between models (Fig. 4.6c). The area where at least one model predicted drought (61.1% of total area for October 1983) was much larger than the area for which all models agreed (6.1% of total area), demonstrating the difficulty of drawing any specific conclusion based on a single global model only (Fig. 4.6c). In this chapter, the maximum area in drought for all of Africa during this drought event was found at the end of 1983 and again in August 1984. According to Sheffield et al. (2009), this event spread over Africa and reached its maximum extent earlier, namely in April 1983. Although this timing is different, the spatial extents of the drought over Africa in April 1983 and August 1984 found in the ensemble median were similar to the extents indicated by Sheffield et al. (2009). Differences could be caused by the use of a different drought identification method, which mainly affects dry areas, the use of multiple models instead of a single model, or identification of drought in different variables (runoff vs. soil moisture).

The temporal distribution for the years 1981–1986 of the percentage of area in drought for the WAF region determined from precipitation (1-month and 3-month data), the ensemble median and the individual models is given in Fig. 4.6e-f. These time series show the difference between drought in runoff and in precipitation regarding the timing and extent of the event (Fig. 4.6f). The drought identified in 1-month precipitation data was less extreme and shorter than the drought in 3-month precipitation data. The ensemble median identified drought events more linked to the 3-month precipitation data, indicating the memory and storage included in the models. Even though the models generally showed a fast reaction to precipitation in this region (Fig. 4.3), a lag and lengthening of the drought event occurred in the propagation to a runoff drought, which indicates that the models add information that cannot be derived from aggregated precipitation deficits. The individual model results showed a variability in the length of the drought event, related to the different model structures determining the response time (Fig. 4.6e).

1976 drought event in Europe

The 1976 drought event in Europe (Fig. 4.7) is illustrated in a similar way as the event in Africa. The spatial distributions of the drought are given in Fig. 4.7a-d for three different months, derived from the precipitation data (1-month and 3-month data), from the runoff of each model and from the ensemble median. The temporal distribution of the percentage of area in drought for the NEU region for the years 1974–1977 is shown in Fig. 4.7e-f. The meteorological drought determined from monthly precipitation data (Fig. 4.7a) differed substantially in spatial extent with the drought determined from the 3-month data (Fig. 4.7b). The latter covered a much larger area of northern Europe in July 1976. The spatial extent of the runoff drought identified with the ensemble median (Fig. 4.7d) was more in line with the 3-month data, pointing out that the models have a memory of several months when translating the meteorological drought into a hydrological drought. Time series of the percentage of drought for the NEU region also show this difference between the drought in precipitation and runoff (Fig. 4.7e-f). A lengthening of the precipitation event was seen in 1976. The extreme meteorological drought event identified in 1974 was not as extreme in terms of the runoff values (80% of the area in drought for precipitation and 57% of the area in drought regarding runoff from ensemble median). This is also an indication that models reacted more slowly to precipitation in this region than in other regions.

All models started with a drought in Russia and western Europe, which moved to northwestern Europe and ended towards the end of 1976. The spatial extent of the drought event differed substantially among models in all months (in extreme cases the area in drought varied with 30% in the beginning of 1976, Fig. 4.7e), which also implied that the drought duration produced by each model will differ. Some models interrupted the drought event with lower percentages of area in drought, while others showed a longer continuous event with high percentages (Fig. 4.7e). Compared to the literature (e.g. Zaidman and Rees, 2000; Zaidman et al., 2002; Stahl, 2001), the expectation was that all models would give a large area in drought in July 1976. The results presented here, however, show that only for a limited area in Europe all models agreed on July being in drought (5.8% of the total area), although the area in drought for one or more models was much larger (56.5% of the total area had value 1 or larger for July 1976, Fig. 4.7c). In addition, not all models gave the same end date of the drought event (drought recovery). Overall, the median of the models gave qualitatively the same development of the drought event as results of hydrological drought analysis presented in the literature (Zaidman and Rees, 2000).

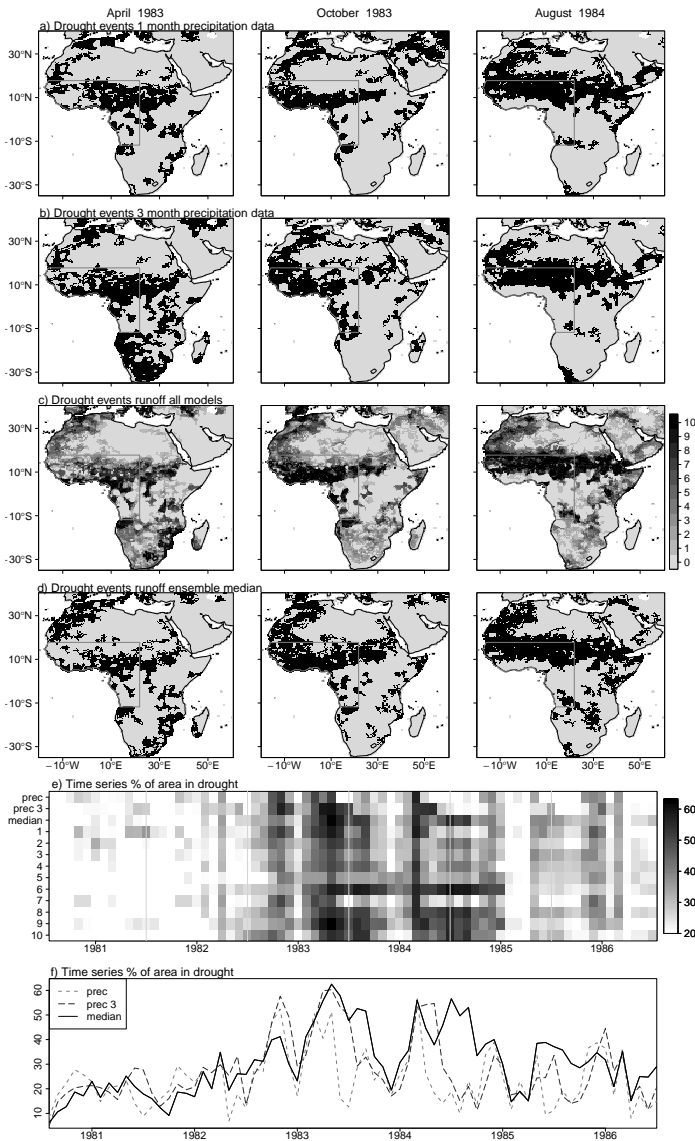


Figure 4.6: Spatial distribution of the historical drought event in Africa for April 1983 (left), October 1983 (middle) and August 1984 (right), a) Spatial extent of drought for 1-month precipitation data, b) Spatial extent of drought for 3-month precipitation data, c) Distribution of drought in runoff for all models (10 means all models identify drought, 0 means none of the models identifies drought), d) Spatial extent of drought for ensemble median, e) Temporal development for meteorological drought based on 1-month and 3-month data and runoff drought based on ensemble median and individual models (1–10) given as percentage of area in drought for Western Africa (WAF) region (indicated with grey box in a–d), and f) Percentage of area in drought for meteorological drought based on 1-month (prec) and 3-month (prec 3) data and runoff drought based on ensemble median for WAF region.

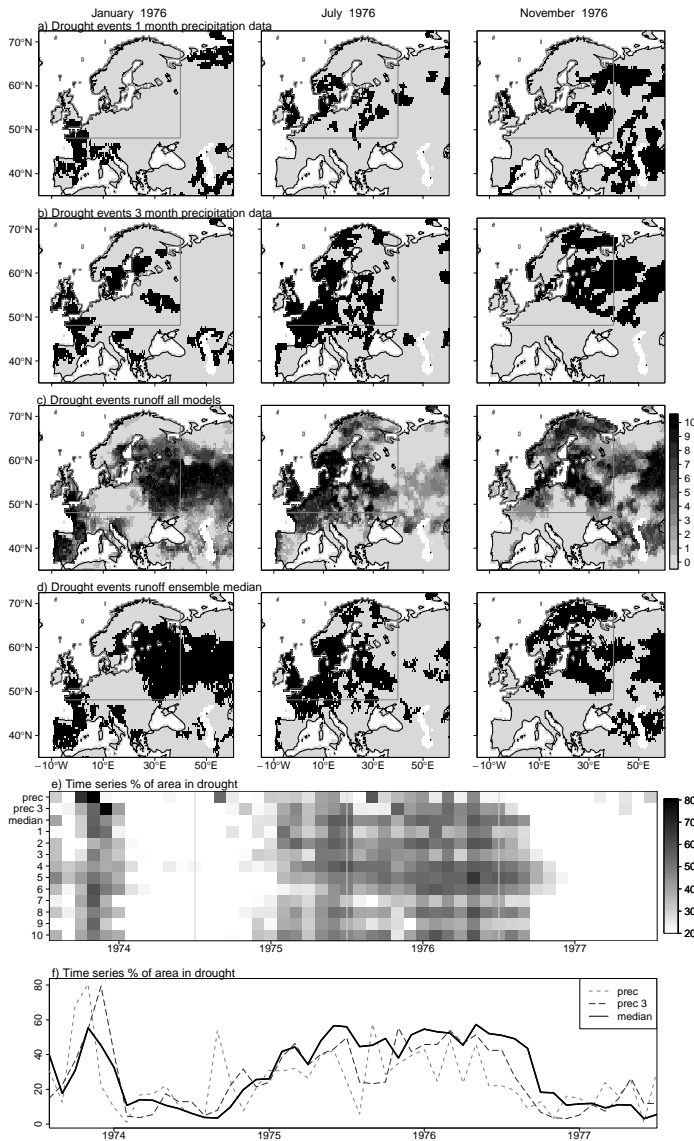


Figure 4.7: Identical to Fig. 4.6, but for the historical drought event in Europe for January 1976 (left), July 1976 (middle) and November 1976 (right) and the Northern Europe region (NEU, indicated with grey box in a–d).

4.5 Discussion

In this chapter, we have used a multi-model ensemble to assess whether large-scale models are suitable for drought analysis. A large variability in model results was found, which means the identified drought events can be very different for individual models. The reason for this variability is difficult to determine, since the many different model structures and parameter values for individual cells make it very difficult to understand the differences between models (e.g. Gud-

mundsson et al., 2012b). Therefore, the focus in this chapter was not on the individual models, but instead on the ensemble median and variability. The use of multiple models has been quite common in climate studies, however, for impacts studies often only one single hydrological model has been used. With the importance of using multiple impacts models now increasingly being appreciated, the latest climate change impacts projects, for example, the ISI-MIP project (www.isi-mip.org), will employ multiple hydrological models.

To reduce the uncertainties between models, performance of the models across a range of output variables, such as evaporation, soil moisture storage, groundwater storage, and their covariance, could be investigated. Suitability of different models for different regions in the world could be determined with this kind of analysis, which was beyond the scope of this study. By including additional variables, propagation of drought could be studied in more detail and processes not represented in the models could be identified. Van Loon et al. (2012) have performed such an analysis for several individual grid cells with contrasting climate and concluded that storage and evaporation processes could be improved in the models. Until a perfect model exists for analysis across the globe with among others ideal stores and parameters included, the use of multiple models is recommended to account for a range of uncertainty.

The largest spread between the models was found in the dry regions of the world. This is consistent with the results of Haddeland et al. (2011), showing a relatively large spread of simulated runoff in arid and semi-arid regions. This can partly be explained by the use of different evapotranspiration and infiltration methods in the models. Since runoff is low in these regions, small differences in evaporation lead to relatively large differences in runoff (Haddeland et al., 2011). Most large-scale models overestimate the runoff in dry regions due to several processes not being included in these models, e.g., the transmission loss along the river channel or infiltration and evaporation of surface runoff (Gosling and Arnell, 2011; Haddeland et al., 2011).

With respect to the temporal development of drought, relatively large differences among the models were also observed in cold regions (e.g., ALA and TIB). Other studies, focusing specifically on Europe, have found that model performance in simulating the observed hydrological response is lower in regions with snow influence than in regions without snow (Stahl et al., 2012; Gudmundsson et al., 2012b). This can be explained by the different implementations of snow processes, such as accumulation, sublimation and melt, and differences in the partitioning of precipitation into rainfall and snowfall between the models (Haddeland et al., 2011).

In general, we found that the ensemble median is capable of identifying the major drought events. Because all models have the same forcing data and major drought events are climate-driven, all models capture the occurrence of these events. This suggests that large-scale models could be used for the simulation of major drought events, as previously concluded by Prudhomme et al. (2011), who compared three different large-scale models for Europe and found these models are able to some extent to simulate low runoff anomalies. However, this study shows that the duration and spatial extent of simulated drought events are less consistent. These drought characteristics depend on catchment characteristics, such as hydrogeology (Tallaksen and Van Lanen, 2004). Some models showed a very fast runoff response to precipitation, implying that simulation of storage-related processes is limited. This lead to deviations in drought events in parts of the world, where stores (e.g., groundwater, lakes) play an important role in drought propagation (Van Loon and Van Lanen, 2012). These results are consistent with the conclusions of Wang et al. (2009), Stahl et al. (2012) and Gudmundsson et al. (2012a). Stahl et al. (2012) noted for areas with groundwater-dominated systems that the nature and magnitude of such complex storages cannot be replicated by the simplified storage schemes used in the current generation of large-scale models. This relatively fast reaction in runoff also explains the lack of multi-year drought events, since generally hydrological drought ended too soon (e.g. Van Loon et al., 2012).

Even though in this study we made a first step to determine the suitability of large-scale models for hydrological drought analysis, validation of the model output remains difficult due to the lack of observations and the limited number of independent drought studies at a global scale for runoff

or streamflow. Global observations of river flow cannot be directly compared with gridded runoff values of the models, because this would require a proper routing procedure and, because of the scale of the models, relatively large river basins (e.g. Haddeland et al., 2011), which are often affected by dams and abstractions.

4.6 Conclusions

One of the main objectives of this chapter was to investigate whether large-scale models are able to reproduce the spatio-temporal development of hydrological drought at the global and continental scale. In this chapter, variability (spread and range) between ten different large-scale models, their ensemble median of runoff as well as precipitation data were used for drought analysis. For all models, a set of general runoff drought characteristics, e.g., number and duration per cell, was derived. As expected, all models yielded many short drought events in areas with high runoff and few long drought events in areas with low runoff values. The largest spread was found in very dry areas and very cold areas, and the smallest spread in areas with high runoff. The differences between the models were caused by the different model structures and parameterizations. Therefore conclusions on global drought occurrence based on single models vary strongly depending on the model used.

Time series of percentage of area in drought for selected regions across the world lead to a similar conclusion, with a large range in model outcomes in cold and dry areas and a small range in high runoff areas. However, simulated drought durations differed substantially between the models. The models showed limitations in identification of multi-year drought events. Due to imperfect simulation of storage-related processes in some models, the runoff reacted very fast to precipitation and long-term memory effects were lacking in some regions. However, by using a multi-model ensemble, the impact of this problem was alleviated, since some of the models do have larger groundwater storages. The correlation between meteorological drought events and runoff drought events derived from the ensemble median showed a distinct spatial pattern across the globe for several aggregation periods of precipitation. This indicates that at a global scale runoff drought cannot be determined from precipitation data alone using a constant aggregation period. Given the uncertainty caused by the variability among the models, the results presented here clearly encourage the use of multiple global hydrological models instead of one single model.

Overall, when focusing on major drought events, a multi-model ensemble gives new insight into the development of drought in space and time at global and continental scales. Further improvement of large-scale models is possible and will lead to improved ability to simulate hydrological drought events.



Changes in hydrological drought characteristics towards the future

Abstract

Drought severity and related socio-economic impacts are expected to increase due to climate change. To better adapt to these impacts, more knowledge on changes in future hydrological drought characteristics (e.g., frequency, duration) is needed rather than only knowledge on changes in meteorological or soil moisture drought characteristics. In this chapter, effects of climate change on drought events in several river basins across the globe were investigated. Down-scaled and bias-corrected data from three General Circulation Models (GCMs) for the SRES A2 emission scenario were used as forcing for large-scale models. Results from five large-scale hydrological models (GHMs) run within the EU-WATCH project were used to identify low flows and hydrological drought characteristics in the control period (1971–2000) and the future period (2071–2100). Low flows were defined by the monthly 20th percentile from discharge (Q_{20}). The variable threshold level method was applied to determine hydrological drought characteristics. The climatology of normalized Q_{20} from model results for the control period was compared with the climatology of normalized Q_{20} from observed discharge of the Global Runoff Data Centre. An observation-constrained selection of model combinations (GHM and GCM) was made based on this comparison. Prior to the assessment of future change, the selected model combinations were evaluated against observations in the period 2001–2010 for a number of river basins. The majority of the combinations (82%) that performed sufficiently in the control period, also performed sufficiently in the period 2001–2010. With the selected model combinations, future changes in drought for each river basin were identified. In cold climates, model combinations projected a regime shift and increase in low flows between the control period and future period. Arid climates were found to become even drier in the future by all model combinations. Agreement between the combinations on future low flows was low in humid climates. Changes in hydrological drought characteristics relative to the control period did not correspond to changes in low flows in all river basins. In most basins (around 65%), drought duration and deficit were projected to increase by the majority of the selected model combinations, while a decrease in low flows was projected in less basins (around 51%). Even if low discharge (monthly Q_{20}) was not projected to decrease for each month, drought events became more severe, for example in some basins in cold climates. This is partly caused by the use of the threshold of the control period to determine drought events in the future, which led to unintended drought events in terms of expected impacts. It is important to consider both low discharge and hydrological drought characteristics to anticipate on changes in drought for implementation of correct adaptation measures to safeguard future water resources.

Adapted from Van Huijgevoort, M.H.J., H.A.J. van Lanen, A.J. Teuling, R. Uijlenhoet, 2014: Identification of changes in hydrological drought characteristics from a multi-GCM driven ensemble constrained by observed discharge. *Journal of Hydrology*, 512, 421–434, doi:10.1016/j.jhydrol.2014.02.060

5.1 Introduction

Drought events and their related impacts on society and environment are expected to increase in severity due to changing climate (e.g. Bates et al., 2008; Dai, 2011; Romm, 2011). Drought occurs across the world in all climatic regions and is still difficult to quantify (Wilhite, 2000; Tallaksen and Van Lanen, 2004; Mishra and Singh, 2010). Drought remains one of the natural hazards for which predictions are most uncertain. Many studies have investigated the effect of climate change on discharge regimes (e.g. Arnell, 1999b; Nijssen et al., 2001a; Manabe et al., 2004; Milly et al., 2005; Nohara et al., 2006; Sperna Weiland et al., 2012). Besides investigating changes in the regime, low flows are included in some studies as well (e.g. Arnell and Gosling, 2013). The main conclusions about the expected changes are in agreement. For example, the discharge is expected to increase in cold climates and a shift of the snow melt peak in these areas is projected (e.g. Sperna Weiland et al., 2012). In addition to the impact of climate change on discharge, effects on drought have been investigated. In the 21st century, drought may intensify in parts of Europe, central North America, Central America and Mexico, northeast Brazil and southern Africa (IPCC, 2012). Studies on drought in the future have mainly focused on soil moisture (e.g. Sheffield and Wood, 2008b; Vidal et al., 2012; Dai, 2013; Orlowsky and Seneviratne, 2013). A decrease in soil moisture was detected at the global scale by Sheffield and Wood (2008b), leading to more soil moisture drought events. Vidal et al. (2012) found that all characteristics of soil moisture or agricultural drought events in France increased in the 21st century. Severe drought conditions in the 21st century over large parts of the globe were determined with the PDSI by Dai (2013). A large range in soil moisture drought projections at a global scale was found by Orlowsky and Seneviratne (2013), but increased drought was consistent in several regions, namely the Mediterranean, South Africa and Central America/Mexico. Less is known about changes in hydrological drought events (drought in groundwater and surface water). Hirabayashi et al. (2008) have studied changes in number of drought days at the global scale by taking the annual drought days from discharge data. Significant increases in drought were found for many regions across the globe (Hirabayashi et al., 2008). For Europe, Feyen and Dankers (2009) investigated changes in streamflow drought by deriving low flows and drought deficits. They concluded that in many rivers, with the exception of rivers in the most northern and northeastern parts of Europe, minimum river flows and flow deficit volumes became more severe in the frost-free season. Most studies on changes in discharge are carried out at the catchment scale instead of the global scale. For example, Madadgar and Moradkhani (2013) used trivariate copulas to determine changes in drought characteristics for a specific catchment in Oregon. They concluded that drought events will become less severe in the future in this catchment. Knowledge on hydrological drought events is important for water resources and needed for adequate planning and assessment of drought impacts in the future. This knowledge across the globe is rather limited.

In recent years, more and more gridded models have been developed for hydrological studies at the global scale. However, many scenario studies employ only one global hydrological model (GHM) in combination with one or an ensemble of General Circulation Models (GCMs) that provide forcing data (e.g. Sperna Weiland et al., 2012; Arnell and Gosling, 2013). Because GHMs can show large differences in the representation of runoff for the previous century (Chapter 4), including multiple GHMs for future analysis is important (e.g. Gudmundsson et al., 2012b; Van Huijgevoort et al., 2013). This was also concluded by Hagemann et al. (2013), who used 8 GHMs and 3 GCMs to analyse water resources and found that spread in hydrological models in some regions is larger than that of climate models. They recommend that analyses of global climate change impacts should use results from multiple impact (hydrological) models.

To reduce or to better adapt to the impacts of hydrological drought across the globe, more knowledge regarding changes in hydrological drought characteristics (e.g., frequency, duration) in the future is needed in addition to already existing knowledge regarding changes in meteorological and soil moisture drought. In this chapter, effects of a climate change scenario on drought

in several river basins across the globe with contrasting climates and catchment characteristics were investigated using a multi-model analysis. The aim of this chapter is to investigate changes in both low flows and drought events, and to illustrate the challenges associated with this kind of drought analysis. Results of five GHMs forced with three GCMs have been used for the analysis over two periods, the control period (1971–2000) and future period (2071–2100). As a first step towards reducing the range of projected changes in drought, model combinations (GHM and GCM) have been constrained for analysis in the future period through comparison with observed discharge in the control period. Monthly low discharge values from selected model combinations for the control period and future period and changes therein have been determined. Changes in hydrological drought characteristics relative to the control period were identified from the selected model combinations using the variable threshold level method.

5.2 Data

5.2.1 Observed river discharge

From the Global Runoff Data Centre (GRDC, 2013) discharge data were available for selected river basins across the globe. The locations of the discharge gauges of these 41 selected (sub)basins are given in Fig. 5.1. Table 5.1 gives an overview with the names of the rivers, abbreviations, locations of gauging stations, periods of data used for comparison with large-scale models and the basin areas. The selection of the river basins was based on the following criteria:

1. The basins should be located in as many climate zones as possible (Fig. 5.1). Climate zones are based on the Köppen-Geiger classification (Peel et al., 2007) of the WATCH forcing data, see Wanders et al. (2010). The five major climate types are the equatorial (A), arid (B), warm temperature (C), snow (D), and polar climates (E).
2. The length of available discharge time series was important, because for drought analysis long time series are needed. Preferably time series were at least 30 years long and covered the control period (1971–2000, Sect. 5.2.2). However, to include all climate zones, ten river basins with shorter time series (less than 25 years) were also selected as a compromise. A subset of the selected river basins was used to evaluate the methodology for selecting model combinations (Sect. 5.3) in the period 2001–2010.
3. Basin area should include enough grid cells of the large-scale models to allow a comparison.
4. Since naturalised runs of the large-scale models were used, the basins should be as undisturbed as possible in terms of human influences, like dams.

The selection of the basins is somewhat biased to the northern colder climates, because more streamflow records were available there and reservoir storage is less important than in warmer, drier climates (Nijssen et al., 2001b).

5.2.2 Forcing data

In this chapter, we used model output from runs with three different GCMs for the SRES A2 scenario (Nakićenović and Swart, 2000). The A2 scenario was chosen to investigate the most extreme changes in drought events. The three GCMs, made available through the European WATCH project (Water and Global Change, www.eu-watch.org), were: ECHAM5/MPIOM of the Max Planck Institute for Meteorology (Jungclaus et al., 2006), CNRM-CM3 of the National Centre for Meteorological Research (Royer et al., 2002; Salas Mélia, 2002) and IPSL-CM4 of the Institute Pierre Simon Laplace (Hourdin et al., 2006; Fichetfet and Morales Maqueda, 1997; Goosse and Fichetfet, 1999). The three GCMs chosen within WATCH belong to different model families and partly cover the range from the CMIP3 ensemble in projected precipitation change (Masson and Knutti, 2011).

Table 5.1: Information about the selected river basins

River	Abbreviation	Longitude ^a	Latitude ^a	Period	Area (*10 ³ km ²)
Vaal ^b	VAA	24.60	-28.50	1971–2000	121
Zambezi	ZAM	23.25	-16.12	1971–2000	285
Sanaga	SANA	10.07	3.77	1971–1980	132
Sangha	SANG	16.05	1.62	1971–1983	158
Ubangi ^c	UBA	18.58	4.37	1971–2007	500
Ashburton	ASH	115.50	-22.54	1972–2000	71
Roper ^c	ROP	134.42	-14.70	1971–2010	47
Mitchell (N Au) ^c	MIT (N.AU)	142.38	-15.95	1972–2010	46
Burdekin ^c	BUR	147.24	-19.76	1971–2010	130
Barwon (Trib. Darling, Murray)	BAR	146.87	-29.95	1971–2000	298
Darling ^b	DAR	145.94	-30.09	1971–2000	386
Murrumbidgee	MUR	149.09	-36.16	1971–2000	1.9
Mitchell (Se Au) ^c	MIT (SE.AU)	147.37	-37.76	1971–2010	3.9
Irrawaddy	IRR	96.10	21.98	1978–1988	118
Mekong	MEK	105.80	15.12	1971–1993	545
Usumacinta	USU	-91.48	17.43	1971–2000	48
Içá	ICA	-69.52	-2.94	1973–1993	108
Jurua ^c	JUR	-66.85	-4.84	1972–2010	162
Madeira	MAD	-63.92	-8.75	1971–2000	976
Aripuana ^c	ARI	-60.65	-7.21	1974–2010	131
Amazon	AMA	-55.51	-1.92	1971–2000	4680
Araguaia	ARA	-49.26	-8.27	1971–2000	320
Rio Das Mortes ^b	MOR	-52.36	-14.67	1971–2000	25
Bermejo	BER	-64.22	-23.10	1971–1980	25
Chubut	CHU	-68.50	-43.85	1971–1994	16
Meuse ^c	MEU	5.72	50.87	1971–2010	21
Rhine ^{b,c}	RHI	6.11	51.84	1971–2010	161
Vistula (Wisla)	VIS	18.80	54.10	1971–1994	194
Yellowstone ^c	YEL	-104.16	47.68	1971–2010	179
Fraser ^c	FRA	-121.45	49.38	1971–2010	217
Hay ^c	HAY	-115.86	60.74	1971–2010	52
Liard ^c	LIA	-121.22	61.75	1972–2010	275
Yukon ^c	YUK	-141.20	64.79	1971–2010	294
Mackenzie ^c	MAC	-133.74	67.46	1972–2010	1660
Amur	AMUR	140.47	52.53	1971–1987	1790
Anadyr	ANA	169.00	65.08	1971–1988	47
Kolyma	KOL	153.67	67.37	1971–2000	361
Indigirka	IND	147.35	69.58	1971–1998	305
Lena	LENA	126.80	72.37	1971–2000	2460
Pechora	PEC	52.10	65.45	1971–1998	248
Severnaya Dvina (Northern Dvina)	SEV	41.92	64.15	1971–2000	348

a) Coordinates of gauging station.

b) River basins not included in the analysis of the future period, because none of the model combinations reached the criterion (Sect. 5.3).

c) River basins used to evaluate the selection criterion.

In an assessment of GCM skill in simulating persistence by Johnson et al. (2011), all three chosen GCMs were ranked among the best performing models for their skill in predicting global precipitation, sea surface temperature and surface pressure.

Bias-corrected forcing data were available from 1960 to 2100. We have taken the period 1971–2000 as the control period and 2071–2100 as the future period. A shorter period 2001–2010 was used to evaluate our methodology for selecting model combinations (Sect. 5.3) in a number of river basins (Table 5.1). All GCM output was downscaled to 0.5° and was bias corrected with the WATCH forcing data (Weedon et al., 2011) for rainfall, snowfall, and minimum, mean and maximum air temperature. The procedure for the statistical bias correction of GCM output is described by Piani et al. (2010), Chen et al. (2011), Haerter et al. (2011) and Hagemann et al. (2011). The WATCH forcing data consist of gridded time series of meteorological variables for 1958–2001 and originate from modification (bias-correction and downscaling) of the ECMWF ERA-40 re-

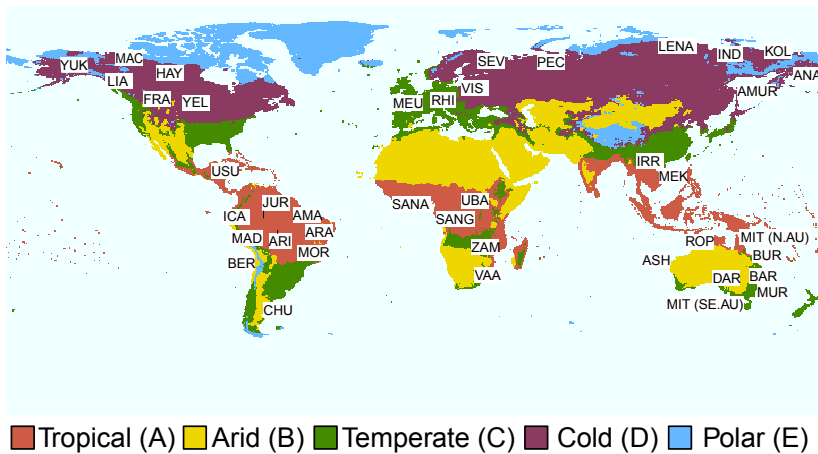


Figure 5.1: Location of the gauging station for each river basin in the major climate zones (see Table 5.1 for river basin abbreviations).

analysis data (Weedon et al., 2011).

Figure 5.2 gives the difference in precipitation for the three GCMs between the control period and the future period. Largest differences in mean daily precipitation are given by IPSL (please note the different scale). For some regions all GCMs agree on the direction of change, for example a decrease in precipitation in Central America, southern Europe and parts of Australia. Other regions have changes that differ for each GCM, for example in the Amazon region. For temperature, all GCMs indicate an increase across the globe, although the magnitude of the increase differs (not shown).

5.2.3 Large-scale hydrological models

Results from 5 different gridded large-scale hydrological models were made available through the WATCH project. The models used in this chapter are: (1) JULES, (2) LPJml, (3) MPI, (4) WaterGAP and (5) Orchidee. They all have a resolution of $0.5^\circ \times 0.5^\circ$. All models are run with the same forcing data for the period 1960–2100 (Sect. 5.2.2) and have the same routing network. The main characteristics of the models and references are given in Appendix A, more information can be found in Haddeland et al. (2011).

Daily time series of discharge were used in this chapter to investigate low flows and hydrological drought, and to be able to compare the model results with observations. Time series of routed discharge were taken from the grid cell in which the gauging stations are located. Discharge values consist of spatially aggregated gridded total runoff (sum of surface and subsurface runoff) from the grid cells in the models that represent the basin. Total runoff has been routed with the same network in each model.

5.3 Low flow and drought identification

The forcing data for the models is obtained from GCMs. These GCMs do not reproduce time series of historical weather in the control period, but the average climate conditions. This implies that time series of modelled discharge and observed discharge cannot directly be compared either. Therefore, as a measure of low flows, the 20th percentile (Q_{20}) for each month was calculated,

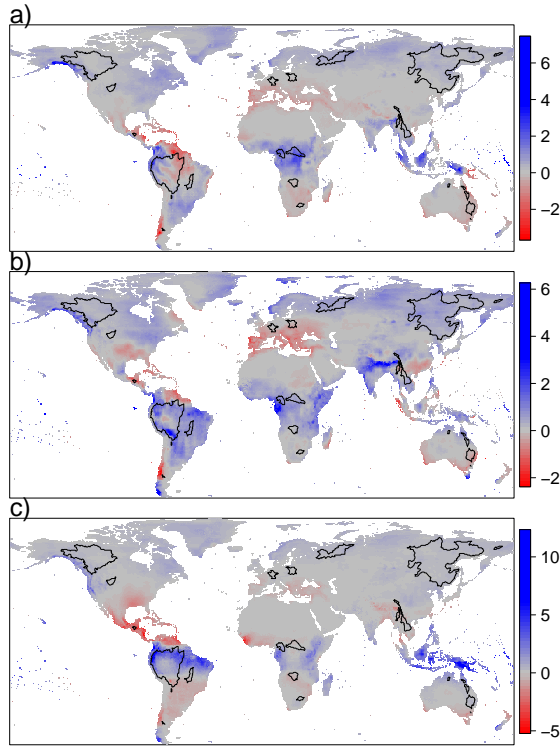


Figure 5.2: Difference between future period (2071–2100) and control period (1971–2001) in mean daily precipitation (mm day^{-1}) for three GCMs (a: ECHAM5, b: CNRM, c: IPSL) for the A2 scenario. River basins are indicated with black polygons.

which is defined as the value that is equalled or exceeded 80% of the time, for observed discharge and simulated discharge. When comparing the climatology of Q_{20} values of the simulated discharges against observations, there was a large difference in absolute values for most basins. The large differences between observations and model results can have different causes, for example, weaknesses in climate forcing, model structure and observations, and has been found in previous studies, e.g., Sperna Weiland et al. (2010). Because drought events were derived from anomalies, all monthly Q_{20} values were normalized by dividing the Q_{20} values by the yearly mean,

$$Q_{20}^*(i) = Q_{20}(i) / \overline{Q_{20}}, \quad (5.1)$$

where i is month of the year. This way the models could be judged on their ability to simulate the regime, which is important for drought analysis.

A selection has been made from the 15 model combinations (GHM and GCM) for analysis in the future based on the Nash-Sutcliffe coefficient (Nash and Sutcliffe, 1970) between the climatology of Q_{20}^* of observed discharge and the climatology of Q_{20}^* of simulated discharge in the control period. A value of 1 indicates a perfect match between model results and observations, while a value below 0 indicates that taking the observed mean is a better predictor than the model results. All model combinations with a Nash-Sutcliffe coefficient of 0.4 or higher were used for analysis of future drought. The criterion of 0.4 is rather arbitrary, but it was chosen based on visual inspection of the climatology of Q_{20}^* for simulated discharges and to keep as many acceptable model combinations as possible in the future analysis.

To analyse hydrological drought events and determine drought characteristics, the variable threshold level method (e.g. Yevjevich, 1967; Hisdal et al., 2004) was used. The start of a drought event is indicated by the point in time when discharge falls below the threshold and the event continues until the threshold is exceeded again. A monthly threshold derived from the 20th percentile of the time series was applied in this study. The discrete monthly threshold values were smoothed by applying a centred moving average of 30 days (Van Loon and Van Lanen, 2012). Drought characteristics derived in this study are the number of drought events, the average duration of drought events and the standardised mean deficit volume (Hisdal et al., 2004; Van Lanen et al., 2013). Due to the definition of the standardised mean deficit volume (deficit volume divided by the mean discharge), it has unit 'day', which indicates the number of days that mean flow is required to equal the deficit volume. To identify changes in drought events between the control period and the future period, drought events were determined with the same threshold, based on the control period.

5.4 Results and discussion

5.4.1 Comparison of large-scale models and observations

The climatologies of Q_{20}^* from the model combinations (GHM and GCM) were compared with the observed Q_{20}^* climatology. A selection of model combinations was made based on a Nash-Sutcliffe efficiency (NS) above 0.4 for the control period. Figure 5.3 shows the model combinations that met this criterion for each river with at least one combination selected. After this selection 37 river basins were left (Table 5.1). Clearly, the number of model combinations and the selected combinations were different for each river basin (Fig. 5.3). The range of all 15 model combinations is also given in Fig. 5.3. In all rivers, the range was reduced by the selection, except for the Meuse river for which all model combinations had a NS above 0.4. In most river basins, the hydrological model had more influence on the simulation than the GCM (e.g., Murrumbidgee river with selected combinations 3a, 3b, 3c, 4a, 4b, 4c; Chubut river with combinations 3a, 3b, 3c, 5b; Madeira river with combinations 1a, 1b, 1c, 3a, 3b, 3c, 4b, 5a, 5b, 5c). In most river basins, the selection of model combinations included one or multiple GHMs with all three GCMs. So forcing was less important than the hydrological model, which supports the findings of Hagemann et al. (2013). However, there are also river basins in which the simulations were dominated by the choice of the GCM (e.g., Içá river with combinations 1b, 2b, 4b; Mackenzie river with combinations 4b, 5b; Zambezi river with combinations 4b, 5b).

The number of model combinations left for further analysis depended on the NS value used for the selection. Figure 5.4 shows how the number of selected models decreased with increasing NS threshold values (averaged over all basins). Based on this analysis, we adopted 0.4 as the selection criterion. A NS of 0.4 is generally accepted to reflect a reasonable model performance, while with higher NS values, the number of model combinations quickly dropped. By using the criterion of 0.4, the median of the model combinations left was 7 across all river basins.

The selection of GHM and GCM combinations has been made to reduce the range, and thereby uncertainty, in projections. Previous studies have argued not to make a selection of the models or a ranking, because information could get lost (e.g. Gosling et al., 2011). Furthermore, it has been argued that results based on historical information might not determine model performance in the future (Reifen and Toumi, 2009). However, other studies (Hall and Qu, 2006; Stegehuis et al., 2013) have shown that if GCMs are constrained with observations, the uncertainty in the future is reduced. We believe that in order to achieve projections of future hydrological drought to determine the effects on water resources, a reduction of the large range in model projections is necessary. Some model combinations resulted in negative NS even for the Q_{20}^* climatology, which means that even the regimes of the rivers were not modelled correctly. It is questionable if these model combinations could give any useful information about future changes in discharge in

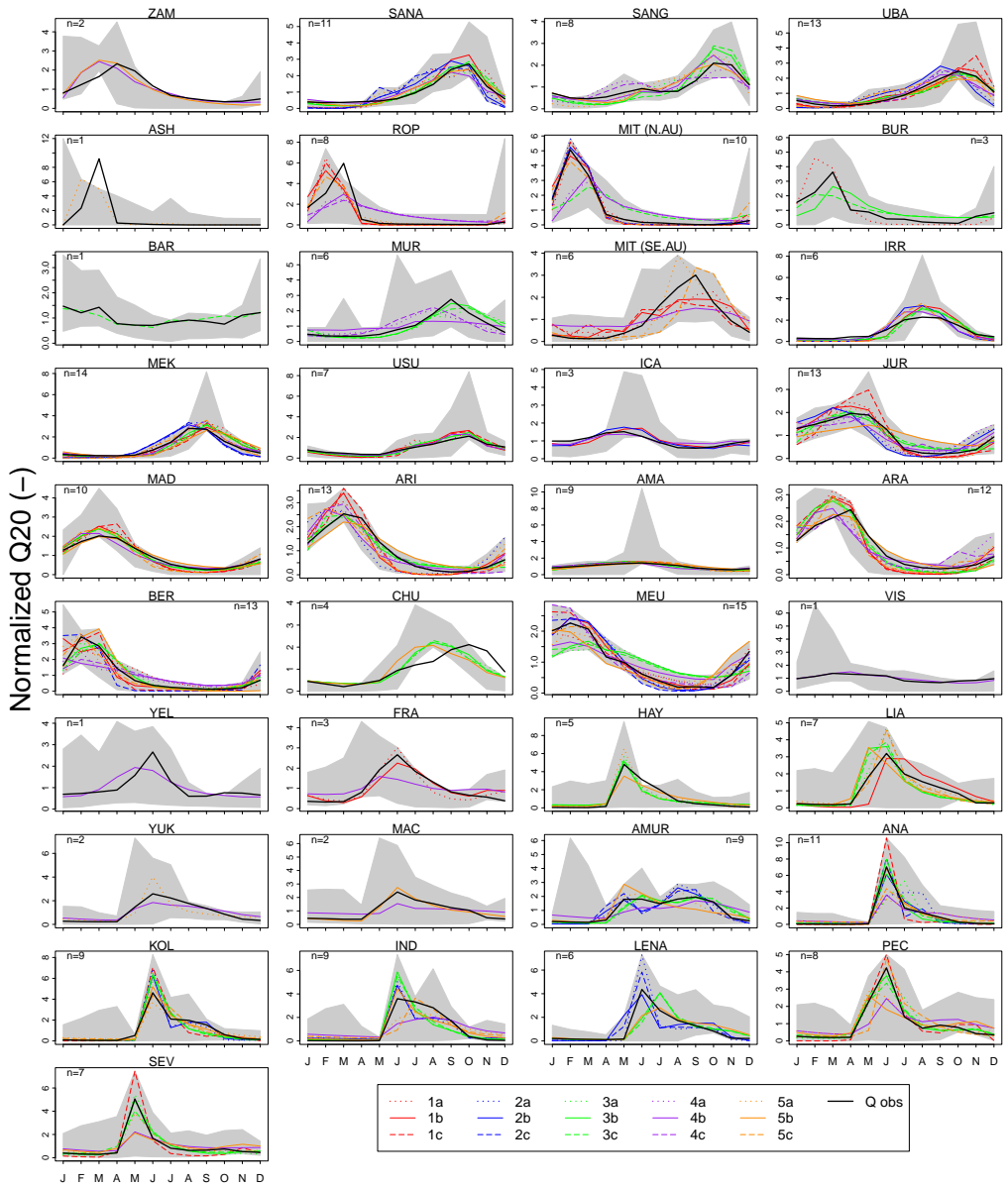


Figure 5.3: Climatology of normalized Q_{20} values of simulated discharge and observed discharge (Q_{obs}). Model combinations (GHM and GCM) shown are selected for analysis of future drought (number of combinations is given by n), the grey areas indicate the range of all 15 model combinations. The number indicated in the legend refers to the hydrological model (Sect. 5.2.3), the character to the GCM (a: ECHAM5, b: CNRM, and c: IPSL).

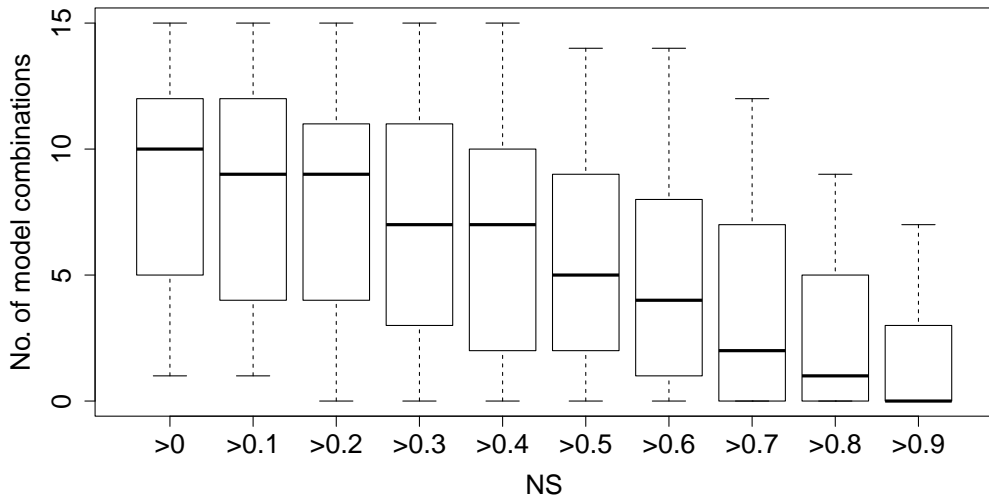


Figure 5.4: Number of model combinations selected per basin based on different Nash-Sutcliffe efficiency thresholds. The black line indicates the median, the box indicates the 25th and 75th quantiles, and the whiskers give the minimum and maximum number of selected model combinations.

these rivers. The selection made in this chapter is subjective in terms of selecting the NS as criterion and the magnitude of the NS. It should be considered as a first step towards a methodology to reduce the range in future hydrological drought. Other additional criteria to select models could be included in the methodology.

To investigate the robustness of the assumption that model combinations with a very low NS should be excluded, the NS was also calculated for a subset of rivers (Table 5.1) for the period 2001–2010. This period was not used in the comparison of GCM output and forcing data to derive the bias-correction method (Sect. 5.2.2) and can thus be regarded as near future relative to the control period. Figure 5.5 gives the NS values for the river basins with available observed data for two periods, 1971–2000 (p1) and 2001–2010 (p2). Overall, the NS values are reasonably constant, i.e., the majority of the combinations with a NS value above 0.4 in the control period also gave a NS value above 0.4 in the following period (82%). This means that only 18% of the model combinations with a value above 0.4 in the control period dropped below 0.4 in the next period. Only two model combinations with NS above 0.4 in the control period dropped below a NS of zero (both for the Mitchell river (Se Au), combinations 5a and 5c). Model combinations with a very low NS value (even below -2) did not recover in the following period. Although the threshold choice (NS = 0.4) is arbitrary, Fig. 5.5 indicates that performance in the past can provide an indication for the future.

Clearly, it is difficult to judge the effect of selecting only models that perform well in the control period given that all projections are uncertain. Nevertheless we believe that models that perform better against observations, have a higher plausibility and as a consequence the range in the projected changes can be reduced. However, river basins with only one or a few selected model combinations left, need to be investigated more in detail, since such a small selection might not be representative (Hagemann et al., 2013). For these specific river basins with a limited number of acceptable model combinations, other hydrological models with a different structure or model runs including human influence might be better suited. Although river basins were selected to be as undisturbed as possible, because the model results did not take into account human influence, it was difficult to find completely undisturbed basins in some regions and therefore human influence

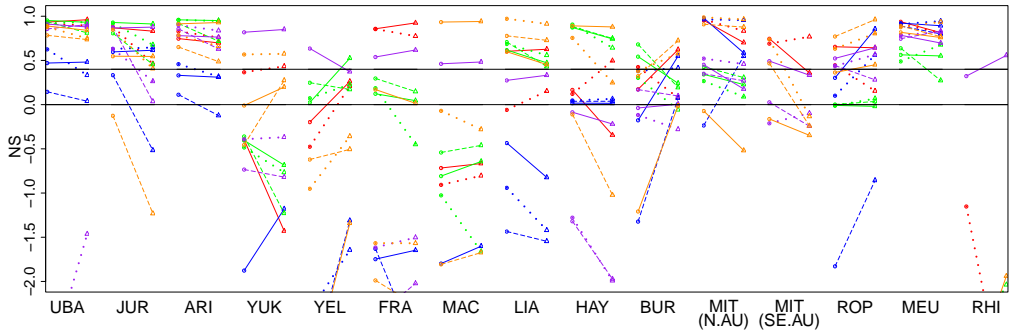


Figure 5.5: Direction of change in Nash-Sutcliffe efficiency for a subset of river basins between period 1971–2000 (p1, circle) and period 2001–2010 (p2, triangle). See Table 5.1 for exceptions in data availability in these periods for some river basins. Black horizontal lines indicate NS values of 0 and 0.4 (the selection criterion). Other colours and line styles are similar to Fig. 5.3.

might be larger than expected. To analyse climate change in these specific river basins a detailed analysis is needed, which is beyond the scope of this chapter. The selection of the model combinations is determined by the chosen criterion. For specific basins other criteria might be more suitable. More research is needed to determine additional criteria for the selection of suitable model combinations. Besides additional criteria for the selection of suitable model combinations, another option would be to keep all model combinations, but use a model averaging method instead. For the selection made in this chapter, model results below a certain NS value are removed from the analysis for the future. When using an averaging method, all model results are taken into account. By using Bayesian model averaging (BMA), model results with a better performance are given larger weights in the ensemble average (Duan et al., 2007). Different ways to implement the BMA are described by Parrish et al. (2012). The BMA method was applied by Najafi et al. (2011) to assess uncertainties of hydrological model selection in a climate change impact study for a specific catchment. They found that the BMA allowed for quantifying model structure uncertainties and performing ensemble estimation. However, they also mention that models with poor performances may reduce the performance of the BMA and removing poor results increases the performance of the BMA (Najafi et al., 2011). This may indicate that selecting models based on certain criteria, including a model averaging method, is the most promising way to assess climate change impact.

5.4.2 Influence of climate change on low flows

To investigate the influence of climate change, the difference between the climatology of Q_{20} (monthly Q_{20} values derived from model results) in the future period and the climatology of Q_{20} in the control period was calculated for all river basins for the selected model combinations (Fig. 5.6). The agreement between the model combinations regarding the changes is indicated in Fig. 5.6 by the intensity of the colours. There was no overall consistent drying or wetting trend in all selected rivers across the globe. The number of selected model combinations that agreed on the direction of change in low discharges differed between the river basins (ranging from 50% to 100% for the mean of the monthly changes in Q_{20} , from now on indicated as mean change Q_{20}). In most major climate zones, however, the direction of changes in low discharges for the river basins was largely similar. In the arid climates, models tended to agree on a decrease in the low discharge. For example, this was the case for the Murrumbidgee river and the Mitchell river (Se Au, third row in Fig. 5.6) for which all models agreed on negative mean change Q_{20} (i.e., will become drier). Also

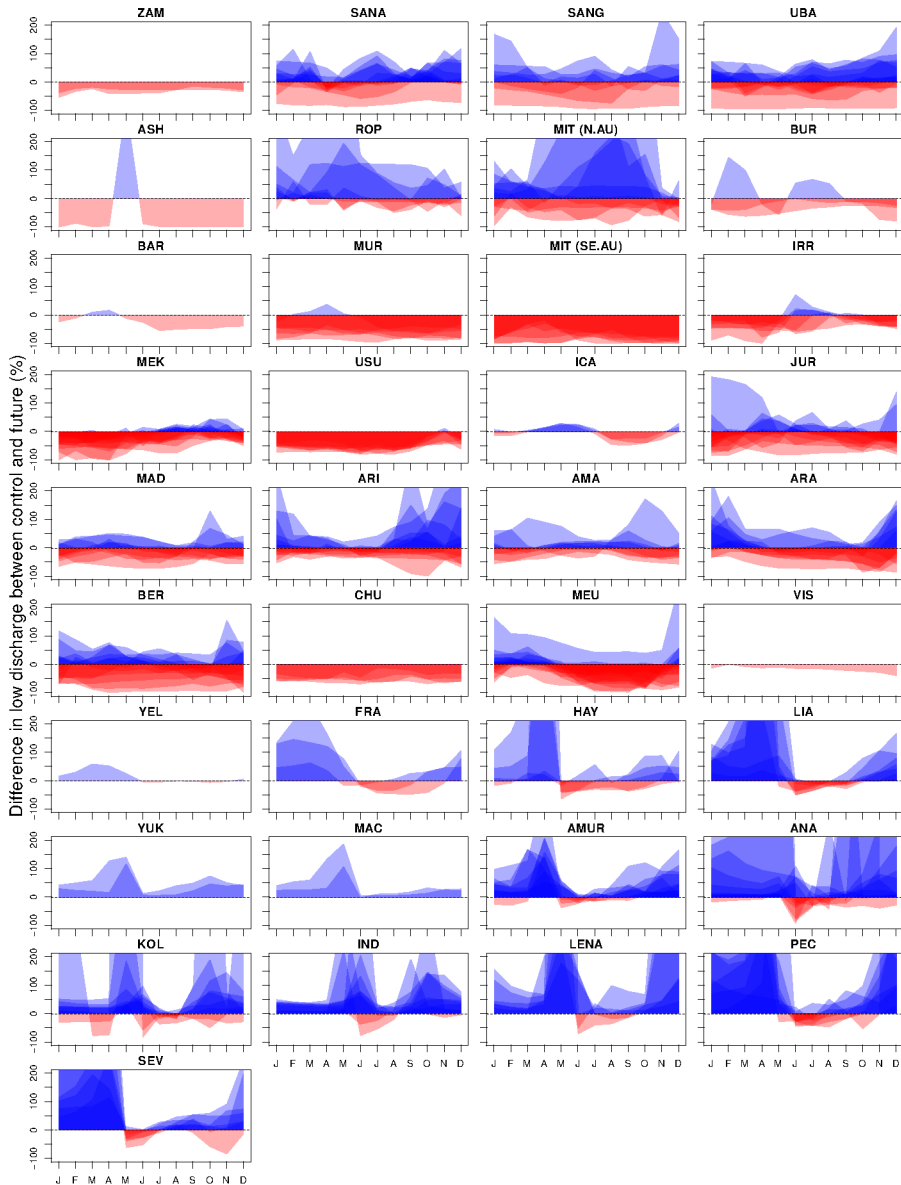


Figure 5.6: Relative change in low flows (Q_{20}) between future period (2071–2100) and control period (1971–2000) given as percentage of low discharge in the control period. Red indicates a decrease in Q_{20} in the future period, blue indicates an increase in Q_{20} . All selected model combinations (GHM and GCM) for each river basin are shown. The darker the colour, the more models have the same difference.

rivers on the border of the arid climate zone, like the Zambezi river and the Chubut river, showed a decrease in low discharge. For other rivers at this border, the Roper river and the Mitchell river (N Au), changes were less uniform (around 50% of the models agreed on the direction of mean change Q_{20}). Models did not all agree on increase or decrease of low discharges in these basins. The projected changes in low discharge corresponded with the changes in precipitation (Fig. 5.2). Precipitation decreased in southern Australia, the Zambezi river basin and Chubut river basin, while increases or no changes were obtained for northern Australia.

For rivers located mainly in tropical (A) climates, models disagreed on the changes, although this differed per continent. All rivers in the humid climates in Africa (Sanaga, Sangha and Ubangi, first row in Fig. 5.6) and most rivers in the Amazon region (Jurua, Madeira, Aripuana, Amazon and Araguaia, fourth and fifth row in Fig. 5.6) showed changes in low discharges in both directions, and thus it was difficult to predict changes in drying or wetting for these regions (model agreement on the direction of mean change Q_{20} was between 50% and 75%). For the river basins in Africa, the GCMs indicated an increase or no change in precipitation. This is not directly visible in low discharge changes because of other processes that determine discharge as well, e.g., changes in evapotranspiration and storage. This highlights the importance of using hydrological models for hydrological drought analysis instead of only GCMs which generally have a more crude land surface model component. For the Amazon region, changes in precipitation were not uniform among the GCMs and again other hydrological processes affect discharge changes. One exception regarding low discharge changes in the Amazon region was the Içá river. For this river all selected model combinations indicated an increase in low discharge for the months April to July, followed by a decrease in low discharge. For the Içá river, the selection of model combinations resulted in only one GCM (CNRM, Fig. 5.3), which could explain the uniform changes in discharge. Other rivers in humid climates (Irrawaddy, Mekong and Usumacinta, third and fourth row in Fig. 5.6) showed a decrease in low discharge for most models for the whole year or at least a large part of the year (all models agreed on a negative mean change Q_{20}). For the Usumacinta river, however, all GCMs projected a large decrease in precipitation, which translated in a decrease in low discharge. For the Mekong river and Irrawaddy river projected precipitation changes were less uniform.

There were almost no rivers in the selection in temperate climates (Fig. 5.1), partly because rivers in these regions were often largely affected and partly because model performance was poor for these rivers. For the Meuse river, most models gave an increased low discharge in winter and decreased low discharge in summer. This means that the low discharges in wet periods became higher and in dry periods became lower, as was the case for the Içá river. The Bermejo river is on the border of climate zones (Fig. 5.1) and showed differences in low discharges in both directions and little model agreement, which was triggered by the GCMs that disagreed on precipitation change.

Changes in river discharges in the cold climates (D and E, bottom four rows in Fig. 5.6) were dominated by a shift in the regime caused by an earlier snow melt peak and less snowfall due to higher temperatures. The mean yearly low discharge (mean Q_{20}) in these rivers increased according to most models. The change in timing of the snow melt peak is shown in Fig. 5.7, where the month with the highest Q_{20} value in the year is given for both the control period and the future period for each model combination. In most river basins, there is only one month difference between the models for the timing of the peak. Not for all rivers in cold climates a change in the timing of the snow melt peak was predicted by the models (e.g., Kolyma river, Anadyr river). However, in some cases models agreed that the snow melt peak would occur one month earlier in the future (e.g., Lena river, MacKenzie river, Pechora river).

An overview of previous studies on the change in runoff or discharge caused by climate change is given by Sperna Weiland et al. (2012). Their overview mentions regions found to be affected either by an increase or a decrease of discharge or runoff. Although most previous studies focused on mean discharge instead of on low flows, we have compared our results with their findings here by lack of studies on low streamflow at the global scale. The shift in regime in northern

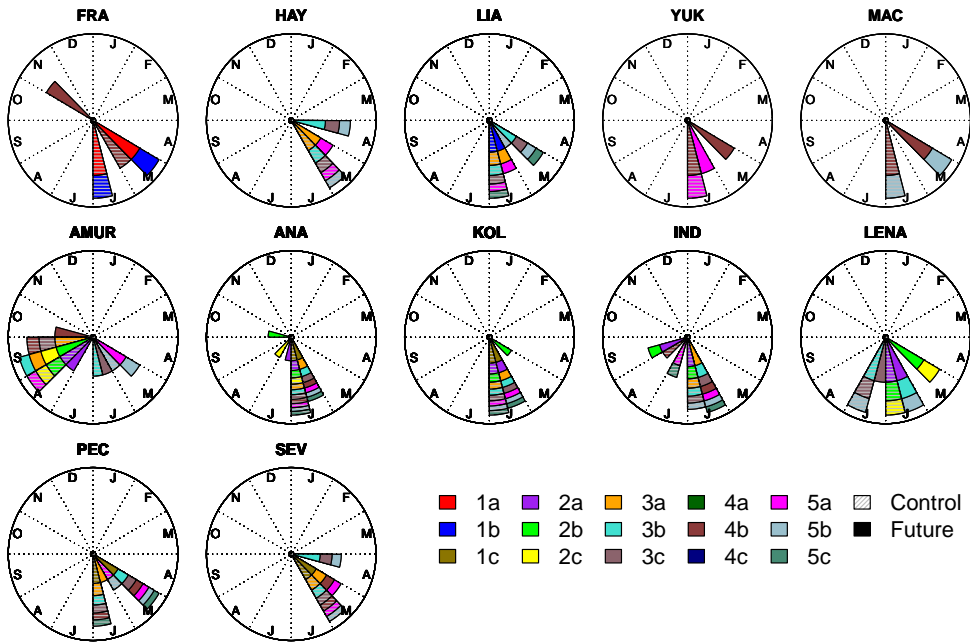


Figure 5.7: Timing of the seasonal peak in Q_{20} between the control period (shaded colours) and the future period (full colours) given for all river basins in cold climates that showed differences for the selected model combinations (GHM and GCM). (The length of the radius of the segments is determined by the number of selected model combinations and has no additional meaning.)

colder river basins and the increase in low discharge found in this chapter corresponded well with results on discharge changes from e.g., Arnell and Gosling (2013), Sperna Weiland et al. (2012), Nohara et al. (2006) and Milly et al. (2005). Also our findings that arid river basins will become drier in the future corresponded well with previous studies (e.g. Tang and Lettenmaier, 2012; Nohara et al., 2006; Sperna Weiland et al., 2012; Milly et al., 2005). Changes in low discharge for the rivers in the Amazon region were less certain in this chapter. There was less agreement with previous studies and these previous studies disagree on changes. Arnell (2003), Arnell and Gosling (2013) and Arora and Boer (2001) found a decrease in discharge or runoff in this region, while Nijssen et al. (2001a), Manabe et al. (2004) and Nohara et al. (2006) found an increase in mean annual discharge for the Amazon. The decrease of low discharges during large parts of the year in the Asian rivers, Irrawaddy and Mekong, found here is not in agreement with all other studies (e.g. Nijssen et al., 2001a; Sperna Weiland et al., 2012), which showed an increase in discharge for the Mekong, although Manabe et al. (2004) and Arora and Boer (2001) also found a decrease for the Mekong. Changes in low discharge found for the Meuse river in this chapter correspond with findings of De Wit et al. (2007) that seasonality in the discharge regime of the Meuse will be enhanced. However, they also stated that groundwater storage is important in the Meuse basin and a decrease in mean summer discharge might not necessarily lead to more severe low flows. Differences between climate change studies and the current study are caused by a different focus of the studies (e.g., mean discharge instead of low flows) and the use of different hydrological models, climate models and emission scenarios.

5.4.3 Influence of climate change on hydrological drought characteristics

With the variable threshold level method (Sect. 5.3), drought events and their characteristics have been determined for the control period and the future period. The changes in drought characteristics, mean drought duration and standardised deficit volume, between the future period and the control period are shown in Fig. 5.8 for each river basin. It was expected that when model combinations projected a decrease in low discharges, drought characteristics would show an increase. In general, differences in hydrological drought characteristics (Fig. 5.8) showed the same pattern as the differences in Q_{20} (Fig. 5.6). In river basins with a good model agreement for changes in Q_{20} , drought characteristics also showed good agreement and followed the direction of change in Q_{20} with a negative correlation as expected. For example, all model combinations showed an increase in drought duration and standardised deficit volume for the Usumacinta river (USU, Fig. 5.8), which also showed a decrease in low discharge (Fig. 5.6). The rivers in arid regions (Mur-

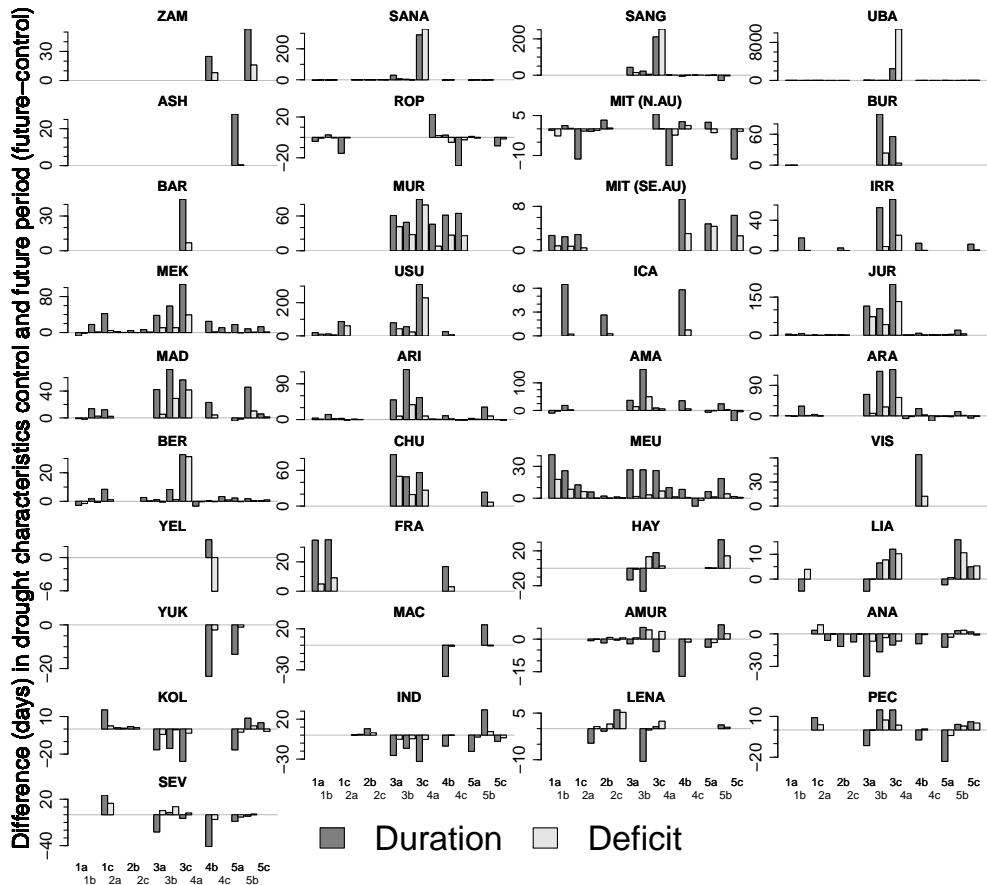


Figure 5.8: Change in drought characteristics (mean duration and mean standardised deficit volume) between future period (2071–2100) and control period (1971–2000) for the selected combinations of GCM and GHM. Codes for the combinations are equal to Fig. 5.3. Positive change means longer drought events or higher standardised deficit volumes in the future, whereas negative change means the opposite.

rumbidgee and Mitchell (Se Au)) also showed a decrease in low discharge and this resulted in an increase in drought characteristics. Especially in these dry regions this could have large impacts, since there is already little water available.

There was better model agreement regarding differences in drought characteristics than regarding changes of the climatology of Q_{20} in other river basins, e.g., Madeira river, Jurua river, Amazon river. For these rivers, both drought characteristics showed an increase (Fig. 5.8), while the model combinations did not agree on a clear increase or decrease for Q_{20} (Fig. 5.6). This means severity and impact of drought events will likely increase in these basins, although uncertainty in changes of low discharge was large.

For the Meuse river and Içá river, the model combinations projected seasonality in low discharges would become more extreme (Fig. 5.6). The drought analysis showed that the increase in seasonality led to an increase in both drought characteristics for almost all selected model combinations. So, even though Q_{20} values were higher during the wet period, drought duration increased and drought impacts will be more severe in the future because of the decrease in summer discharge.

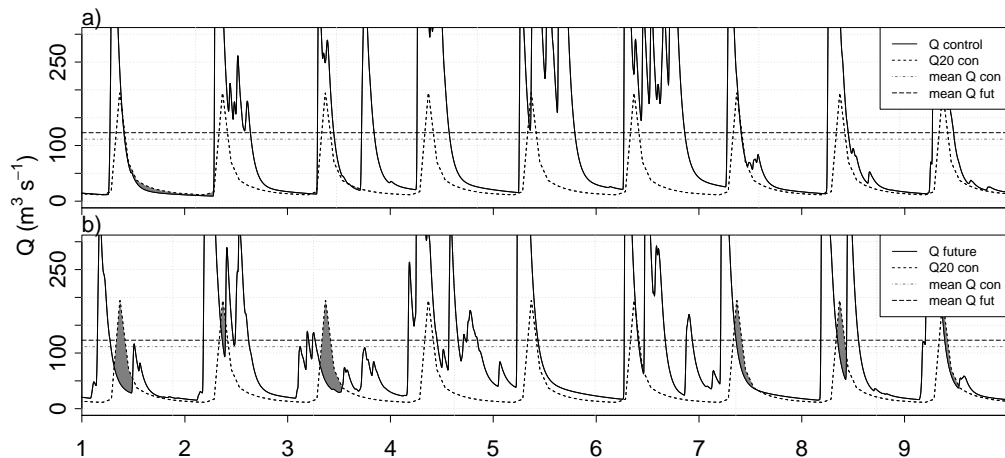


Figure 5.9: Influence of a threshold derived from the control period on identification of drought events (grey polygons) in the future in case of a regime shift: a) Drought events identified from simulated discharge in the control period, b) Drought events identified from simulated discharge in the future period.

In some river basins in cold climates that showed a clear snow melt peak, there were model combinations that gave an opposite signal in drought characteristics as compared to the signal in discharge, e.g., the Liard river and the Fraser river. The overall Q_{20} discharge in these basins seemed to increase (Fig. 5.6), whereas the drought duration and standardised deficit volume also increased (Fig. 5.8). This was partly caused by the application of the threshold level method to the future period using a threshold derived from the control period (Fig. 5.9). In case of a shift in the timing of the snow melt peak in the Q_{20} values, anomalies in discharge behind the peak could be inadvertently identified as drought (in terms of expected impacts), even though the mean discharge increases from the control period to the future period. However, the increase in drought characteristics was also caused by a decrease of summer discharge as projected by some model combinations (Fig. 5.6). In that case, the number of summer drought events will increase in these regions even if mean discharge increases. Adaptation measures will be necessary to prevent large impacts of these summer drought events.

Figure 5.9 indicates that it is not straightforward to determine hydrological drought events with the variable threshold method using the same threshold both in the control period and in the future period. The use of the threshold derived from the control period can lead to unintended drought events in terms of expected impacts. The natural variability of the climate over 100 years is not taken into account and it is difficult to determine the impact of drought events in the future, because possible adaptation to the changing conditions could occur. This adaptation could be included by linking the drought threshold to adaptation scenarios like Vidal et al. (2012). This would require more information to formulate accurate scenarios, but could be an important step in future hydrological drought identification studies. Drought identification in the future is very dependent on the identification method used and should include both drought characteristics and low flows to indicate changes. If only low flows are considered, effects on drought events in the future could be underestimated, for example as seen in the rivers in the Amazon region (Figs. 5.6 and 5.8).

5.5 Conclusions

For adequate adaptation to the impacts of hydrological drought events, robust predictions about changes in their characteristics in the future is important. In this chapter, an ensemble of Global Hydrological Models (GHMs) forced with different General Circulation Models (GCMs) was used to analyse low flows and drought events. To reduce the range in future drought projections, a selection of model combinations (GHM and GCM) was made by comparing model results with observed discharge in the control period (1971–2001). Selected model combinations differed per river basin and included both different GCMs and different GHMs. This highlights the importance of using multiple hydrological models as well as multiple climate models. Models showed large differences in absolute discharge values compared to observations, so model improvement is still an important step for impact studies as well. GHMs use different model structures and parameters and will not all perform uniformly across the globe. In this study, the selection of model combinations was based on a single criterion as a first step towards a set of criteria that will reduce the range of projected changes in hydrological drought. The selected model combinations based upon the single criterion were evaluated against observations in the period 2001–2010 (the near future with respect to the control period) and model combinations showed a fairly consistent performance across the control period and the evaluation period. More research is needed both to find the best set of criteria and to improve the models, to reduce the uncertainty in projections, which is important to derive adequate adaptation measures.

With the selected model combinations (GHM and GCM), different effects of climate change on low flows were found in the river basins across the world. River basins in arid regions were projected to become even drier. In cold regions, a shift of the snow melt peak and an increase in low discharges was found. For most rivers in humid and temperate climates, model combinations gave uncertain results. Overall, results corresponded with previous studies on the effects of climate change on discharge. The change in low discharge was not everywhere equal to the change in precipitation, because discharge, of course, is affected by other processes as well (e.g., evapotranspiration) and catchment characteristics. This emphasizes the importance of the use of multiple hydrological models in climate change studies.

Besides the changes in low flows, also changes in hydrological drought characteristics (mean duration and standardised deficit volume) were determined. The drought characteristics showed an increase in most river basins, which means impacts and severity of drought events are expected to increase as well. The increase in characteristics was not always consistent with the changes in low flows. Partly, this can be caused by the drought identification method. In case of a regime shift, unintended drought events in terms of expected impacts were identified with the threshold level method. However, drought characteristics add information about changes in drought impacts. For example, model combinations did not project a clear increase or decrease in low flows

for river basins in the Amazon region, while model agreement on the amplification of drought characteristics was much larger. Given the large societal and environmental impacts of hydrological drought events, it is important to progress with finding the best drought identification method for future hydrological drought to anticipate on possible drought impacts.

Influence of multi-year storage variation on hydrological drought

Abstract

Storage processes in catchments have a large influence on river discharge. Hydrological drought events are therefore also affected by the amount of storage and storage dynamics in catchments. Since drought is expected to become more severe in the future in multiple regions due to climate change, understanding drought development is important. In this chapter, the influence of long-term storage variation on drought duration was analysed. Discharge time series were decomposed in three components with a Seasonal-Trend decomposition procedure based on Loess (STL). The trend (slow-varying) component gives long term changes and is taken as a metric for storage processes. Discharge data from 1737 river catchments in Europe and the United States were used. Three catchments, the Noor, the Pang and the Ourthe, were studied in more detail using observations of precipitation, discharge and groundwater level. Drought events were identified with the variable threshold method. In slowly-responding catchments the contribution of the trend component to total discharge variation was higher than in fast-responding catchments. The contribution of the trend component to the total discharge variation (fraction of the trend component) was linked to mean drought duration. Higher fractions of the trend component were associated with longer drought events. This means it is important to adequately include storage processes in hydrological models to determine drought characteristics correctly. Without an adequate description of storage processes, drought duration will be underestimated and drought frequency will be overestimated. This will affect other characteristics (e.g., deficits) and predicted impacts.

6.1 Introduction

Storage processes have a large influence on discharge dynamics of river catchments (Tallaksen and Van Lanen, 2004; Teuling et al., 2010; Birkel et al., 2011; Brauer et al., 2013; Creutzfeldt et al., 2014). The amount of groundwater storage, lakes and other stores determine the reaction time of discharge to precipitation events. Especially the potential for storage change is important. A large storage potential usually implies a slow response to precipitation. The more water that can be stored in a catchment, the longer water can be released from the storage to feed the river (Van Lanen et al., 2004).

Drought is defined as a period of below-average natural water availability due to relatively low precipitation and/or high evaporation rates (Tallaksen and Van Lanen, 2004). A drought propagates through the hydrological system from precipitation through soil moisture to groundwater and river discharge. When a drought affects the groundwater and discharge, it is referred to as hydrological drought. This propagation of drought is dependent on climate and catchment characteristics (e.g. Van Loon and Van Lanen, 2012). Groundwater systems, which have storage change potential, and other stores have a major impact on the development of hydrological drought (Eltahir and Yeh, 1999; Van Lanen et al., 2013). Van Lanen et al. (2013) reported that “groundwater systems are as important as climate control for the development of hydrological drought”. The capacity of a catchment to store water (e.g., in lakes, aquifers, snowpack, wetlands, groundwater and the upper soil layers) is considered as one of the most important factors in drought propagation (Sheffield and Wood, 2011).

Hydrological drought events are highly dependent on the reaction time of a catchment to precipitation and thus on available storage within the catchment. Several studies have focused on the propagation of drought through the hydrological cycle (e.g. Peters et al., 2003, 2006; Van Loon and Van Lanen, 2012) and the effect of groundwater systems on drought (e.g. Eltahir and Yeh, 1999; Van Lanen et al., 2013). Most of these studies have investigated single catchments in detail (Peters et al., 2006; Tallaksen et al., 2006, 2009), a limited number of catchments (Eltahir and Yeh, 1999; Van Loon and Van Lanen, 2012), a series of virtual catchments (Peters et al., 2003), or used modelled data (Van Lanen et al., 2013). They all concluded that there are less and longer drought events in discharge in catchments that are dominated by slowly-responding groundwater systems. Long-term variation in discharge caused by multi-year variation in storage determines the length, impact and recovery of drought events in slow-responding catchments (Van Lanen et al., 2004).

Drought is expected to increase in the future in multiple areas of the world, for example, in parts of Europe and Middle-America (e.g. Bates et al., 2008; Dai, 2011; Romm, 2011; Seneviratne et al., 2012; Prudhomme et al., 2014). Besides increased drought, discharge is projected to decrease in large parts of the world (Milly et al., 2005; Nohara et al., 2006; Sperna Weiland et al., 2012). The increase of drought events will have large societal and environmental impacts, so it is important to improve knowledge on future discharge changes and associated drought development, especially at small scales where local storage controls may be strong. Studies on the future changes in discharge at the global scale (e.g. Sperna Weiland et al., 2012; Arnell and Gosling, 2013; Van Huijgevoort et al., 2014) use large-scale models to simulate discharge. These large-scale models often lack a comprehensive representation of storage processes, which is relevant for smaller spatial units (e.g., subgrid level and catchments). Previous studies on historical drought events that compared large-scale models with observed river flow (Stahl et al., 2012; Van Loon et al., 2012; Gudmundsson et al., 2012b; Van Huijgevoort et al., 2013) reported a fast reaction of runoff in the models to precipitation. As a consequence they found the largest differences between simulated drought events and observed drought events in catchments where storage plays an important role. Improving the implementation of storage processes is one of the many challenges in the development of hyperresolution global models (e.g. Wood et al., 2011).

The aim of this chapter is to study the influence of multi-year storage variations on hydrological drought characteristics and to quantify this relation. Data from 1737 catchments in Europe and

the United States were used to establish a relation between storage processes and drought. This was done by dividing the discharge time series in three components, i.e. a seasonal component, trend (slow-varying) component, and remainder (fast-varying) component. The trend component was taken as a metric for the long-term variation reflecting storage change. This component was associated with the mean drought duration in the river catchments.

6.2 Data

Discharge data from catchments in Europe and the United States were used to analyse the influence of storage variation on drought characteristics. Three catchments in Europe were studied in more detail: Noor, Pang and Ourthe. The small catchment of the Noor (10.6 km²) is situated in the southern part of the Netherlands and partly in Belgium (Van Lanen and Dijkma, 1999, 2004). Discharge (daily), precipitation (daily) and groundwater level (monthly) data were available from 1992 to 2006. The Noor catchment has deep groundwater levels and a thick unsaturated zone. Therefore the catchment has a large potential for storage change, and as a result the brook reacts slowly to precipitation (Van Lanen and Dijkma, 2004). The Pang catchment (170 km²) is situated in the United Kingdom (Peters et al., 2006). Daily discharge data were available from 1968 to 2012, daily precipitation data from 1961 to 1997 and monthly groundwater data from 1974 to 2012. The Pang catchment has, similar to the Noor catchment, deep groundwater levels. The total discharge is by 2/3 composed of deep groundwater (Peters and Van Lanen, 2005), which means that the catchment reacts slowly to precipitation. The Upper-Ourthe catchment (around 1600 km²) is located in the Belgian Ardennes (Driessen et al., 2010). Daily discharge and precipitation data were available for several stations from 1990 to 2009. The discharge data from Tabreux in the Upper-Ourthe catchment were used in this chapter. Groundwater data were available at several locations, however, measurement intervals were irregular. The Ourthe is a fast reacting system with shallow soils overlying impermeable bedrock in many places (Rakovec et al., 2012).

Long-term variation in subsurface storage preferably is derived from groundwater data, but these data are often not available or irregularly measured in most catchments. Therefore we have used a metric derived from discharge data to determine the influence of storage variation on drought (Sect. 6.3.1). In addition to the three catchments, which were investigated in detail, discharge data from 1734 catchments were used for this analysis (Fig. 6.1). In Europe, discharge

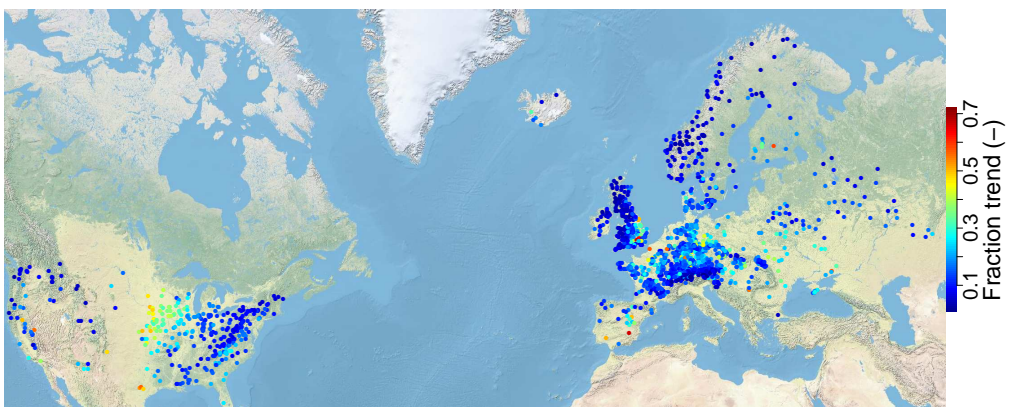


Figure 6.1: Location of the discharge gauges in Europe and the United States and fraction of the variation in discharge time series explained by the trend component (see Sect. 6.3.1).

data for 1354 catchments were available from the European Water Archive (EWA) of the UNESCO IHP FRIEND Water programme. The time series from EWA were selected based on the length of the period (at least 30 years) and on the criterion of less than one year of missing values. Besides discharge from EWA, discharge series were used from several subbasins in the Meuse basin (Netherlands and Belgium, Uijlenhoet et al., 2001), the Rhine basin (measured at Lobith, Netherlands), the Narsjø catchment (Norway), the Upper-Metuje catchment (Czech Republic), the Upper-Sázava catchment (Czech Republic) and the Nedožery catchment (Slovakia). For the United States, discharge data were taken from the MOPEX (Model Parameter Estimation Project) dataset (Duan et al., 2006). This dataset includes a wide range of river catchments. In this chapter, discharge data from 345 US catchments (Fig. 6.1) were used based on the criterion of less than one year of missing values.

The distribution of catchment size is given in Fig. 6.2. Most catchments have an area between 100 and approximately 3000 km². It was anticipated that storage variation had a larger influence in smaller catchments. In addition, selected catchments should have little human influence, so fewer larger catchments were selected.

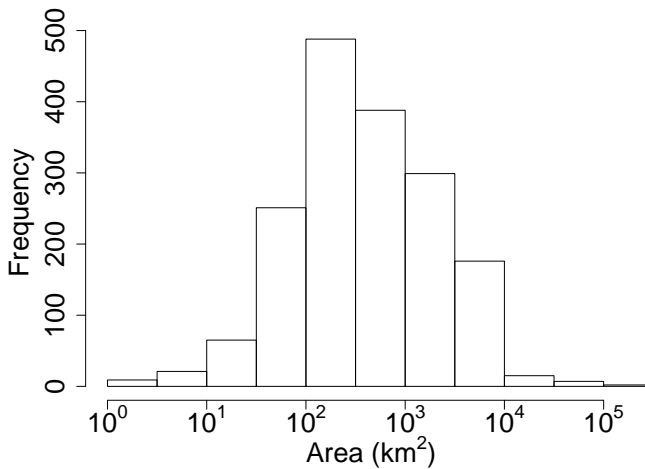


Figure 6.2: Distribution of the 1737 catchment areas used in this chapter.

6.3 Methodology

6.3.1 Decomposition of discharge time series

To find the influence of long-term storage variation on the discharge data, the time series of discharge were decomposed with a Seasonal-Trend decomposition procedure based on Loess (STL) (Cleveland et al., 1990). This method divides time series (Y_t) in three components:

$$Y_t = T_t + S_t + R_t, \quad (6.1)$$

where Y_t is the observed value at time t , T_t is the trend (slow-varying) component, S_t is the seasonal component and R_t is the remainder or residual (fast-varying) component. The STL method is based on locally weighted regression and applies a series of smoothing operations (Cleveland

et al., 1990). The method was applied after taking the logarithmic values of the discharge, because discharges generally follow a log-normal distribution rather than a normal distribution and the local regression technique works better on variables that are symmetric.

The contribution of the variance of the trend component to the variance of the total series has been taken as a metric for the importance of storage changes in the catchment. For each of the three components the variance was determined and divided by the sum of the variances of the three components. In this chapter, the resulting value of that division is defined as the fraction of that component. The sum of the variances of the three components is not completely equal to the variance of the original time series (Y_i), however, we assume that the covariances between the components are small, because this is defined by the decomposition method.

6.3.2 Drought identification

To identify drought events and determine their drought characteristics, the variable threshold level method (e.g. Yevjevich, 1967; Hisdal et al., 2004) was used (Chapter 2). The start of a drought event is indicated by the point in time when discharge (or another variable of interest) falls below the threshold and the event continues until the threshold is exceeded again. A monthly threshold derived from the 20th percentile of the time series of discharge, precipitation, or groundwater was applied in this study. The discrete monthly threshold values were smoothed by applying a centred moving average of 30 days (Van Loon and Van Lanen, 2012). Drought characteristics derived in this chapter are the number of drought events, the average duration of drought events and the standardized mean deficit volume (Hisdal et al., 2004; Van Lanen et al., 2013). To exclude short drought events, the drought analysis was done after smoothing the discharge series and precipitation series with a moving average of 30 days and a minimum drought duration of 3 days was taken.

6.4 Results and discussion

6.4.1 Decomposition of the discharge time series

The discharge series of all catchments were decomposed in three components with the STL method. The three components of the series for the Noor and Ourthe catchments are given as example in Fig. 6.3. Both discharge series had a seasonal component, however, the contribution of the seasonal component to the total series was substantially larger for the Ourthe catchment (0.54) than for the Noor catchment (0.06). In the Noor catchment the contribution of the trend component was much higher than in the Ourthe catchment (0.72 vs 0.08). Since the Noor is a slowly-responding catchment and the Ourthe fast-responding, these contributions confirmed the hypothesis.

The influence of groundwater on the discharge in the three catchments that were studied in detail was analysed on the basis of groundwater level observations. A high correlation between groundwater level and discharge at the same time step was found for the Noor (0.83) and Pang (0.71) catchments. The time series of the trend component found with the STL method also showed a high correlation with groundwater level in these catchments (Noor: 0.78, Pang: 0.73). This suggests that in these catchments the long-term trend component is closely connected to groundwater. In the Ourthe catchment, a lower correlation was found for groundwater level and discharge (0.61), and for groundwater level and the time series of the trend component (0.35). Hence, the long term trend component in the Ourthe catchment had a weaker connection with groundwater and discharge was apparently influenced more by the precipitation and quickly responding catchment units (e.g., peat areas in headwaters). These correlations were in line with the hypothesis based on the knowledge of the catchments.

The fractions of the trend component for all 1737 catchments are shown in Fig. 6.1. For the 1734 additional catchments only discharge data were used. Within Europe the larger catchments,

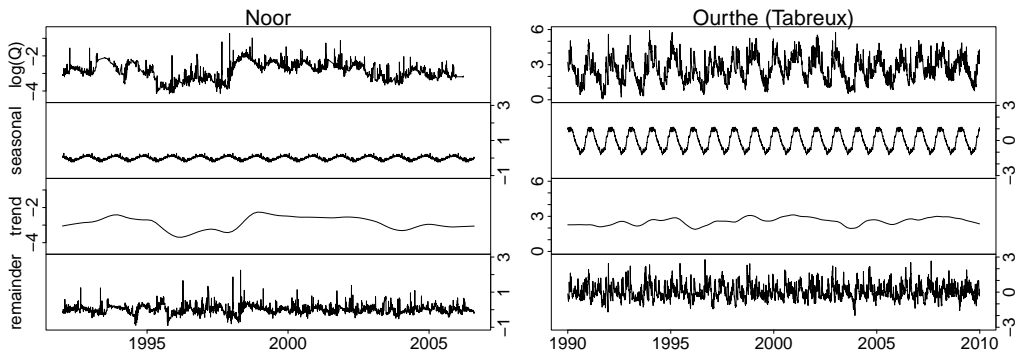


Figure 6.3: Example of the decomposition of time series for the discharge of the Noor (left) and the Ourthe river (right). The panels represent the logarithmic discharge data (upper) and the three components derived with the STL method (seasonal component: second panel, trend component: third panel, remainder component: fourth panel).

the Meuse and the Rhine, had a low fraction of the trend component (0.18 and 0.25). Storage could become less important in larger catchments, since those catchments usually consist of subcatchments of which some likely have a fast reaction, which influences the total discharge. For instance, subcatchments of the Meuse had both high and low fractions. The Hoyoux (small subcatchment of 94 km²) had a high fraction (0.56), whereas the Ourthe subcatchment (discharge measured at Tabreux) had a low fraction (0.08).

Considering all catchments, the higher fractions of the trend component were found in the catchments with an area between 10 and 10 000 km² (Fig. 6.4). In the smallest catchments (<10 km²) only low fractions of the trend component were found (maximum 0.2). These smallest catchments are mainly headwater catchments with steep slopes and shallow soils, leading to low fractions of the trend component. The number of catchments with a catchment size below 10 km² included in this chapter is limited (Fig. 6.2), so small catchments with higher fractions could exist, but were not sampled. The median of the fraction of the trend component increases with the catchment area from 0.07 to 0.23 (Fig. 6.4). In the largest catchments (>10⁴ km²) the higher fractions of the trend component were around 0.4. However, also the number of the larger catchments is limited in this chapter (Fig. 6.2). The larger the catchment, the more subcatchments are included leading to an increased median fraction of the trend component.

For the Upper-Metuje catchment a small fraction of the trend component (0.11) was found, which was not expected, because it contains multiple aquifers (Rakovec et al., 2009). The discharge of the Upper-Metuje catchment, however, included a fast reaction component that caused discharge peaks when available storage in the catchment still was not filled. In the Upper-Metuje catchment the potential for storage change rather than total storage determines the drought development. This potential is somewhat low, because the catchment showed a fast reaction due to the high conductivity of porous sandstones, which prevents large phreatic water table variation.

The majority of the catchments in Europe had a fairly low contribution of the trend component. The mean fraction of the trend component was 0.15 for all European catchments. Only 2.5% of all European catchments (35 catchments) had a fraction of the trend component of 0.4 or higher. Especially the catchments in the Alps, Norway and northern parts of the United Kingdom had a low fraction of the trend component. In parts of Spain, the southeastern part of the United Kingdom, the northern part of France, and parts of Germany, some catchments with a high fraction of the trend component were found (above 0.4).

For the river basins in the United States, a slightly higher mean fraction of the trend component was found (0.18), and 6.1% of the catchments in the United States (21 catchments) had a fraction

of the trend component above 0.4. A distinct spatial pattern was found across the United States, with most higher fractions of the trend component in the middle of the country (Fig. 6.1). This is not the same pattern as found previously by Santhi et al. (2008) for the Base Flow Index (BFI) for the United States, which also reflects catchment response. The difference between these metrics might be caused by seasonality in the signal. Seasonality is filtered out by the STL method, but still included in the BFI. For example, in regions with a distinct snow melt peak of several weeks, BFI is often overestimated, because a large portion of this peak is included in the baseflow.

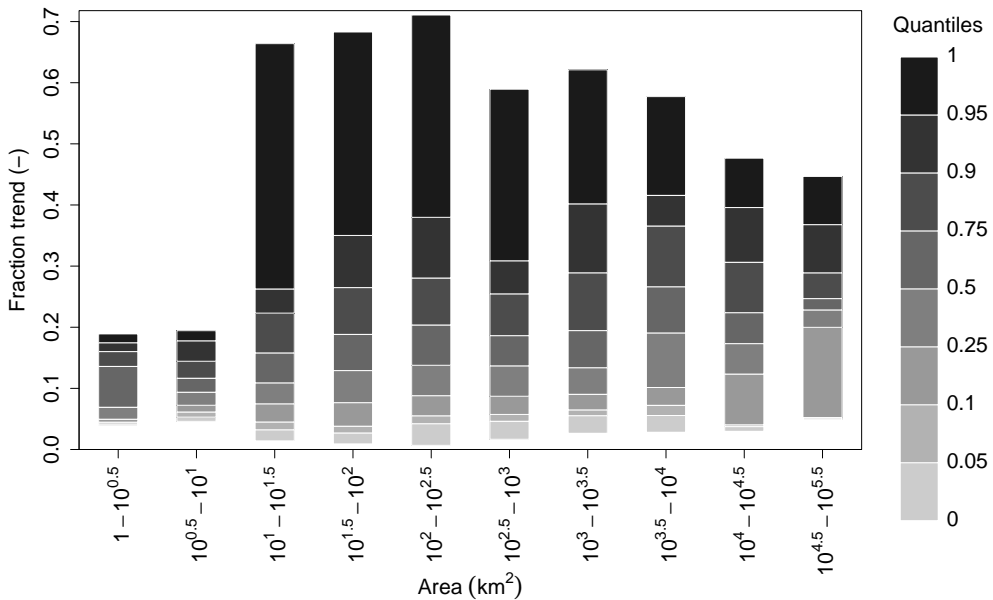


Figure 6.4: Distribution of quantile values from the fraction of the trend component over the catchment size.

6.4.2 Drought analysis

Drought events were identified in all catchments using the observed discharge time series. In the Noor, Pang and Ourthe catchments, drought events were determined in precipitation and groundwater as well to analyse propagation of drought. The drought occurrence for the Noor and Ourthe catchments in all variables is shown in Fig. 6.5. In both catchments the features of drought propagation (pooling, attenuation, lengthening and lag; Van Loon and Van Lanen, 2012) were visible to some extent as the drought signal moves through the hydrological cycle. In the Noor catchment, the reaction of discharge and groundwater on precipitation was slow, as expected because of the large potential to store water in the thick unsaturated zone and the associated slow water table response. Multiple drought events in precipitation, therefore, led to long events in discharge and groundwater in the period 1996–1998. The discharge drought partly recovered in this period because of peaks caused by small wetland areas with a fast response in the catchment, but the groundwater drought did not end before mid 1998. Measurements of the groundwater level were missing in this part of 1998, but discharge and groundwater drought would otherwise end around the same time. Meteorological drought events were more frequent and shorter, and did not always cause a drought in discharge. The Pang catchment showed a similar behaviour in dry years (not shown). This was different in the Ourthe catchment. Because of the fast reaction of

the discharge to precipitation due to low potential to store water in the unsaturated zone and the quick response of the water table, there was some delay in the propagation, but drought events in discharge and groundwater largely coincided with meteorological drought events. They occurred more often and were shorter than in the Noor catchment.

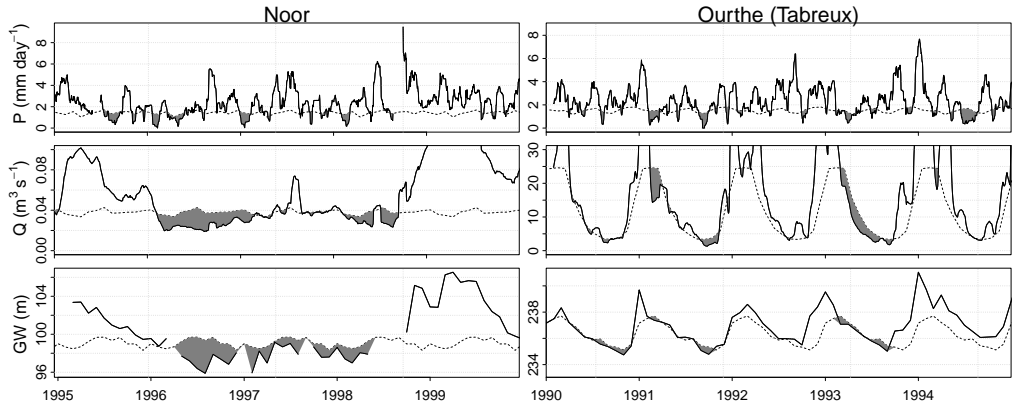


Figure 6.5: Drought occurrence (grey areas) in the Noor (left) and Ourthe (right) for precipitation (P), discharge (Q) and groundwater (GW). The black lines are the observations (for P and Q after smoothing), the dashes lines are the thresholds (based on monthly 20th percentiles).

6.4.3 Link between discharge components and drought

The influence of storage variation on drought duration is shown in Fig. 6.6. The fractions of all three components are given together with the mean drought duration (Fig. 6.6 top) and the relation between the fraction of the trend component and the mean drought duration (Fig. 6.6 bottom). The median of the drought duration found in all catchments was 41 days and there were 34 catchments with a mean duration longer than 80 days. There is a tendency that a higher fraction of the trend component led to longer drought events in discharge. An exception was the Noor catchment with a relatively short drought duration (mean average duration of 55 days). A small part of the Noor catchment reacts fast to precipitation (due to the presence of wetland areas), which caused short-lived peaks in the discharge. The daily discharge was smoothed with a 30-day moving average, but still some peaks interrupted drought events in discharge. Such interruptions end the drought, hence drought duration was shorter than expected. A pooling method could be applied to remove small peaks (Fleig et al., 2006). Other catchments that were found to have a higher trend fraction, i.e. the Pang and Hoyoux catchments, had long drought events as expected (mean average duration 113 days for Pang and 103 days for Hoyoux). The Ourthe catchment had a low trend fraction and many short drought events, which resulted in a rather low average drought duration (34 days). The larger catchments of the Meuse and the Rhine experienced short drought events as well (mean average duration of 45 days for the Meuse and 50 days for the Rhine).

In smaller catchments (between 10 and 10 000 km², the mean drought duration is clearly influenced by the fraction of the trend component. This means storage processes and the potential for storage change are important for correct drought prediction and identification. These storage processes should be included in hydrological models, otherwise drought duration will be underestimated for smaller catchments.

The potential for storage change influences drought characteristics, which is in line with the conclusions of Bloomfield and Marchant (2013). They concluded that maximum drought duration for groundwater is related to average unsaturated zone thickness and aquifer hydraulic diffusivity

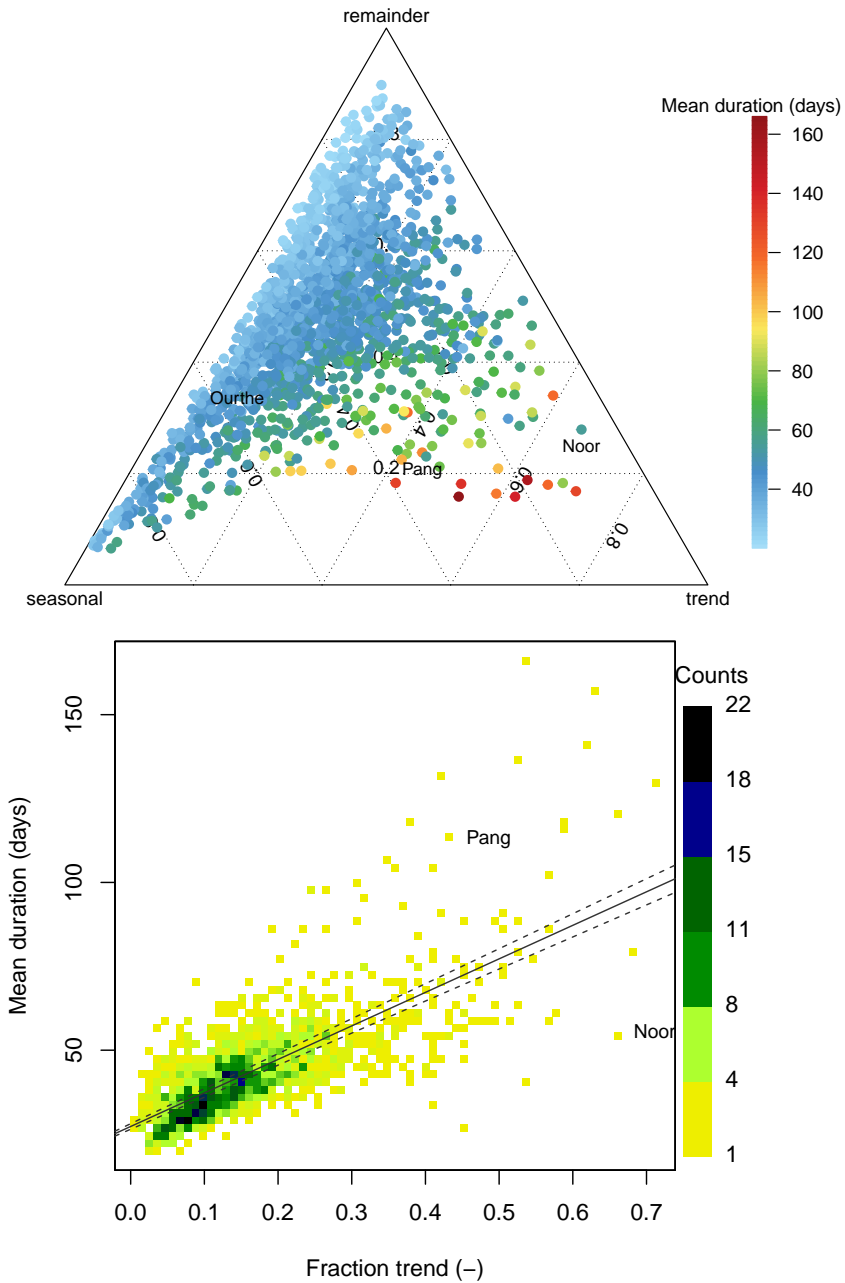


Figure 6.6: Link between the three discharge components and mean drought duration for all basins. Top) Fraction of the three components associated with mean drought duration. Bottom) Density plot for the relation between fraction of trend component and mean drought duration. The straight line is the linear regression line with confidence bounds for the 5th and 95th percentile (dashed lines).

depending on the aquifer type (e.g., fractured or granular). The findings here also correspond well with earlier studies on the propagation of drought and the role of the groundwater system (Eltahir and Yeh, 1999; Van Lanen et al., 2004; Peters et al., 2003, 2006; Van Loon and Van Lanen, 2012; Van Lanen et al., 2013). These studies also reported an increase in drought duration in slowly-responding catchments, which can have deep water tables, rather low aquifer diffusivity, high storage coefficients and low drainage density.

Besides storage processes as illustrated by the trend component, seasonality also influenced drought duration. A high fraction of the seasonality component in combination with a still relatively low fraction of the trend component also led to a longer average drought duration (Fig. 6.6 top).

The fraction of the trend component as determined with the STL method also depends on the length of the period with available data and the precipitation signal in that period. The robustness of the relation between the fraction of the trend component and the mean drought duration was evaluated for the Noor and Pang catchments. Several periods of respectively 7 years for the Noor and 10 years for the Pang were taken from the total period with available data and the fraction of the trend component and mean drought duration were determined for these periods. Although the fraction and mean duration differed considerably between the periods (not shown), they followed the relationship found in Fig. 6.6 (bottom). It is important to account for this dependence on the length of the time series when analysing discharges to identify the relation between the trend component and drought duration by testing periods of different lengths.

Overall, the number of catchments with a high fraction of the trend component found in this chapter is limited. However, there was a bias in the available data towards headwater catchments with shallow impervious layers. These catchments generally have lower fractions of the trend component, because potential for storage change is limited. The investigation of the importance of storage variation could be expanded across the globe by using the decomposition of the discharge data as an indicator. Since the analysis is based on discharge data only and these data are available in more catchments than other hydrological data, like groundwater levels, more catchments in other climate zones could be included in future research.

With the fractions of the trend component of the catchments used in this chapter, we investigated the relation between these fractions and other catchment characteristics. The locations of the catchments were linked to geology (i.e. rock type, pubs.usgs.gov/atlas/geologic and onegeology-europe.brgm.fr/), aquifer distribution (i.e. aquifer type; recharge; www.whymap.org) and the spatially-distributed simulated depth to water table (Fan et al., 2013). All these catchment characteristics play a role in the potential for storage change in a catchment, but no straightforward relationship was found with the available data, partly because some data sources provide only a broad range. Future research aims at a multivariate analysis including these and other catchment characteristics that links the occurrence of catchments with higher fractions of the trend component to the characteristics. This would indicate in which areas across the globe the storage variation is dominant.

6.5 Conclusions

Storage processes play an important role in generating the discharge of catchments, implying that hydrological drought characteristics are influenced by long-term storage variation as well. In this chapter, the storage variation was represented by the trend component of the discharge after decomposing the time series with the STL method. The fraction of the trend component was linked to mean drought duration. Slowly-responding catchments gave a higher fraction of the trend component than fast-responding catchments and the correlation between groundwater observations and the time series of the trend component was found to be high. Higher fractions of the trend component were connected to longer drought events. The fraction of the trend component also depends on the size of the catchment. Very small catchments and large catchments are less influenced by

storage variation than catchments with areas between 10 and 10 000 km². The decomposition of discharge series also depends on the length of the period with available data and the precipitation in this period. However, a robust relation was found between the fraction of the trend component and mean drought duration for periods of different lengths. This means it is important to adequately include storage processes in (large-scale) hydrological models to determine drought events correctly. In particular, the potential for storage change is critical for drought development. Without accounting for storage processes, drought duration will be underestimated. Especially large-scale models often do not include a comprehensive description of the storage processes that are important in smaller spatial units. When developing models at a higher resolution (i.e. hyper-resolution models as suggested by Wood et al., 2011), new processes that adequately account for long-term storage variation should be included to improve drought identification and prediction.

CHAPTER

7

Synthesis



7.1 Summary of results

The main objective of this thesis was to investigate the space-time development of large-scale hydrological drought for historic and future drought events through a multi-model analysis. To reach this objective three steps with different research questions were taken (Sect. 1.4). In this chapter, the main conclusions of the previous chapters will be summarized and linked to the different steps and research questions.

Multi-model hydrological drought analysis at a global scale for the 20th century

One of the objectives within this first step was to find the best way to determine the characteristics of large-scale drought. For the characterisation of hydrological drought at the global scale an identification method was needed that determined the development of drought across the globe in a consistent manner (Chapter 2). By combining two existing drought identification methods, the threshold level method and the consecutive dry period method, a more robust method was created. Drought events are allowed to start in a period with runoff and continue in a zero-runoff period. With this combined method, drought can be identified in the different climate regions across the world in a consistent way. The method is especially important for the transitional areas, where both periods with runoff and periods without runoff occur.

With the combined method the space-time development of large-scale drought was determined at a global scale (Chapters 3 and 4). Simulated time series of runoff from 10 large-scale models (Land Surface Models, LSMs, and Global Hydrological Models, GHMs) were used to identify drought. Across the world short drought events were found in areas with high runoff and long drought events in areas with low runoff, as would be expected (Fig. 4.1). Differences between the models were found for drought duration and drought occurrence caused by the model structures and parameterizations (Figs. 4.6 and 4.7). In general, major drought events could be identified in the model results.

Another objective of this step in the research was to find the relation between hydrological drought and meteorological drought at the global scale (drought propagation). The correlation between drought in runoff and drought in precipitation for several aggregation periods of precipitation differed across the globe (Chapter 4, Fig. 4.4). This means that different processes and catchment characteristics determine the propagation of drought for each climate and, therefore, runoff drought cannot be determined from precipitation data alone using a constant aggregation period across the globe.

A multi-model ensemble can be used to study major drought events at large-scale. However, spread caused by the models has to be taken into account in the drought analysis. Conclusions on global drought occurrence based on single models vary strongly depending on the model used, so a multi-model ensemble should be taken instead.

Multi-model hydrological drought analysis at a global scale for the 21st century

The impact of projected climate change on hydrological drought was investigated with three General Circulation Models (GCMs) for the A2 emission scenario in combination with five large-scale hydrological models (Chapter 5). Multiple river basins across the globe were studied and observed discharge was used to select model combinations (GHM and GCM) that performed well enough based on the Nash-Sutcliffe efficiency. The selected model combinations were used to identify changes in low flows and drought characteristics between the control period (1971–2001) and the future period (2071–2100).

Different effects of climate change on low flows were found for river basins depending on the climate zones (Fig. 5.6). Catchments in arid regions were predicted to become even drier in the future period. In cold regions, a shift of the snow melt peak and an increase in low discharges was found. For most rivers in humid and temperate climates, a large uncertainty was found in the

directionality of the changes and results were highly influenced by the combination of GHM and GCM.

The impact of climate change was also considered by investigating the changes in hydrological drought characteristics (mean duration and mean standardised deficit volume, Fig. 5.8). The drought characteristics showed an increase in most river basins towards the future, which means impacts and severity of drought events will increase as well. Changes in low flows and in drought characteristics were not always in agreement. The two methodologies of assessing the impact of climate change on low flow and drought should be used in a complementary way to get as much information as possible about changes in water availability and its variability towards the future.

Representation of drought by large-scale models

At the global scale, observed discharge data are often not available for periods that are long enough to be used for drought analysis with sufficient spatial coverage. Therefore, models are used to simulate discharges, however, validation of model results is difficult without observations. In Chapter 3, drought events derived from simulated time series of a multi-model ensemble were compared with known drought events described in literature. This led to the conclusion that major drought events in the second part of the 20th century were reproduced by the model ensemble median. Duration and spatial extent of these events, however, differed between the models and from reported events (Chapter 3). The comparison between known events and model results is difficult because of the lack of global hydrological drought studies, so different drought types had to be compared (e.g., hydrological drought with soil moisture drought). However, major drought events occur in all variables and are caused by precipitation deficits linked to climatic patterns, for example the El Niño Southern Oscillation. In Chapter 4 it was concluded by comparing drought in runoff with drought in precipitation that the large-scale models in general simulated a fast reaction of runoff to precipitation (Fig. 4.3). This indicates that the models do not include all stores that are important for runoff generation.

The influence of storage variation in a catchment on drought characteristics was investigated with observed data on smaller scales (Chapter 6). Observed discharge data for 1737 catchments or subcatchments across Europe and the United States were used. Especially the potential for storage change within a catchment is important for drought development. The long-term trend (slow-varying) component in discharge, which was obtained through a Seasonal-Trend decomposition procedure, was taken as a metric for the potential for storage change. Slowly-responding catchments, that have a higher potential for storage change, were influenced more by the long-term trend component and experienced longer drought events than fast-responding catchments. Without an adequate inclusion of storage processes in large-scale hydrological models, drought duration will be underestimated.

7.2 Discussion

With this thesis, we have contributed to the knowledge on drought development at large scales, but challenges still remain. In this section, these challenges for future work are discussed and results of this research are put into context.

7.2.1 Drought versus water scarcity

This thesis has followed the drought definition of Tallaksen and Van Lanen (2004) that “drought is a sustained and regionally extensive occurrence of below average natural water availability and can be seen as a deviation of the normal conditions”. We specifically did not take into account the human influence on drought, but only considered natural conditions (Sect. 1.2). The used model results originated from naturalised runs without human influences like, for example, abstractions,

land use change, and dams. For the drought analysis with observed discharge, catchments were chosen that were as undisturbed as possible, similar to Stahl et al. (2010, 2012). However, in large parts of the world finding catchments that are not influenced by humans at all is nearly impossible. Many catchments are influenced by dams, irrigation, land use change, and other human impacts (e.g. Dynesius and Nilsson, 1994; Vörösmarty et al., 1997; Nilsson et al., 2005). Unaffected catchments are mainly found in the northern (colder) parts of the world (Dynesius and Nilsson, 1994; Nijssen et al., 2001b). Haddeland et al. (2014) investigated the impact of human influence on water resources. They concluded that, although human impact on the long-term global terrestrial water balance was small, in several river basins the impacts are significant and even stronger than the projected changes for climate change. This raises the question whether drought can be studied without taking into account human influence and whether it is possible to completely separate drought from water scarcity.

An observation-modelling framework to distinguish between drought (natural causes) and water scarcity (human influence) was proposed by Van Loon and Van Lanen (2013). They demonstrate the framework for a catchment in Spain that is heavily influenced and show that drought events were much longer in the situation with human influence than in a naturalised situation. Wada et al. (2013a) performed a similar analysis to quantify human influence at the global scale. According to Wada et al. (2013a), human influence intensifies hydrological drought (with natural causes) in large parts of the world and managing water demand is important to cope with drought conditions.

Besides the direct effect of human water demand on water scarcity, it is also important to take into account the ability of a region to cope with dry conditions. The vulnerability of a region largely determines the consequences of a drought. By separating natural causes and human influences on the water availability, management plans can be developed focused on adaptation to (changes in) climate variability or on reduction of the human water demand (Van Loon and Van Lanen, 2013). Because large parts of the world are heavily influenced by humans, drought research should not be restricted to natural causes only, but water scarcity should be integrated more in the future.

7.2.2 Drought identification methods

In this thesis, a drought identification method was developed for analysis at the global scale. Many indices already exist to identify the different drought types (meteorological, soil moisture, and hydrological). All these indices make it difficult to compare the outcomes of drought research. These outcomes are very dependent on the identification method and definitions that are used (e.g. Seneviratne et al., 2012). For example, Sheffield et al. (2012) showed that the method used for calculation of the potential evaporation in one particular drought index, i.e. the Palmer Drought Severity Index (PDSI), has a very large effect on the change in global area in drought over the past 60 years. Using a different method to calculate the potential evaporation in the PDSI, they estimated that there was little change in soil moisture drought, whereas Dai (2011, 2013) found an increase in drought severity. The difference between these specific studies (Sheffield et al., 2012; Dai, 2013) was explained in more detail by Trenberth et al. (2014). They concluded that the differences between the changes in drought are not only caused by the PDSI calculation, but mainly by the disparities between precipitation data sets.

We believe that the combined method described in this thesis (Chapter 2) can be an important additional analytical tool for global drought studies to deal with areas where intermittent runoff is common. The threshold level method, which is applied to rivers with perennial runoff, has advantages and disadvantages. Choices have to be made to determine the threshold value if this value is not provided by potentially impacted sectors (e.g., ecological minimum flow). In this thesis, the 20th percentile was chosen as a threshold to be consistent with other drought studies (e.g. Andreadis et al., 2005; Sheffield and Wood, 2007; Tallaksen et al., 2009; Van Lanen et al.,

2013; Wada et al., 2013a). Also the choice for a minimum drought duration or a pooling method is subjective (Fleig et al., 2006).

In order to obtain more consistent drought studies, the use of a set of common indices addressing each of the different drought types could be a step forward. We have shown that the use of one index to describe all drought types is not desirable. The Standardised Precipitation Index (SPI) is regularly used as a hydrological drought index by taking several aggregation periods of the precipitation (e.g. Nalbantis and Tsakiris, 2009; Zhai et al., 2010; Dai, 2011). In Chapter 4 we have shown that the development of meteorological and hydrological drought differs. Bloomfield and Marchant (2013) found a very site specific relation between SPI and their Standardised Groundwater level Index (SGI). For each site a different SPI aggregation period led to the strongest correlation between SPI and SGI. Hydrological drought events are affected by more factors than just the precipitation, such as groundwater storage, lakes and other catchment characteristics (Tallaksen and Van Lanen, 2004; Van Loon et al., 2012; Van Lanen et al., 2013).

To study drought across the hydrological cycle while taking into account the different processes that affect each drought type, a set of different indices to cover all drought types could be used. The US drought monitor (droughtmonitor.unl.edu) from the National Drought Mitigation Center is based on several drought indices to take into account multiple variables in the identification of drought. The Joint Research Centre monitors the drought situation across Europe with the European Drought Observatory (edo.jrc.ec.europa.eu/). Several indices are compared and a combined drought index is calculated to determine the current drought situation. An agreed set of indices (and guidelines on how to calculate them) applicable to all different drought types and adapted to the specific purpose of each drought study, e.g., for a specific impact, should become available to enable comparison between all drought studies.

7.2.3 Large-scale modelling

In this thesis, results from multiple large-scale models made available through the WATCH project were used to identify drought. It was specifically not our intention to evaluate individual models or to judge individual model performance. Because all models have different parameterizations and model structures, it is not possible to indicate what causes the differences between model results, so results from a multi-model ensemble were taken instead. From this ensemble, several processes could be identified that cause differences in the drought analysis between the models and observations. Examples are the implementation of snow processes, such as accumulation, sublimation and melt, and differences in the partitioning of precipitation into rainfall and snowfall between the models (Haddeland et al., 2011). We have found larger differences between drought characteristics in cold climates, which corresponds with other studies for Europe that have found that model performance in simulating the observed hydrological response is lower in regions with snow influence than in regions without snow (Stahl et al., 2012; Gudmundsson et al., 2012b).

In Fig. 7.1 a general representation of a large-scale hydrological model is given. This representation already indicates that some processes are missing in the large-scale models. In this thesis, one of the main processes found to be missing or not adequately represented was storage, in particular a groundwater store. In general, the models showed a fast reaction to precipitation and lacked multi-year drought events. These results are consistent with the conclusions of Wang et al. (2009), Stahl et al. (2012) and Gudmundsson et al. (2012a). More research on the propagation of drought in the large-scale models, as was done by Van Loon et al. (2012) for several grid cells, is important to determine model performance in more detail. A range of output variables, such as evaporation, soil moisture storage, and groundwater storage, if available, could be used for such an analysis. Besides a lack of storage, also lateral interaction of the groundwater (between cells) is missing in the large-scale models. A coupling between a land-surface model and groundwater model was made by Sutanudjaja et al. (2011), which is an important step towards improving groundwater processes in large-scale models.

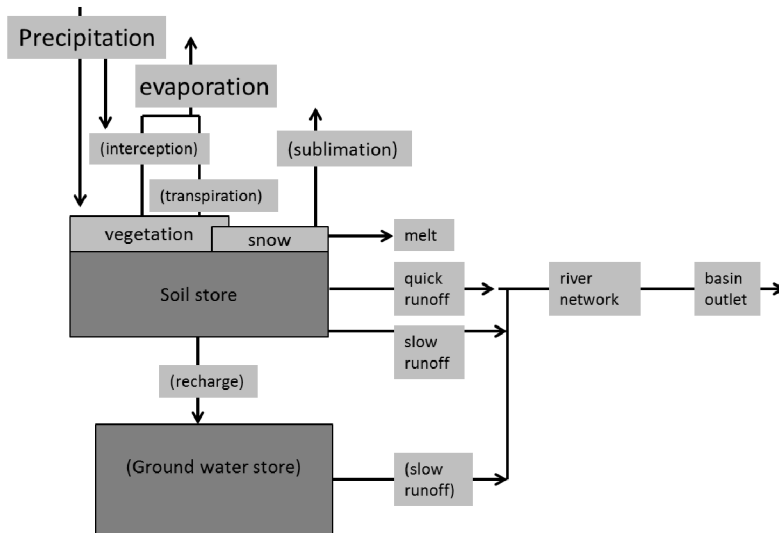


Figure 7.1: General model structure of large-scale hydrological models as presented by Harding et al. (2011). Processes missing in some models are indicated by brackets. ©American Meteorological Society. Used with permission.

Identifying the missing processes is an important step towards the improvement of the models. Another step is modelling at a higher resolution. The development of a hyperresolution model is indicated as “a grand challenge for hydrology” (Wood et al., 2011). This model could be used to address all sorts of questions involving the terrestrial water cycle. However, before such a model can be developed, knowledge about hydrological processes at the hyperresolution scale has to be increased, including hyperresolution data. Beven and Cloke (2012) indicate that only moving to finer resolutions will not be enough. One of the main challenges in developing such a model is improving the surface and subsurface interaction at finer resolution (Wood et al., 2011).

As we have shown in Chapter 6 of this thesis, the potential for storage in a catchment is an important factor for a proper assessment of drought characteristics. In Chapter 6, observed discharge data from an extensive set of catchments across Europe and the United States were used to quantify the relation between long-term storage variation and drought duration. To show the differences between large-scale model results and observations, which is complementary to the results described in Chapter 6, drought characteristics were also identified from the model discharge results for the grid cells in which the catchments are located (Fig. 7.2). The model results and observed data are not directly comparable, because of the difference between the size of the catchments and the size of the grid cells. Most catchments were rather small (Fig. 6.2) compared to the size of the grid cells. The different grid cells of a certain model gave a range of drought characteristics, indicating the differences in storage processes between the grid cells. The model results gave a large spread in mean duration of the drought events (Fig. 7.2). Mean drought duration was very low compared to observations in some models (H08 and LPJml), whereas other models (JULES and WaterGAP) gave mean drought durations that were more comparable with the observed data. Results from MATSIRO showed an overestimation of the drought duration and much more slowly-responding systems than the other model results. This indicates the different implementation of storage processes in each model. This distinction between models was also found by Tallaksen and Stahl (2014), who separated a slightly different set of large-scale models in two groups based on the persistence in drought and reaction time: Group 1 (GWAVA, HTESSEL, JULES and WaterGAP) and Group 2 (LPJml, MPI-HM and Orchidee). These groups correspond

well with the behaviour of the models found in Fig. 7.2. However, the relation between the importance of each discharge component and the mean duration is quite similar between the models and between model results and observed data. Long drought events were only found in combination with a high fraction of the trend (slow-varying) component (red points in the right corner, Fig. 7.2) and low fractions of the trend component were combined with short durations (blue points in the upper corner, Fig. 7.2). A combination of a long mean duration and low fraction of the trend component was not found. Overall, improvement of the implementation of storage processes could lead to less uncertainty between the models and more robust drought predictions.

To determine in which parts of the world storage plays an important role, information is needed about groundwater occurrence, aquifer thickness and water table depths across the globe. The water table depth is linked to the potential of storage change. A global map with groundwater level observations is not available yet. Fan et al. (2013) have studied the groundwater table depth at the global scale. They simulated the global water table depth based on observations and model results and found that 22 to 32% of the global land area is influenced by shallow groundwater (Fan et al., 2013). This indicates again the need to improve the implementation of groundwater and storage processes in large-scale models.

Another important step towards improving large-scale models (GHMs and LSMs) is model validation. Observed hydrological data are needed to validate models, but these data are often missing at the global scale. Improved large-scale datasets and more flexible data structures are needed to support spatially detailed research with large-scale models (Lehner and Grill, 2013). Lehner and Grill (2013) describe a global hydrological database (HydroSHEDS) and a new river network routing model (HydroROUT) that can be used for such research. Satellite remote sensing also provides new opportunities for data collection (Wood et al., 2011). For example, the gravity-based terrestrial water storage can be determined from the Gravity Recovery and Climate Experiment (GRACE), but time series are rather short for drought analysis. Observed datasets are also important to avoid overparameterization of the models; more data can help constrain the parameters and by improving knowledge on the processes less parameters are needed in the models (Kirchner, 2006). Large-scale datasets with hydrometeorological observations are essential for the assessment of hydrological changes across the globe and to increase our knowledge of the hydrological system at a global scale.

7.2.4 Drought and climate change

Even though drought is expected to increase in severity and intensity in multiple regions in many studies (e.g. Bates et al., 2008; Dai, 2011; Romm, 2011; Seneviratne et al., 2012; Prudhomme et al., 2014), the IPCC (Stocker et al., 2013) still considers the “regional and global-scale projections of soil moisture and drought relatively uncertain compared to other aspects of the water cycle”. This indicates more research is still needed to assess the effects of climate change on drought occurrence. Trends in hydrological drought for the 20th century have shown both increases and decreases in the land area affected by drought, which resulted in a low confidence assessment of observed and attributable large-scale trends (Stocker et al., 2013). The main reasons indicated by the IPCC (Stocker et al., 2013) for this low confidence are “lack and quality of direct observations, dependencies of inferred trends on the index choice, geographical inconsistencies in the trends and difficulties in distinguishing decadal scale variability from long term trends”. This again stresses the need for improved observational datasets and the use of a set of uniform drought indices (Sect. 7.2.2).

Despite the low confidence in past drought trends, likely drying in soil moisture is projected in the Mediterranean, southwestern U.S. and south African regions under the extreme RCP8.5 scenario (Stocker et al., 2013). Regarding changes in annual runoff, decreases are likely in southern Europe and the Middle East, while increases are likely in high northern latitude regions (Stocker et al., 2013). These changes are in correspondence with the changes found in Chapter 5 of this thesis and other studies (e.g. Nohara et al., 2006; Sperna Weiland et al., 2012; Arnell and Gosling, 2013; Forzieri et al., 2014).

Multiple hydrological models were used to assess changes in discharge across the globe. Although uncertainty in projections increases by using multiple models, an ensemble is recommended to include all possible model structures (Haddeland et al., 2011). Since discharge is dependent on catchment characteristics and not only on the change in precipitation, hydrological models have to be included in climate change impact studies instead of determining changes from GCM output directly (Hagemann et al., 2013; Prudhomme et al., 2014). However, increasing the number of models in impact studies is not the ultimate solution to improve confidence in future projections. As stated by Harding et al. (2011): “The improvement of our simulations of regional precipitation will take many years, if not decades. In the meantime, the community needs to find ways of providing meaningful assessments of future water resources to policy makers and other stakeholders. This must include a realistic discussion of uncertainty and risk that does not swamp the key message that the hydrological cycle will change in the future under the combined pressures of changing climate and increasing demands of agriculture, industry, and water supply.”

A realistic view of the uncertainties in projected climate change effects on drought and reducing these uncertainties is important for adequate measures to ensure water availability in the future. In Chapter 5, an attempt was made to reduce the uncertainty by selecting model combinations (GHM and GCM) based on their performance in the past. Although some previous studies have argued not to select models to keep as much information as possible in the ensemble and have stated that performance in the past might not be representative for the future (Reifen and Toumi, 2009; Gosling et al., 2011), it is clear that a reduction of the large range in model projections is necessary. We believe that models with a very low performance against observations should not be included in future projections. However, more research is needed to determine the best methods to judge the performance of models in the past. A set of criteria to compare observations and model results might be the best way forward.

Another source of uncertainty in future projections of hydrological drought is the drought identification method that is applied. In Chapter 5 we have shown that it is important to include both low flows and drought characteristics to assess changes in the future. The variable threshold level method showed difficulties with drought identification in cold climates due to a shift in the snow melt peak (Fig. 5.9). Using the same threshold in the control period and future period ignores the natural variability of the climate over 100 years and the ability of the system to adapt to changes. Vidal et al. (2012) include this adaptation by linking the threshold to adaptation scenarios. Although these adaptation scenarios could add uncertainty to the assessment, this could be a promising way to identify drought in the future.

Uncertainty in drought projections caused by the drought index used was also found in studies for different drought types (Burke and Brown, 2008; Burke, 2011; Taylor et al., 2013). Different reactions to changes in the climate were found for indices representing the different drought types, namely SPI, Soil Moisture Anomaly (SMA), PDSI, and Standardised Runoff Index (SRI). Each of these indices projected different increases or decreases of the areas in drought (Taylor et al., 2013). Taylor et al. (2013) suggest that only one index may not be representative for all possible future changes in drought. Overall, finding the best drought identification methods both for the past and for the future remains an important challenge in drought research.

7.3 Outlook for large-scale drought analysis

Several recommendations for future research were given in the previous section. Although some aspects of drought analyses in general could be improved, it is not my intention to change this kind of analyses completely. Large-scale models can and should be improved, but already provide useful information about drought development at the global scale. Especially in assessing the influence of climate change on drought, they can play an important role. In Fig. 7.3, a schematic overview of the different steps in large-scale drought analysis both for historic and future drought is given. This framework follows the steps taken in traditional drought analysis, but some im-

provements and areas for future research mentioned above are indicated. The framework starts with forcing data on the left hand side (a in Fig. 7.3), these forcing data can be either observed data, modelled data, or a combination. This thesis has focused on hydrological drought and therefore the uncertainty in the forcing data was not explicitly taking into account. The forcing data used to run the models in this thesis are developed with state-of-the-art bias-correction and down-scaling methods. Time series of runoff and discharge can be simulated with an ensemble of large-scale models (b in Fig. 7.3b). From these time series hydrological drought can be identified with a suitable set of indices (d in Fig. 7.3).

I will focus here on the main challenges for hydrological drought analysis using large-scale models only, not including the forcing data. This research has contributed to meeting these challenges. Two main challenges left are:

- improvement of the structure of large-scale models to reduce uncertainties in the simulations,
- agreement on a set of indices suitable for historic and future hydrological drought analysis and concise development of guidelines on how to calculate these indices.

To face the challenge of model structure improvement, it is essential to have observed data to validate the models and to increase knowledge on hydrological processes. Process understanding is needed to develop adequate model structures (e.g. Beven and Cloke, 2012). Especially the storage processes at smaller scales have to be incorporated more accurately in large-scale models. Many other studies have indicated the lack of reliable observations as problematic for hydrological modelling (e.g. Kirchner, 2006). Differences in observations (i.e. precipitation data sets) can have a large influence on the results of drought analysis (Trenberth et al., 2014). Therefore, investments to obtain large-scale observed datasets are as important as investments to develop (hyperresolution) hydrological models.

Overall, large-scale models are an important tool to assess water availability at the global scale and can be employed to estimate current and future drought situations. The knowledge gained by evaluating these model results, in combination with increased hydrological process understanding derived from observed data, can play an important role in safeguarding water availability for future generations.

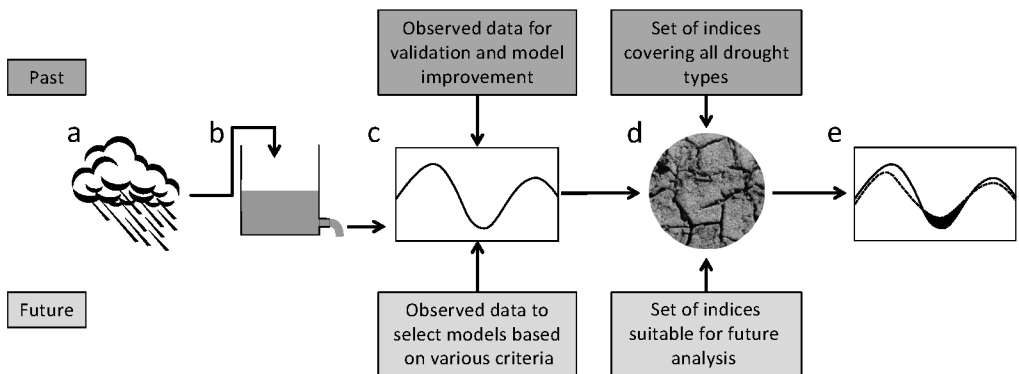


Figure 7.3: Framework for large-scale drought analysis. Main challenges for future research are indicated. The framework starts with forcing data (a) on the left side, these data are then used in hydrological models (b), and a drought analysis (d) can be performed on the model output (c), which results in identified drought events (e).



APPENDIX

A

Main characteristics of the large-scale models



Table A.1: Main characteristics of the selected models (derived from Haddeland et al., 2011)

Model name	Model time step	Meteorological forcing variables ^a	Energy balance	Evapotranspiration scheme ^b	Runoff scheme ^c	Snow scheme	Reference(s)
GWAVA	Daily	P, T, W, Q, LWn, SW, SP	No	Penman-Monteith	Saturation excess/ Beta function	Degree day	Meigh et al. (1999)
H08	6 h	R, S, T, W, Q, LW, SW, SP	Yes	Bulk formula	Saturation excess/ Beta function	Energy balance	Hanasaki et al. (2008)
HTESEL	1 h	R, S, T, W, Q, LW, SW, SP	Yes	Penman-Monteith	Variable infiltration capacity/ Darcy	Energy balance	Balsamo et al. (2009)
JULES	1 h	R, S, T, W, Q, LW, SW, SP	Yes	Penman-Monteith	Infiltration excess/ Darcy	Energy balance	Best et al. (2011); Clark et al. (2011)
LPJmL	Daily	P, T, LWn, SW	No	Priestley-Taylor	Saturation excess	Degree day	Bondeau et al. (2007); Rost et al. (2008)
Mac-PDM	Daily	P, T, W, Q, LWn, SW	No	Penman-Monteith	Saturation excess/ Beta function	Degree day	Arnell (1999a); Gosling and Arnell (2011)
MATSIRO	1 h	R, S, T, W, Q, LW, SW, SP	Yes	Bulk formula	Infiltration and saturation excess/ Groundwater	Energy balance	Takata et al. (2003); Koirala (2010)
MPI-HIM	Daily	P, T	No	Thorntwaite	Saturation excess/ Beta function	Degree day	Hagemann and Gates (2003); Hagemann and Dümenil (1998)
Orchidee	15 min	R, S, T, W, Q, SW, LW, SP	Yes	Bulk formula	Saturation excess	Energy balance	De Rosnay and Polcher (1998)
WaterGAP	Daily	P, T, LWn, SW	No	Priestley-Taylor	Beta function	Degree day	Alcamo et al. (2003)

a) R: Rainfall rate, S: Snowfall rate, P: Precipitation (rain or snow distinguished in the model), T: air temperature, W: Wind speed,

Q: Specific humidity, LW: Longwave radiation flux (downward), LWn: Longwave radiation flux (net),

SW: Shortwave radiation flux (downward), SP: Surface pressure

b) Bulk formula: Bulk transfer coefficients are used when calculating the turbulent heat fluxes.

c) Beta function: Runoff is a nonlinear function of soil moisture.



Bibliography

- Alcamo, J., Döll, P., Henrichs, T., Kaspar, F., Lehner, B., Rösch, T., Siebert, S., 2003. Development and testing of the WaterGAP 2 global model of water use and availability. *Hydrol. Sci. J.* 48 (3), 317–337, doi: 10.1623/hysj.48.3.317.45290.
- Alley, W. M., 1984. The Palmer Drought Severity Index - Limitations and Assumptions. *J. Clim. Appl. Meteorol.* 23 (7), 1100–1109, doi:10.1175/1520-0450(1984)023<1100:TPDSIL>2.0.CO;2.
- Andreadis, K. M., Clark, E. A., Wood, A. W., Hamlet, A. F., Lettenmaier, D. P., 2005. Twentieth-century drought in the conterminous United States. *J. Hydrometeorol.* 6 (6), 985–1001, doi:10.1175/JHM450.1.
- Andreadis, K. M., Lettenmaier, D. P., 2006. Trends in 20th century drought over the continental United States. *Geophys. Res. Lett.* 33 (10), L10403, doi:10.1029/2006GL025711.
- Anyah, R. O., Weaver, C. P., Miguez-Macho, G., Fan, Y., Robock, A., 2008. Incorporating water table dynamics in climate modeling: 3. Simulated groundwater influence on coupled land-atmosphere variability. *J. Geophys. Res., Atmos.* 113 (D7), D07103, doi:10.1029/2007JD009087.
- Arnell, N. W., 1999a. A simple water balance model for the simulation of streamflow over a large geographic domain. *J. Hydrol.* 217 (3–4), 314–335, doi:10.1016/S0022-1694(99)00023-2.
- Arnell, N. W., 1999b. Climate change and global water resources. *Glob. Environ. Chang.* 9, Supplement 1 (0), S31–S49, doi:10.1016/S0959-3780(99)00017-5.
- Arnell, N. W., 2003. Effects of IPCC SRES* emissions scenarios on river runoff: a global perspective. *Hydrol. Earth System Sci.* 7 (5), 619–641, doi:10.5194/hess-7-619-2003.
- Arnell, N. W., Gosling, S. N., 2013. The impacts of climate change on river flow regimes at the global scale. *J. Hydrol.* 486 (0), 351–364, doi:10.1016/j.jhydrol.2013.02.010.
- Arora, V. K., Boer, G. J., 2001. Effects of simulated climate change on the hydrology of major river basins. *J. Geophys. Res., Atmos.* 106 (D4), 3335–3348, doi:10.1029/2000JD900620.
- Balsamo, G., Viterbo, P., Beljaars, A., Van Den Hurk, B., Hirschi, M., Betts, A. K., Scipal, K., 2009. A revised hydrology for the ECMWF model: Verification from field site to terrestrial water storage and impact in the integrated forecast system. *J. Hydrometeorol.* 10 (3), 623–643, doi:10.1175/2008JHM1068.1.
- Bates, B. C., Kundzewicz, Z. W., Wu, S., Palutikof, J. P. (Eds.), 2008. *Climate Change and Water*. Technical Paper of the Intergovernmental Panel on Climate Change, Intergovernmental Panel on Climate Change, Geneva.
- Bell, G. D., Halpert, M. S., 1998. Climate assessment for 1997. *Bull. Am. Meteorol. Soc.* 79 (5), S1–S50, doi: 10.1175/1520-0477(1998)079<1014:CAF>2.0.CO;2.
- Best, M. J., Pryor, M., Clark, D. B., Rooney, G. G., Essery, R. L. H., Ménard, C. B., Edwards, J. M., Hendry, M. A., Porson, A., Gedney, N., Mercado, L. M., Sitch, S., Blyth, E., Boucher, O., Cox, P. M., Grimmond, C. S. B., Harding, R. J., 2011. The Joint UK Land Environment Simulator (JULES), model description - Part 1: Energy and water fluxes. *Geosci. Model Dev.* 4 (3), 677–699, doi:10.5194/gmd-4-677-2011.
- Beven, K. J., Cloke, H. L., 2012. Comment on “Hyperresolution global land surface modeling: Meeting a grand challenge for monitoring Earth’s terrestrial water” by Eric F. Wood et al. *Water Resour. Res.* 48, W01801, doi: 10.1029/2011WR010982.
- Birkel, C., Soulsby, C., Tetzlaff, D., 2011. Modelling catchment-scale water storage dynamics: reconciling dynamic storage with tracer-inferred passive storage. *Hydrol. Process.* 25 (25), 3924–3936, doi: 10.1002/hyp.8201.
- Bloomfield, J. P., Marchant, B. P., 2013. Analysis of groundwater drought building on the standardised precipitation index approach. *Hydrol. Earth System Sci.* 17 (12), 4769–4787, doi:10.5194/hess-17-4769-2013.
- BoM, 1997. *Living with Drought*. Tech. rep., Australian Bureau of Meteorology, accessed: 07-2011. URL <http://www.bom.gov.au/climate/drought/livedrought.shtml>
- Bondeau, A., Smith, P. C., Zaehle, S., Schaphoff, S., Lucht, W., Cramer, W., Gerten, D., 2007. Modelling the role of agriculture for the 20th century global terrestrial carbon balance. *Glob. Chang. Biol.* 13 (3), 679–706,

- doi:10.1111/j.1365-2486.2006.01305.x.
- Bordi, I., Fraedrich, K., Sutera, A., 2009. Observed drought and wetness trends in Europe: an update. *Hydrol. Earth System Sci.* 13 (8), 1519–1530, doi:10.5194/hess-13-1519-2009.
- Bradford, R. B., 2000. Drought events in Europe. In: Vogt, J. V., Somma, F. (Eds.), *Drought and Drought Mitigation in Europe*. Vol. 14 of *Advances in natural and technological hazards research*. Kluwer Academic Publishers, Dordrecht, The Netherlands, pp. 7–20.
- Brauer, C. C., Teuling, A. J., Torfs, P. J. F., Uijlenhoet, R., 2013. Investigating storage-discharge relations in a lowland catchment using hydrograph fitting, recession analysis, and soil moisture data. *Water Resour. Res.* 49 (7), 4257–4264, doi:10.1002/wrcr.20320.
- Burke, E. J., 2011. Understanding the Sensitivity of Different Drought Metrics to the Drivers of Drought under Increased Atmospheric CO₂. *J. Hydrometeorol.* 12 (6), 1378–1394, doi:10.1175/2011JHM1386.1.
- Burke, E. J., Brown, S. J., 2008. Evaluating uncertainties in the projection of future drought. *J. Hydrometeorol.* 9 (2), 292–299, doi:10.1175/2007JHM929.1.
- Chang, F., Chen, C. J., Lu, C. J., 2004. A linear-time component-labeling algorithm using contour tracing technique. *Comput. Vis. Image Und.* 93 (2), 206–220, doi:10.1016/j.cviu.2003.09.002.
- Chen, C., Haerter, J. O., Hagemann, S., Piani, C., 2011. On the contribution of statistical bias correction to the uncertainty in the projected hydrological cycle. *Geophys. Res. Lett.* 38 (20), L20403, doi:10.1029/2011GL049318.
- Chiew, F. H. S., McMahon, T. A., 2002. Global ENSO-streamflow teleconnection, streamflow forecasting and interannual variability. *Hydrol. Sci. J.* 47 (3), 505–522, doi:10.1080/02626660209492950.
- Clark, D. B., Mercado, L. M., Sitch, S., Jones, C. D., Gedney, N., Best, M. J., Pryor, M., Rooney, G. G., Essery, R. L. H., Blyth, E., Boucher, O., Harding, R. J., Huntingford, C., Cox, P. M., 2011. The Joint UK Land Environment Simulator (JULES), model description - Part 2: Carbon fluxes and vegetation dynamics. *Geosci. Model Dev.* 4 (3), 701–722, doi:10.5194/gmd-4-701-2011.
- Cleveland, R. B., Cleveland, W. S., McRae, J. E., Terpenning, I., 1990. STL: A Seasonal-Trend Decomposition Procedure Based on Loess. *Journal of Official Statistics* 6 (1), 3–73.
- Corzo Perez, G. A., Van Huijgevoort, M. H. J., Voß, F., Van Lanen, H. A. J., 2011. On the spatio-temporal analysis of hydrological droughts from global hydrological models. *Hydrol. Earth System Sci.* 15 (9), 2963–2978, doi:10.5194/hess-15-2963-2011.
- Covey, C., AchutaRao, K. M., Cubasch, U., Jones, P., Lambert, S. J., Mann, M. E., Phillips, T. J., Taylor, K. E., 2003. An overview of results from the Coupled Model Intercomparison Project. *Global Planet. Change* 37 (1-2), 103–133, doi:10.1016/S0921-8181(02)00193-5.
- Creutzfeldt, B., Troch, P. A., Güntner, A., Ferré, T. P. A., Graeff, T., Merz, B., 2014. Storage-discharge relationships at different catchment scales based on local high-precision gravimetry. *Hydrol. Process.* 28 (3), 1465–1475, doi:10.1002/hyp.9689.
- Dai, A., 2011. Drought under global warming: a review. *WIREs Clim. Change* 2 (1), 45–65, doi:10.1002/wcc.81.
- Dai, A., 2013. Increasing drought under global warming in observations and models. *Nature Clim. Change* 3 (1), 52–58, doi:10.1038/nclimate1633.
- Dai, A., Qian, T. T., Trenberth, K. E., Milliman, J. D., 2009. Changes in Continental Freshwater Discharge from 1948 to 2004. *J. Clim.* 22 (10), 2773–2792, doi:10.1175/2008JCLI2592.1.
- Dai, A., Trenberth, K. E., Qian, T. T., 2004. A global dataset of Palmer Drought Severity Index for 1870–2002: Relationship with soil moisture and effects of surface warming. *J. Hydrometeorol.* 5 (6), 1117–1130, doi:10.1175/JHM-386.1.
- Davie, J. C. S., Falloon, P. D., Kahana, R., Dankers, R., Betts, R., Portmann, F. T., Wisser, D., Clark, D. B., Ito, A., Masaki, Y., Nishina, K., Fekete, B., Tessler, Z., Wada, Y., Liu, X., Tang, Q., Hagemann, S., Stacke, T., Pavlick, R., Schaphoff, S., Gosling, S. N., Franssen, W., Arnell, N., 2013. Comparing projections of future changes in runoff from hydrological and biome models in ISI-MIP. *Earth Syst. Dynam.* 4 (2), 359–374, doi:10.5194/esd-4-359-2013.
- De Rosnay, P., Polcher, J., 1998. Modelling root water uptake in a complex land surface scheme coupled to a GCM. *Hydrol. Earth System Sci.* 2 (2-3), 239–255, doi:10.5194/hess-2-239-1998.
- De Wit, M. J. M., Van Den Hurk, B., Warmerdam, P. M. M., Torfs, P. J. F., Roulin, E., Van Deursen, W. P. A., 2007. Impact of climate change on low-flows in the river Meuse. *Clim. Chang.* 82 (3-4), 351–372, doi:

- 10.1007/s10584-006-9195-2.
- Deni, S. M., Jemain, A. A., 2009. Mixed log series geometric distribution for sequences of dry days. *Atmos. Res.* 92 (2), 236–243, doi:10.1016/j.atmosres.2008.10.032.
- Dirmeyer, P. A., Gao, X., Zhao, M., Guo, Z., Oki, T., Hanasaki, N., 2006. GSWP-2: Multimodel Analysis and Implications for Our Perception of the Land Surface. *Bull. Amer. Meteor. Soc.* 87 (10), 1381–1397, doi:10.1175/BAMS-87-10-1381.
- Dracup, J. A., Lee, K. S., Paulson, E. G., 1980. On the definition of droughts. *Water Resour. Res.* 16 (2), 297–302, doi:10.1029/WR016i002p00297.
- Driessen, T. L. A., Hurkmans, R. T. W. L., Terink, W., Hazenberg, P., Torfs, P. J. J. F., Uijlenhoet, R., 2010. The hydrological response of the Ourthe catchment to climate change as modelled by the HBV model. *Hydrol. Earth System Sci.* 14 (4), 651–665, doi:10.5194/hess-14-651-2010.
- Duan, Q., Ajami, N. K., Gao, X., Sorooshian, S., 2007. Multi-model ensemble hydrologic prediction using Bayesian model averaging. *Adv. Water Resour.* 30 (5), 1371–1386, doi:10.1016/j.advwatres.2006.11.014.
- Duan, Q., Schaake, J., Andréassian, V., Franks, S., Goteti, G., Gupta, H., Gusev, Y., Habets, F., Hall, A., Hay, L., Hogue, T., Huang, M., Leavesley, G., Liang, X., Nasonova, O., Noilhan, J., Oudin, L., Sorooshian, S., Wagener, T., Wood, E., 2006. Model Parameter Estimation Experiment (MOPEX): An overview of science strategy and major results from the second and third workshops. *J. Hydrol.* 320 (1-2), 3–17, doi:10.1016/j.jhydrol.2005.07.031.
- Dutra, E., Magnusson, L., Wetterhall, F., Cloke, H. L., Balsamo, G., Boussetta, S., Pappenberger, F., 2013. The 2010-2011 drought in the Horn of Africa in ECMWF reanalysis and seasonal forecast products. *Int. J. Climatol.* 33 (7), 1720–1729, doi:10.1002/joc.3545.
- Dynesius, M., Nilsson, C., 1994. Fragmentation and Flow Regulation of River Systems in the Northern Third of the World. *Science* 266 (5186), 753–762, doi:10.1126/science.266.5186.753.
- Eltahir, E. A. B., Yeh, P. J.-F., 1999. On the asymmetric response of aquifer water level to floods and droughts in Illinois. *Water Resour. Res.* 35 (4), 1199–1217, doi:10.1029/1998WR900071.
- EurAqua, 2004. Towards a European Drought Policy. Discussion document. EurAqua Secretariat, CEH, Wallingford, UK.
- European Commission, 2006. Water Scarcity and Drought First Interim Report. Brussels, Belgium.
- European Commission, 2007. Communication Addressing the challenge of water scarcity and droughts in the European Union, (COM(2007) 414), Brussels, Belgium.
- European Environment Agency, 2010. Mapping the impacts of natural hazards and technological accidents in Europe. An overview of the last decade. Tech. Rep. 13, Copenhagen, Denmark.
- Fan, Y., Li, H., Miguez-Macho, G., 2013. Global Patterns of Groundwater Table Depth. *Science* 339 (6122), 940–943, doi:10.1126/science.1229881.
- Feyen, L., Dankers, R., 2009. Impact of global warming on streamflow drought in Europe. *J. Geophys. Res., Atmos.* 114, 17, doi:10.1029/2008JD011438.
- Fichefet, T., Morales Maqueda, M. A., 1997. Sensitivity of a global sea ice model to the treatment of ice thermodynamics and dynamics. *J. Geophys. Res. Oceans* 102 (C6), 12609–12646, doi:10.1029/97JC00480.
- Fischer, E. M., Seneviratne, S. I., Luethi, D., Schaer, C., 2007. Contribution of land-atmosphere coupling to recent European summer heat waves. *Geophys. Res. Lett.* 34 (6), L06707, doi:10.1029/2006GL029068.
- Fleig, A. K., Tallaksen, L. M., Hisdal, H., Demuth, S., 2006. A global evaluation of streamflow drought characteristics. *Hydrol. Earth System Sci.* 10 (4), 535–552, doi:10.5194/hess-10-535-2006.
- Forzieri, G., Feyen, L., Rojas, R., Flörke, M., Wimmer, F., Bianchi, A., 2014. Ensemble projections of future streamflow droughts in Europe. *Hydrol. Earth System Sci.* 18 (1), 85–108, doi:10.5194/hess-18-85-2014.
- Fraser, E. D. G., Simelton, E., Termansen, M., Gosling, S. N., South, A., 2013. “Vulnerability hotspots”: Integrating socio-economic and hydrological models to identify where cereal production may decline in the future due to climate change induced drought. *Agric. For. Meteorol.* 170, 195–205, doi:10.1016/j.agrformet.2012.04.008.
- Fundel, F., Jörg-Hess, S., Zappa, M., 2013. Monthly hydrometeorological ensemble prediction of streamflow droughts and corresponding drought indices. *Hydrol. Earth System Sci.* 17 (1), 395–407, doi:10.5194/hess-17-395-2013.

- Gao, X., Dirmeyer, P. A., 2006. A multimodel analysis, validation, and transferability study of global soil wetness products. *J. Hydrometeorol.* 7 (6), 1218–1236, doi:10.1175/JHM551.1.
- Giorgi, F., Francisco, R., 2000. Uncertainties in regional climate change prediction: a regional analysis of ensemble simulations with the HADCM2 coupled AOGCM. *Clim. Dyn.* 16 (2-3), 169–182, doi:10.1007/PL00013733.
- Goosse, H., Fichefet, T., 1999. Importance of ice-ocean interactions for the global ocean circulation: A model study. *J. Geophys. Res. Oceans* 104 (C10), 23337–23355, doi:10.1029/1999JC900215.
- Gosling, S. N., Arnell, N. W., 2011. Simulating current global river runoff with a global hydrological model: model revisions, validation, and sensitivity analysis. *Hydrol. Process.* 25 (7), 1129–1145, doi:10.1002/hyp.7727.
- Gosling, S. N., Taylor, R. G., Arnell, N. W., Todd, M. C., 2011. A comparative analysis of projected impacts of climate change on river runoff from global and catchment-scale hydrological models. *Hydrol. Earth System Sci.* 15 (1), 279–294, doi:10.5194/hess-15-279-2011.
- GRDC, 2013. Global Runoff Data Centre, D - 56002 Koblenz, Germany.
URL <http://www.bafg.de/GRDC>
- Griffiths, M. L., Bradley, R. S., 2007. Variations of twentieth-century temperature and precipitation extreme indicators in the northeast United States. *J. Clim.* 20 (21), 5401–5417, doi:10.1175/2007JCLI1594.1.
- Groisman, P. Y., Knight, R. W., 2008. Prolonged dry episodes over the conterminous United States: New tendencies emerging during the last 40 years. *J. Clim.* 21 (9), 1850–1862, doi:10.1175/2007JCLI2013.1.
- Gudmundsson, L., Tallaksen, L. M., Stahl, K., Clark, D. B., Dumont, E., Hagemann, S., Bertrand, N., Gerten, D., Heinke, J., Hanasaki, N., Voss, F., Koirala, S., 2012a. Comparing large-scale hydrological model simulations to observed runoff percentiles in Europe. *J. Hydrometeorol.* 13, 604–620, doi:10.1175/JHM-D-11-083.1.
- Gudmundsson, L., Wagener, T., Tallaksen, L. M., Engeland, K., 2012b. Evaluation of nine large-scale hydrological models with respect to the seasonal runoff climatology in Europe. *Water Resour. Res.* 48, W11504, doi:10.1029/2011WR010911.
- Guo, Z., Dirmeyer, P. A., Gao, X., Zhao, M., 2007. Improving the quality of simulated soil moisture with a multi-model ensemble approach. *Q. J. Roy. Meteor. Soc.* 133 (624, Part a), 731–747, doi:10.1002/qj.48.
- Haddeland, I., Clark, D. B., Franssen, W., Ludwig, F., Voss, F., Arnell, N. W., Bertrand, N., Best, M., Folwell, S., Gerten, D., Gomes, S., Gosling, S. N., Hagemann, S., Hanasaki, N., Harding, R., Heinke, J., Kabat, P., Koirala, S., Oki, T., Polcher, J., Stacke, T., Viterbo, P., Weedon, G. P., Yeh, P., 2011. Multi-model estimate of the global terrestrial water balance: Setup and first results. *J. Hydrometeorol.* 12 (5), 869–884, doi:10.1175/2011JHM1324.1.
- Haddeland, I., Heinke, J., Biemans, H., Eisner, S., Flörke, M., Hanasaki, N., Konzmann, M., Ludwig, F., Masaki, Y., Schewe, J., Stacke, T., Tessler, Z. D., Wada, Y., Wisser, D., 2014. Global water resources affected by human interventions and climate change. *Proc. Natl. Acad. Sci. U.S.A.* 111 (9), 3251–3256, doi:10.1073/pnas.1222475110.
- Haerter, J. O., Hagemann, S., Moseley, C., Piani, C., 2011. Climate model bias correction and the role of timescales. *Hydrol. Earth System Sci.* 15 (3), 1065–1079, doi:10.5194/hess-15-1065-2011.
- Hagemann, S., Chen, C., Clark, D. B., Folwell, S., Gosling, S. N., Haddeland, I., Hanasaki, N., Heinke, J., Ludwig, F., Voss, F., Wiltshire, A. J., 2013. Climate change impact on available water resources obtained using multiple global climate and hydrology models. *Earth Syst. Dynam.* 4 (1), 129–144, doi:10.5194/esd-4-129-2013.
- Hagemann, S., Chen, C., Haerter, J. O., Heinke, J., Gerten, D., Piani, C., 2011. Impact of a Statistical Bias Correction on the Projected Hydrological Changes Obtained from Three GCMs and Two Hydrology Models. *J. Hydrometeorol.* 12 (4), 556–578, doi:10.1175/2011JHM1336.1.
- Hagemann, S., Dümenil, L., 1998. A parametrization of the lateral waterflow for the global scale. *Clim. Dyn.* 14 (1), 17–31, doi:10.1007/s003820050205.
- Hagemann, S., Gates, L. D., 2003. Improving a subgrid runoff parameterization scheme for climate models by the use of high resolution data derived from satellite observations. *Clim. Dyn.* 21 (3-4), 349–359, doi:10.1007/s00382-003-0349-x.
- Hall, A., Qu, X., 2006. Using the current seasonal cycle to constrain snow albedo feedback in future climate change. *Geophys. Res. Lett.* 33, L03502, doi:10.1029/2005GL025127.

- Hanasaki, N., Kanae, S., Oki, T., Masuda, K., Motoya, K., Shirakawa, N., Shen, Y., Tanaka, K., 2008. An integrated model for the assessment of global water resources, Part 1: Model description and input meteorological forcing. *Hydrol. Earth System Sci.* 12 (4), 1007–1025, doi:10.5194/hess-12-1007-2008.
- Harding, R., Best, M., Blyth, E., Hagemann, S., Kabat, P., Tallaksen, L. M., Warnaars, T., Wiberg, D., Weedon, G. P., Van Lanen, H., Ludwig, F., Haddeland, I., 2011. WATCH: Current Knowledge of the Terrestrial Global Water Cycle. *J. Hydrometeorol.* 12 (6), 1149–1156, doi:10.1175/JHM-D-11-024.1.
- Hastie, T., Tibshirani, R., Friedman, J., 2001. *The Elements of Statistical Learning: Data Mining, Inference, and Prediction*. Springer Series in Statistics. Springer-Verlag New York.
- He, L., Chao, Y., Suzuki, K., Wu, K., 2009. Fast connected-component labeling. *Pattern Recogn.* 42 (9), 1977–1987, doi:10.1016/j.patcog.2008.10.013.
- Hirabayashi, Y., Kanae, S., Emori, S., Oki, T., Kimoto, M., 2008. Global projections of changing risks of floods and droughts in a changing climate. *Hydrol. Sci. J.* 53 (4), 754–772, doi:10.1623/hysj.53.4.754.
- Hisdal, H., Stahl, K., Tallaksen, L. M., Demuth, S., 2001. Have streamflow droughts in Europe become more severe or frequent? *Int. J. Climatol.* 21 (3), 317–333, doi:10.1002/joc.619.
- Hisdal, H., Tallaksen, L. M., 2003. Estimation of regional meteorological and hydrological drought characteristics: a case study for Denmark. *J. Hydrol.* 281 (3), 230–247, doi:10.1016/S0022-1694(03)00233-6.
- Hisdal, H., Tallaksen, L. M., Clausen, B., Peters, E., Gustard, A., 2004. *Hydrological Drought Characteristics*. In: Tallaksen, L. M., Van Lanen, H. A. J. (Eds.), *Hydrological Drought Processes and Estimation Methods for Streamflow and Groundwater*. Elsevier Science B.V., *Developments in Water Science*, 48, The Netherlands, pp. 139–198.
- Hourdin, F., Musat, I., Bony, S., Braconnot, P., Codron, F., Dufresne, J.-L., Fairhead, L., Filiberti, M.-A., Friedlingstein, P., Grandpeix, J.-Y., Krinner, G., LeVan, P., Li, Z.-X., Lott, F., 2006. The LMDZ4 general circulation model: climate performance and sensitivity to parametrized physics with emphasis on tropical convection. *Clim. Dyn.* 27 (7-8), 787–813, doi:10.1007/s00382-006-0158-0.
- Im, E. S., Jung, I. W., Bae, D. H., 2011. The temporal and spatial structures of recent and future trends in extreme indices over Korea from a regional climate projection. *Int. J. Climatol.* 31 (1), 72–86, doi:10.1002/joc.2063.
- IPCC, 2012. *Summary for Policymakers*. In: Field, C., Barros, V., Stocker, T., Qin, D., Dokken, D., Ebi, K., Mastrandrea, M., Mach, K., Plattner, G.-K., Allen, S., Tignor, M., Midgley, P. (Eds.), *Managing the Risks of Extreme Events and Disasters to Advance Climate Change Adaptation. A Special Report of Working Groups I and II of the Intergovernmental Panel on Climate Change*. Cambridge University Press, Cambridge, UK, and New York, NY, USA, pp. 3–21.
- Jaranilla-Sanchez, P. A., Wang, L., Koike, T., 2011. Modeling the hydrologic responses of the Pampanga River basin, Philippines: A quantitative approach for identifying droughts. *Water Resour. Res.* 47, W03514, doi:10.1029/2010WR009702.
- Johnson, F., Westra, S., Sharma, A., Pitman, A. J., 2011. An Assessment of GCM Skill in Simulating Persistence across Multiple Time Scales. *J. Clim.* 24 (14), 3609–3623, doi:10.1175/2011JCLI3732.1.
- Jungclaus, J. H., Keenlyside, N., Botzet, M., Haak, H., Luo, J.-J., Latif, M., Marotzke, J., Mikolajewicz, U., Roeckner, E., 2006. Ocean Circulation and Tropical Variability in the Coupled Model ECHAM5/MPI-OM. *J. Clim.* 19 (16), 3952–3972, doi:10.1175/JCLI3827.1.
- Kallis, G., 2008. Droughts. *Annu. Rev. Environ. Res.* 33, 85–118, doi:10.1146/annurev.enviro.33.081307.123117.
- Kampragou, E., Apostolaki, S., Manoli, E., Froebrich, J., Assimakopoulos, D., 2011. Towards the harmonization of water-related policies for managing drought risks across the EU. *Environ. Sci. Policy* 14 (7), 815–824, doi:10.1016/j.envsci.2011.04.001.
- Keyantash, J., Dracup, J. A., 2002. The quantification of drought: An evaluation of drought indices. *Bull. Am. Meteorol. Soc.* 83 (8), 1167–1180.
- Kirchner, J. W., 2006. Getting the right answers for the right reasons: Linking measurements, analyses, and models to advance the science of hydrology. *Water Resour. Res.* 42 (3), W03S04, doi:10.1029/2005WR004362.
- Koirala, S., 2010. *Explicit representation of groundwater process in a global-scale land surface model to improve hydrological predictions*. Ph.D. thesis, The University of Tokyo, Japan.
- Koster, R. D., Dirmeyer, P. A., Guo, Z. C., Bonan, G., Chan, E., Cox, P., Gordon, C. T., Kanae, S., Kowalczyk,

- E., Lawrence, D., Liu, P., Lu, C. H., Malyshev, S., McAvaney, B., Mitchell, K., Mocko, D., Oki, T., Oleson, K., Pitman, A., Sud, Y. C., Taylor, C. M., Verseghy, D., Vasic, R., Xue, Y. K., Yamada, T., Team, G., 2004. Regions of strong coupling between soil moisture and precipitation. *Science* 305 (5687), 1138–1140, doi:10.1126/science.1100217.
- Koster, R. D., Suarez, M. J., 2001. Soil moisture memory in climate models. *J. Hydrometeorol.* 2 (6), 558–570, doi:10.1175/1525-7541(2001)002<0558:SMMICM>2.0.CO;2.
- Lehner, B., Grill, G., 2013. Global river hydrography and network routing: baseline data and new approaches to study the world's large river systems. *Hydrol. Process.* 27 (15), 2171–2186, doi:10.1002/hyp.9740.
- Lewis, S. L., Brando, P. M., Phillips, O. L., Van Der Heijden, G. M. F., Nepstad, D., 2011. The 2010 Amazon Drought. *Science* 331 (6017), 554, doi:10.1126/science.1200807.
- Lloyd-Hughes, B., Saunders, M. A., 2002. A drought climatology for Europe. *Int. J. Climatol.* 22 (13), 1571–1592, doi:10.1002/joc.846.
- Madadgar, S., Moradkhani, H., 2013. Drought Analysis under Climate Change Using Copula. *J. Hydrol. Eng.* 18 (7), 746–759, doi:10.1061/(ASCE)HE.1943-5584.0000532.
- Manabe, S., Milly, P. C. D., Wetherald, R., 2004. Simulated long-term changes in river discharge and soil moisture due to global warming. *Hydrol. Sci. J.* 49 (4), –642, doi:10.1623/hysj.49.4.625.54429.
- Marengo, J. A., Tomasella, J., Alves, L. M., Soares, W. R., Rodriguez, D. A., 2011. The drought of 2010 in the context of historical droughts in the Amazon region. *Geophys. Res. Lett.* 38 (12), L12703, doi:10.1029/2011GL047436.
- Markandya, A., Mysiak, J., Palatnik, R., Breil, M., Balzarolo, P., Martin-Ortega, J., 2009. Economic and Social Impacts of Droughts and Demand Side Options - State of the Art Review, Background Document Xerochore.
- Masson, D., Knutti, R., 2011. Climate model genealogy. *Geophys. Res. Lett.* 38 (8), L08703, doi:10.1029/2011GL046864.
- McGlynn, B. L., Blöschl, G., Borga, M., Bormann, H., Hurkmans, R., Komma, J., Nandagiri, L., Uijlenhoet, R., Wagener, T., 2013. A data acquisition framework for runoff prediction in ungauged basins. In: Blöschl, G., Sivapalan, M., Wagener, T., Viglione, A., Savenije, H. (Eds.), *Runoff Prediction in Ungauged Basins*. Cambridge University Press, pp. 29–52.
- McKee, T. B., Doesken, N. J., Kleist, J., 1993. The relationship of drought frequency and duration to time scales. In: *Preprints, Eight Conference on Applied Climatology*. January 17-22, Anaheim, California, pp. 179–184.
- Meehl, G. A., Stocker, T. F., Collins, W. D., Friedlingstein, P., Gaye, A. T., Gregory, J. M., Kitoh, A., Knutti, R., Murphy, J. M., Noda, A., Raper, S. C. B., Watterson, I. G., Weaver, A. J., Zhao, Z.-C., 2007. Global Climate Projections. In: Solomon, S., Qin, D., Manning, M., Chen, Z., Marquis, M., Averyt, K., Tignor, M., Miller, H. (Eds.), *Climate Change 2007: The Physical Science Basis. Contribution of Working Group I to the Fourth Assessment Report of the Intergovernmental Panel on Climate Change*. Cambridge University Press, Cambridge, United Kingdom and New York, NY, USA.
- Meigh, J. R., McKenzie, A. A., Sene, K. J., 1999. A grid-based approach to water scarcity estimates for eastern and southern Africa. *Water Resour. Manag.* 13 (2), 85–115, doi:10.1023/A:1008025703712.
- Milly, P. C. D., Dunne, K. A., Vecchia, A. V., 2005. Global pattern of trends in streamflow and water availability in a changing climate. *Nature* 438 (7066), 347–350, doi:10.1038/nature04312.
- Mishra, A. K., Singh, V. P., 2010. A review of drought concepts. *J. Hydrol.* 391, 202–216, doi:10.1016/j.jhydrol.2010.07.012.
- Najafi, M. R., Moradkhani, H., Jung, I. W., 2011. Assessing the uncertainties of hydrologic model selection in climate change impact studies. *Hydrol. Process.* 25 (18), 2814–2826, doi:10.1002/hyp.8043.
- Nakićenović, N., Swart, R., 2000. *Special Report on Emissions Scenarios: A special report of Working Group III of the Intergovernmental Panel on Climate Change*. Tech. rep., Cambridge University Press.
- Nalbantis, I., Tsakiris, G., 2009. Assessment of hydrological drought revisited. *Water Resour. Manag.* 23, 881–897, doi:10.1007/s11269-008-9305-1.
- Nash, J. E., Sutcliffe, J. V., 1970. River flow forecasting through conceptual models part I - A discussion of principles. *J. Hydrol.* 10 (3), 282–290, doi:10.1016/0022-1694(70)90255-6.
- NCEP, 2012. National Centers for Environmental Prediction, NOAA/ National Weather Service. www.ncep.noaa.gov, accessed: 6-2012.

- Niemeyer, S., 2008. New drought indices. In: Proceedings of the 1st International Conference "Drought management: Scientific and technological innovations". Zaragova, Spain, 12-14 June 2008, pp. 267-274.
- Nijssen, B., O'Donnell, G. M., Hamlet, A. F., Lettenmaier, D. P., 2001a. Hydrologic Sensitivity of Global Rivers to Climate Change. *Clim. Chang.* 50 (1-2), 143-175, doi:10.1023/A:1010616428763.
- Nijssen, B., O'Donnell, G. M., Lettenmaier, D. P., Lohmann, D., Wood, E. F., 2001b. Predicting the Discharge of Global Rivers. *J. Clim.* 14 (15), 3307-3323, doi:10.1175/1520-0442(2001)014<3307:PTDOGR>2.0.CO;2.
- Nilsson, C., Reidy, C. A., Dynesius, M., Revenga, C., 2005. Fragmentation and Flow Regulation of the World's Large River Systems. *Science* 308 (5720), 405-408, doi:10.1126/science.1107887.
- Nohara, D., Kitoh, A., Hosaka, M., Oki, T., 2006. Impact of Climate Change on River Discharge Projected by Multimodel Ensemble. *J. Hydrometeorol.* 7 (5), 1076-1089, doi:10.1175/JHM531.1.
- Orlowsky, B., Seneviratne, S. I., 2013. Elusive drought: uncertainty in observed trends and short- and long-term CMIP5 projections. *Hydrol. Earth System Sci.* 17 (5), 1765-1781, doi:10.5194/hess-17-1765-2013.
- Palmer, W. C., 1965. Meteorological drought. U.S. Weather Bureau, Washington, D.C.
- Parrish, M. A., Moradkhani, H., DeChant, C. M., 2012. Toward reduction of model uncertainty: Integration of Bayesian model averaging and data assimilation. *Water Resour. Res.* 48 (3), W03519, doi:10.1029/2011WR011116.
- Peel, M. C., Finlayson, B. L., McMahon, T. A., 2007. Updated world Köppen-Geiger climate classification map. *Hydrol. Earth System Sci.* 11, 1633-1644, doi:10.5194/hessd-4-439-2007.
- Peel, M. C., McMahon, T. A., Pegram, G. G. S., 2005. Global analysis of runs of annual precipitation and runoff equal to or below the median: Run magnitude and severity. *Int. J. Climatol.* 25 (5), 549-568, doi:10.1002/joc.1147.
- Peters, E., Bier, G., van Lanen, H. A. J., Torfs, P. J. J. F., 2006. Propagation and spatial distribution of drought in a groundwater catchment. *J. Hydrol.* 321, 257-275, doi:10.1016/j.jhydrol.2005.08.004.
- Peters, E., Torfs, P. J. J. F., van Lanen, H. A. J., Bier, G., 2003. Propagation of drought through groundwater - a new approach using linear reservoir theory. *Hydrol. Process.* 17 (15), 3023-3040, doi:10.1002/hyp.1274.
- Peters, E., Van Lanen, H. A. J., 2005. Separation of base flow from streamflow using groundwater levels-illustrated for the Pang catchment (UK). *Hydrol. Process.* 19 (4), 921-936, doi:10.1002/hyp.5548.
- Pfister, C., Weingartner, R., Luterbacher, J., 2006. Hydrological winter droughts over the last 450 years in the Upper Rhine basin: a methodological approach. *Hydrol. Sci. J.* 51 (5), 966-985, doi:10.1623/hysj.51.5.966.
- Piani, C., Weedon, G. P., Best, M., Gomes, S. M., Viterbo, P., Hagemann, S., Haerter, J. O., 2010. Statistical bias correction of global simulated daily precipitation and temperature for the application of hydrological models. *J. Hydrol.* 395, 199-215, doi:10.1016/j.jhydrol.2010.10.024.
- Prudhomme, C., Giuntoli, I., Robinson, E. L., Clark, D. B., Arnell, N. W., Dankers, R., Fekete, B. M., Franssen, W., Gerten, D., Gosling, S. N., Hagemann, S., Hannah, D. M., Kim, H., Masaki, Y., Satoh, Y., Stacke, T., Wada, Y., Wisser, D., 2014. Hydrological droughts in the 21st century, hotspots and uncertainties from a global multimodel ensemble experiment. *Proc. Natl. Acad. Sci. U.S.A.* 111 (9), 3262-3267, doi:10.1073/pnas.1222473110.
- Prudhomme, C., Parry, S., Hannaford, J., Clark, D. B., Hagemann, S., Voss, F., 2011. How well do large-scale models reproduce regional hydrological extremes in Europe? *J. Hydrometeorol.* 12 (6), 1181-1204, doi:10.1175/2011JHM1387.1.
- Rakovec, O., Van Loon, A. F., Horáček, S., Kašpárek, L., Van Lanen, H. A. J., Novický, O., 2009. Drought analysis for the Upper Metuje and Upper Sázava catchments (Czech Republic) using the hydrological model HBV. WATCH Technical Report 19, accessed: 10-2013.
URL <http://www.eu-watch.org/publications/technical-reports>
- Rakovec, O., Weerts, A. H., Hazenberg, P., Torfs, P. J. J. F., Uijlenhoet, R., 2012. State updating of a distributed hydrological model with Ensemble Kalman Filtering: effects of updating frequency and observation network density on forecast accuracy. *Hydrol. Earth System Sci.* 16 (9), 3435-3449, doi:10.5194/hess-16-3435-2012.
- Rees, G., Marsh, T. J., Roald, L., Demuth, S., Van Lanen, H. A. J., Kašpárek, L., 2004. Hydrological Data. In: Tallaksen, L. M., van Lanen, H. A. J. (Eds.), *Hydrological Drought Processes and Estimation Methods for Streamflow and Groundwater*. Elsevier Science B.V., Developments in Water Science, 48, The Netherlands, pp. 99-138.
- Reifen, C., Toumi, R., 2009. Climate projections: Past performance no guarantee of future skill? *Geophys. Res.*

- Lett. 36 (13), L13704, doi:10.1029/2009GL038082.
- Romm, J., 2011. The next dust bowl. *Nature* 478, 450–451, doi:10.1038/478450a.
- Ropelewski, C. F., Halpert, M. S., 1987. Global and Regional Scale Precipitation Patterns Associated with the El Niño/Southern Oscillation. *Mon. Weather Rev.* 115 (8), 1606–1626, doi:10.1175/1520-0493(1987)115<1606:GARSPP>2.0.CO;2.
- Rosenfeld, A., 1970. Connectivity in digital pictures. *J. ACM* 17, 146–160, doi:10.1145/321556.321570.
- Rost, S., Gerten, D., Bondeau, A., Lucht, W., Rohwer, J., Schaphoff, S., 2008. Agricultural green and blue water consumption and its influence on the global water system. *Water Resour. Res.* 44 (9), 1–12, doi:10.1029/2007WR006331.
- Royer, J.-F., Cariolle, D., Chauvin, F., Déqué, M., Douville, H., Hu, R.-M., Planton, S., Rascol, A., Ricard, J.-L., Melia, D. S. Y., Sevault, F., Simon, P., Somot, S., Tyteca, S., Terray, L., Valcke, S., 2002. Simulation des changements climatiques au cours du XXI^e siècle incluant l’ozone stratosphérique. *C. R. Geosci.* 334 (3), 147–154, doi:10.1016/S1631-0713(02)01728-5.
- Salas Mélia, D., 2002. A global coupled sea ice-ocean model. *Ocean Modelling* 4 (2), 137–172, doi:10.1016/S1463-5003(01)00015-4.
- Santhi, C., Allen, P. M., Muttiah, R. S., Arnold, J. G., Tuppad, P., 2008. Regional estimation of base flow for the conterminous United States by hydrologic landscape regions. *J. Hydrol.* 351 (1-2), 139–153, doi:10.1016/j.jhydrol.2007.12.018.
- Schewe, J., Heinke, J., Gerten, D., Haddeland, I., Arnell, N. W., Clark, D. B., Dankers, R., Eisner, S., Fekete, B. M., Colón-González, F. J., Gosling, S. N., Kim, H., Liu, X., Masaki, Y., Portmann, F. T., Satoh, Y., Stacke, T., Tang, Q., Wada, Y., Wisser, D., Albrecht, T., Frieler, K., Piontek, F., Warszawski, L., Kabat, P., 2014. Multimodel assessment of water scarcity under climate change. *Proc. Natl. Acad. Sci. U.S.A.* 111 (9), 3245–3250, doi:10.1073/pnas.1222460110.
- Schmidt, G., Benítez-Sanz, C., 2013. How to distinguish water scarcity and drought in EU water policy? GWF Discussion Paper 1333, Global Water Forum, Canberra, Australia.
- Schneider, U., Fuchs, T., Meyer-Christoffer, A., Rudolf, B., 2008. Global Precipitation Analysis Products of the GPCC. Available from reports and publications section of the GPCC homepage - gpcc.dwd.de, accessed: 10-2012.
- Schnoor, J. L., 2012. The US Drought of 2012. *Environ. Sci. Technol.* 46 (19), 10480, doi:10.1021/es303416z.
- Seneviratne, S. I., Luthi, D., Litschi, M., Schar, C., 2006. Land-atmosphere coupling and climate change in Europe. *Nature* 443 (7108), 205–209, doi:10.1038/nature05095.
- Seneviratne, S. I., Nicholls, N., Easterling, D., Goodess, C. M., Kanae, S., Kossin, J., Luo, Y., Marengo, J., McInnes, K., Rahimi, M., Reichstein, M., Sorteberg, A., Vera, C., Zhang, X., 2012. Changes in climate extremes and their impacts on the natural physical environment. In: Field, C. B., Barros, V., Stocker, T. F., Qin, D., Dokken, D. J., Ebi, K. L., Mastrandrea, M. D., Mach, K. J., Plattner, G. K., Allen, S. K., Tignor, M., Midgley, P. M. (Eds.), *Managing the Risks of Extreme Events and Disasters to Advance Climate Change Adaptation. A Special Report of Working Groups I and II of the Intergovernmental Panel on Climate Change (IPCC)*. Cambridge University Press, Cambridge, UK, and New York, NY, USA, pp. 109–230.
- Sheffield, J., Andreadis, K. M., Wood, E. F., Lettenmaier, D. P., 2009. Global and continental drought in the second half of the twentieth century: Severity-area-duration analysis and temporal variability of large-scale events. *J. Clim.* 22 (8), 1962–1981, doi:10.1175/2008JCLI2722.1.
- Sheffield, J., Goteti, G., Wen, F. H., Wood, E. F., 2004. A simulated soil moisture based drought analysis for the United States. *J. Geophys. Res., Atmos.* 109 (D24), D24108, doi:10.1029/2004JD005182.
- Sheffield, J., Wood, E. F., 2007. Characteristics of global and regional drought, 1950-2000: Analysis of soil moisture data from off-line simulation of the terrestrial hydrologic cycle. *J. Geophys. Res., Atmos.* 112 (D17), D17115, doi:10.1029/2006JD008288.
- Sheffield, J., Wood, E. F., 2008a. Global trends and variability in soil moisture and drought characteristics, 1950-2000, from observation-driven simulations of the terrestrial hydrologic cycle. *J. Clim.* 21 (3), 432–458, doi:10.1175/2007JCLI1822.1.
- Sheffield, J., Wood, E. F., 2008b. Projected changes in drought occurrence under future global warming from multi-model, multi-scenario, IPCC AR4 simulations. *Clim. Dyn.* 31 (1), 79–105, doi:10.1007/s00382-007-0340-z.

- Sheffield, J., Wood, E. F., 2011. Drought : past problems and future scenarios. Earthscan, London.
- Sheffield, J., Wood, E. F., Roderick, M. L., 2012. Little change in global drought over the past 60 years. *Nature* 491 (7424), 435–438, doi:10.1038/nature11575.
- Shukla, S., Wood, A. W., 2008. Use of a standardized runoff index for characterizing hydrologic drought. *Geophys. Res. Lett.* 35 (2), L02405, doi:10.1029/2007GL032487.
- Smith, A. B., Katz, R. W., 2013. US billion-dollar weather and climate disasters: data sources, trends, accuracy and biases. *Nat. Hazards* 67 (2), 387–410, doi:10.1007/s11069-013-0566-5.
- Smith, C. A., Sardeshmukh, P. D., 2000. The effect of ENSO on the intraseasonal variance of surface temperatures in winter. *Int. J. Climatol.* 20 (13), 1543–1557, doi:10.1002/1097-0088(20001115)20:13<1543::AID-JOC579>3.0.CO;2-A.
- Soulé, P. T., 1993. Hydrologic Drought in the Contiguous United-States, 1900-1989 - Spatial Patterns and multiple comparison of means. *Geophys. Res. Lett.* 20 (21), 2367–2370, doi:10.1029/93GL02608.
- Sperna Weiland, F. C., Van Beek, L. P. H., Kwadijk, J. C. J., Bierkens, M. F. P., 2010. The ability of a GCM-forced hydrological model to reproduce global discharge variability. *Hydrol. Earth System Sci.* 14 (8), 1595–1621, doi:10.5194/hess-14-1595-2010.
- Sperna Weiland, F. C., Van Beek, L. P. H., Kwadijk, J. C. J., Bierkens, M. F. P., 2012. Global patterns of change in discharge regimes for 2100. *Hydrol. Earth System Sci.* 16 (4), 1047–1062, doi:10.5194/hess-16-1047-2012.
- Stahl, K., 2001. Hydrological Drought - a Study across Europe. Ph.D. thesis, Albert-Ludwigs-Universität Freiburg, available from: <http://www.freidok.uni-freiburg.de/volltexte/202/>, Freiburg, Germany, accessed: 4-2011.
- Stahl, K., Hisdal, H., Hannaford, J., Tallaksen, L. M., Van Lanen, H. A. J., Sauquet, E., Demuth, S., Fendekova, M., Jódar, J., 2010. Streamflow trends in Europe: evidence from a dataset of near-natural catchments. *Hydrol. Earth System Sci.* 14 (12), 2367–2382, doi:10.5194/hess-14-2367-2010.
- Stahl, K., Tallaksen, L. M., Gudmundsson, L., Christensen, J. H., 2011. Streamflow Data from Small Basins: A Challenging Test to High-Resolution Regional Climate Modeling. *J. Hydrometeorol.* 12 (5), 900–912, doi:10.1175/2011JHM1356.1.
- Stahl, K., Tallaksen, L. M., Hannaford, J., Van Lanen, H. A. J., 2012. Filling the white space on maps of European runoff trends: estimates from a multi-model ensemble. *Hydrol. Earth System Sci.* 16 (7), 2035–2047, doi:10.5194/hess-16-2035-2012.
- Stegehuis, A. I., Teuling, A. J., Ciais, P., Vautard, R., Jung, M., 2013. Future European temperature change uncertainties reduced by using land heat flux observations. *Geophys. Res. Lett.* 40 (10), 2242–2245, doi:10.1002/grl.50404.
- Sternberg, T., 2010. Unravelling Mongolia's extreme winter disaster of 2010. *Nomadic Peoples* 14 (1), 72–86.
- Stocker, T. F., Qin, D., Plattner, G.-K., Alexander, L. V., Allen, S. K., Bindoff, N. L., Bréon, F.-M., Church, J. A., Cubasch, U., Emori, S., Forster, P., Friedlingstein, P., Gillett, N., Gregory, J. M., Hartmann, D. L., Jansen, E., Kirtman, B., Knutti, R., Kumar, K. K., Lemke, P., Marotzke, J., Masson-Delmotte, V., Meehl, G. A., Mokhov, I. I., Piao, S., Ramaswamy, V., Randall, D., Rhein, M., Rojas, M., Sabine, C., Shindell, D., Talley, L. D., Vaughan, D. G., Xie, S.-P., 2013. Technical Summary. In: Stocker, T. F., Qin, D., Plattner, G.-K., Tignor, M., Allen, S. K., Boschung, J., Nauels, A., Xia, Y., Bex, V., Midgley, P. M. (Eds.), *Climate Change 2013: The Physical Science Basis. Contribution of Working Group I to the Fifth Assessment Report of the Intergovernmental Panel on Climate Change*. Cambridge University Press, Cambridge, United Kingdom and New York, NY, USA.
- Sutanudjaja, E. H., Van Beek, L. P. H., De Jong, S. M., Van Geer, F. C., Bierkens, M. F. P., 2011. Large-scale groundwater modeling using global datasets: a test case for the Rhine-Meuse basin. *Hydrol. Earth System Sci.* 15 (9), 2913–2935, doi:10.5194/hess-15-2913-2011.
- Suzuki, K., Horiba, I., Sugie, N., 2003. Linear-time connected-component labeling based on sequential local operations. *Comput. Vis. Image Und.* 89 (1), 1–23, doi:10.1016/S1077-3142(02)00030-9.
- Takata, K., Emori, S., Watanabe, T., 2003. Development of the minimal advanced treatments of surface interaction and runoff. *Global Planet. Change* 38 (1-2), 209–222, doi:10.1016/S0921-8181(03)00030-4.
- Tallaksen, L. M., Hisdal, H., Van Lanen, H. A. J., 2006. Propagation of drought in a groundwater fed catchment, the Pang in the UK. In: *Climate variability and change: hydrological impacts*. IAHS-AISH Publication 308. pp. 128–133.

- Tallaksen, L. M., Hisdal, H., Van Lanen, H. A. J., 2009. Space-time modelling of catchment scale drought characteristics. *J. Hydrol.* 375 (3-4), 363–372, doi:10.1016/j.jhydrol.2009.06.032.
- Tallaksen, L. M., Madsen, H., Clausen, B., 1997. On the definition and modelling of streamflow drought duration and deficit volume. *Hydrol. Sci. J.* 42 (1), 15–33, doi:10.1080/0262669709492003.
- Tallaksen, L. M., Stahl, K., 2014. Spatial and temporal patterns of large-scale droughts in Europe: model dispersion and performance. *Geophys. Res. Lett.* 41 (2), 429–434, doi:10.1002/2013GL058573.
- Tallaksen, L. M., Stahl, K., Wong, G., 2011. Space-time characteristics of large-scale droughts in Europe derived from streamflow observations and WATCH multi-model simulations. WATCH Technical Report 48, accessed: 1-2012.
URL <http://www.eu-watch.org/publications/technical-reports>
- Tallaksen, L. M., Van Lanen, H. A. J. (Eds.), 2004. Hydrological drought : processes and estimation methods for streamflow and groundwater. Elsevier Science BV, Developments in Water Science; 48, The Netherlands.
- Tang, Q., Lettenmaier, D. P., 2012. 21st century runoff sensitivities of major global river basins. *Geophys. Res. Lett.* 39 (6), L06403, doi:10.1029/2011GL050834.
- Taylor, I. H., Burke, E., McColl, L., Falloon, P. D., Harris, G. R., McNeall, D., 2013. The impact of climate mitigation on projections of future drought. *Hydrol. Earth System Sci.* 17 (6), 2339–2358, doi:10.5194/hess-17-2339-2013.
- Teuling, A. J., Lehner, I., Kirchner, J. W., Seneviratne, S. I., 2010. Catchments as simple dynamical systems: Experience from a Swiss prealpine catchment. *Water Resour. Res.* 46 (10), W10502, doi:10.1029/2009WR008777.
- Teuling, A. J., Stoeckli, R., Seneviratne, S. I., 2011. Bivariate colour maps for visualizing climate data. *Int. J. Climatol.* 31 (9), 1408–1412, doi:10.1002/joc.2153.
- Tomasella, J., Borma, L. S., Marengo, J. A., Rodriguez, D. A., Cuartas, L. A., Nobre, C. A., Prado, M. C. R., 2011. The droughts of 1996–1997 and 2004–2005 in Amazonia: hydrological response in the river main-stem. *Hydrol. Process.* 25 (8), 1228–1242, doi:10.1002/hyp.7889.
- Trenberth, K. E., Branstator, G. W., 1992. Issues in establishing causes of the 1988 drought over North America. *J. Clim.* 5 (2), 159–172, doi:10.1175/1520-0442(1992)005<0159:IIECOT>2.0.CO;2.
- Trenberth, K. E., Dai, A., Van Der Schrier, G., Jones, P. D., Barichivich, J., Briffa, K. R., Sheffield, J., 2014. Global warming and changes in drought. *Nature Clim. Change* 4 (1), 17–22, doi:10.1038/nclimate2067.
- Uijlenhoet, R., De Wit, M. J. M., Warmerdam, P. M. M., Torfs, P. J. J. F., 2001. Statistical Analysis of Daily Discharge Data of the River Meuse and its Tributaries (1968–1998): Assessment of Drought Sensitivity. Tech. rep., Wageningen University, The Netherlands.
- UNEP, 1994. United Nations Convention to Combat Desertification in those countries experiencing serious drought and/or desertification, particularly in Africa. Paris, France.
- Uppala, S. M., Kallberg, P. W., Simmons, A. J., Andrae, U., Bechtold, V. D., Fiorino, M., Gibson, J. K., Haseler, J., Hernandez, A., Kelly, G. A., Li, X., Onogi, K., Saarinen, S., Sokka, N., Allan, R. P., Andersson, E., Arpe, K., Balmaseda, M. A., Beljaars, A. C. M., Van De Berg, L., Bidlot, J., Bormann, N., Caires, S., Chevallier, F., Dethof, A., Dragosavac, M., Fisher, M., Fuentes, M., Hagemann, S., Holm, E., Hoskins, B. J., Isaksen, I., Janssen, P., Jenne, R., McNally, A. P., Mahfouf, J. F., Morcrette, J. J., Rayner, N. A., Saunders, R. W., Simon, P., Sterl, A., Trenberth, K. E., Untch, A., Vasiljevic, D., Viterbo, P., Woollen, J., 2005. The ERA-40 re-analysis. *Q. J. Roy. Meteor. Soc.* 131 (612), 2961–3012, doi:10.1256/qj.04.176.
- Van Huijgevoort, M. H. J., Hazenberg, P., Van Lanen, H. A. J., Teuling, A. J., Clark, D. B., Folwell, S., Gosling, S. N., Hanasaki, N., Heinke, J., Koirala, S., Stacke, T., Voss, F., Sheffield, J., Uijlenhoet, R., 2013. Global multi-model analysis of drought in runoff for the second half of the 20th century. *J. Hydrometeorol.* 14 (5), 1535–1552, doi:10.1175/JHM-D-12-0186.1.
- Van Huijgevoort, M. H. J., Hazenberg, P., Van Lanen, H. A. J., Uijlenhoet, R., 2012. A generic method for hydrological drought identification across different climate regions. *Hydrol. Earth System Sci.* 16 (8), 2437–2451, doi:10.5194/hess-16-2437-2012.
- Van Huijgevoort, M. H. J., Van Lanen, H. A. J., Teuling, A. J., Uijlenhoet, R., 2014. Identification of changes in hydrological drought characteristics from a multi-GCM driven ensemble constrained by observed discharge. *J. Hydrol.* 512, 421–434, doi:10.1016/j.jhydrol.2014.02.060.
- Van Lanen, H. A. J., Dijkma, R., 1999. Water flow and nitrate transport to a groundwater-fed stream in the Belgian-Dutch chalk region. *Hydrol. Process.* 13 (3), 295–307, doi:10.1002/(SICI)1099-

- 1085(19990228)13:3<295::AID-HYP739>3.0.CO;2-O.
- Van Lanen, H. A. J., Dijkma, R., 2004. Impact of groundwater on surface water quality: role of the riparian area in nitrate transformation in a slowly responding chalk catchment (Noor, The Netherlands). *Ecohydrology and Hydrobiology* 4 (3), 315–325.
- Van Lanen, H. A. J., Fendekova, M., Kupczyk, E., Kasprzyk, A., Pokojski, W., 2004. Flow Generating Processes. In: Tallaksen, L. M., Van Lanen, H. A. J. (Eds.), *Hydrological Drought. Processes and Estimation Methods for Streamflow and Groundwater*. Elsevier Science B.V., Development in Water Science, 48, The Netherlands, pp. 53–96.
- Van Lanen, H. A. J., Tallaksen, L. M., 2008. Drought in Europe. In: Lambert, M., Daniell, T., Leonard, M. (Eds.), *Proc. Water Down Under 2008*. Adelaide, Australia, 14–17 April 2008, pp. 98–108.
- Van Lanen, H. A. J., Wanders, N., Tallaksen, L. M., Van Loon, A. F., 2013. Hydrological drought across the world: impact of climate and physical catchment structure. *Hydrol. Earth System Sci.* 17 (5), 1715–1732, doi:10.5194/hess-17-1715-2013.
- Van Loon, A. F., 2013. On the propagation of drought : how climate and catchment characteristics influence hydrological drought development and recovery. Ph.D. thesis, Wageningen University, accessed: 10-2013. URL <http://edepot.wur.nl/249786>
- Van Loon, A. F., Van Huijgevoort, M. H. J., Van Lanen, H. A. J., 2012. Evaluation of drought propagation in an ensemble mean of large-scale hydrological models. *Hydrol. Earth System Sci.* 16 (11), 4057–4078, doi: 10.5194/hess-16-4057-2012.
- Van Loon, A. F., Van Lanen, H. A. J., 2012. A process-based typology of hydrological drought. *Hydrol. Earth System Sci.* 16 (7), 1915–1946, doi:10.5194/hess-16-1915-2012.
- Van Loon, A. F., Van Lanen, H. A. J., 2013. Making the distinction between water scarcity and drought using an observation-modeling framework. *Water Resour. Res.* 49 (3), 1483–1502, doi:10.1002/wrcr.20147.
- Van Vliet, M. T. H., Yearsley, J. R., Ludwig, F., Voegele, S., Lettenmaier, D. P., Kabat, P., 2012. Vulnerability of US and European electricity supply to climate change. *Nature Clim. Change* 2 (9), 676–681, doi: 10.1038/nclimate1546.
- Vicente-Serrano, S. M., López-Moreno, J. I., 2005. Hydrological response to different time scales of climatological drought: an evaluation of the standardized precipitation index in a mountainous mediterranean basin. *Hydrol. Earth System Sci.* 9 (5), 523–533, doi:10.5194/hess-9-523-2005.
- Vicente-Serrano, S. M., Lopez-Moreno, J. I., Gimeno, L., Nieto, R., Moran-Tejeda, E., Lorenzo-Lacruz, J., Begueria, S., Azorin-Molina, C., 2011. A multiscalar global evaluation of the impact of ENSO on droughts. *J. Geophys. Res., Atmos.* 116, D20109, doi:10.1029/2011JD016039.
- Vidal, J.-P., Martin, E., Kitova, N., Najac, J., Soubeyroux, J.-M., 2012. Evolution of spatio-temporal drought characteristics: validation, projections and effect of adaptation scenarios. *Hydrol. Earth System Sci.* 16 (8), 2935–2955, doi:10.5194/hess-16-2935-2012.
- Vincent, L. A., Mekis, E., 2006. Changes in daily and extreme temperature and precipitation indices for Canada over the twentieth century. *Atmos. Ocean* 44 (2), 177–193, doi:10.3137/ao.440205.
- Vörösmarty, C. J., Sharma, K. P., Fekete, B., Copeland, A. H., Holden, J., Marble, J., Lough, J. A., 1997. The Storage and Aging of Continental Runoff in Large Reservoir Systems of the World. *Ambio* 26 (4), 210–219.
- Wada, Y., Van Beek, L. P. H., Wanders, N., Bierkens, M. F. P., 2013a. Human water consumption intensifies hydrological drought worldwide. *Environ. Res. Lett.* 8 (3), 034036, doi:10.1088/1748-9326/8/3/034036.
- Wada, Y., Wisser, D., Eisner, S., Flörke, M., Gerten, D., Haddeland, I., Hanasaki, N., Masaki, Y., Portmann, F. T., Stacke, T., Tessler, Z., Schewe, J., 2013b. Multimodel projections and uncertainties of irrigation water demand under climate change. *Geophys. Res. Lett.* 40 (17), 4626–4632, doi:10.1002/grl.50686.
- Wagenknecht, G., 2007. A contour tracing and coding algorithm for generating 2D contour codes from 3D classified objects. *Pattern Recogn.* 40 (4), 1294–1306, doi:10.1016/j.patcog.2006.09.003.
- Wanders, N., Van Lanen, H. A. J., Van Loon, A. F., 2010. Indicators for drought characterization on a global scale. WATCH Technical Report 24, accessed: 4-2011. URL <http://www.eu-watch.org/publications/technical-reports>
- Wang, A., Bohn, T. J., Mahanama, S. P., Koster, R. D., Lettenmaier, D. P., 2009. Multimodel ensemble reconstruction of drought over the continental United States. *J. Clim.* 22 (10), 2694–2712, doi:10.1175/2008JCLI2586.1.

- Wang, A., Lettenmaier, D. P., Sheffield, J., 2011. Soil moisture drought in China, 1950-2006. *J. Clim.* 24 (13), 3257–3271, doi:10.1175/2011JCLI3733.1.
- Warszawski, L., Frieler, K., Huber, V., Piontek, F., Serdeczny, O., Schewe, J., 2014. The Inter-Sectoral Impact Model Intercomparison Project (ISI-MIP): Project framework. *Proc. Natl. Acad. Sci. U.S.A.* 111 (9), 3228–3232, doi:10.1073/pnas.1312330110.
- Weedon, G. P., Gomes, S., Viterbo, P., Shuttleworth, W. J., Blyth, E., Österle, H., Adam, J. C., Bellouin, N., Boucher, O., Best, M., 2011. Creation of the WATCH Forcing Data and its use to assess global and regional reference crop evaporation over land during the twentieth century. *J. Hydrometeorol.* 12 (5), 823–848, doi:10.1175/2011JHM1369.1.
- Wells, N., Goddard, S., Hayes, M. J., 2004. A self-calibrating Palmer Drought Severity Index. *J. Clim.* 17 (12), 2335–2351, doi:10.1175/1520-0442(2004)017<2335:ASPDSI>2.0.CO;2.
- Wetherald, R. T., Manabe, S., 2002. Simulation of hydrologic changes associated with global warming. *J. Geophys. Res., Atmos.* 107 (19), 4379, doi:10.1029/2001JD001195.
- Wilhite, D. (Ed.), 2000. DROUGHT A Global Assessment, Vol I & II. Routledge Hazards and Disasters Series, Routledge, London.
- Wolter, K., Timlin, M. S., 2011. El Niño/Southern Oscillation behaviour since 1871 as diagnosed in an extended multivariate ENSO index (MEI.ext). *Int. J. Climatol.* 31 (7), 1074–1087, doi:10.1002/joc.2336.
- Wong, G., Van Lanen, H. A. J., Torfs, P. J. F., 2013. Probabilistic analysis of hydrological drought characteristics using meteorological drought. *Hydrol. Sci. J.* 58 (2), 253–270, doi:10.1080/02626667.2012.753147.
- Wood, E. F., Roundy, J. K., Troy, T. J., Van Beek, L. P. H., Bierkens, M. F. P., Blyth, E., De Roo, A., Doell, P., Ek, M., Famiglietti, J., Gochis, D., Van De Giesen, N., Houser, P., Jaffe, P. R., Kollet, S., Lehner, B., Lettenmaier, D. P., Peters-Lidard, C., Sivapalan, M., Sheffield, J., Wade, A., Whitehead, P., 2011. Hyperresolution global land surface modeling: Meeting a grand challenge for monitoring Earth's terrestrial water. *Water Resour. Res.* 47, W05301, doi:10.1029/2010WR010090.
- Wu, K., Otoo, E., Suzuki, K., 2009. Optimizing two-pass connected-component labeling algorithms. *Pattern anal. appl.* 12 (2), 117–135, doi:10.1007/s10044-008-0109-y.
- Wu, Z. Y., Lu, G. H., Wen, L., Lin, C. A., 2011. Reconstructing and analyzing China's fifty-nine year (1951–2009) drought history using hydrological model simulation. *Hydrol. Earth System Sci.* 15 (9), 2881–2894, doi:10.5194/hess-15-2881-2011.
- Yan, D. H., Wu, D., Huang, R., Wang, L. N., Yang, G. Y., 2013. Drought evolution characteristics and precipitation intensity changes during alternating dry-wet changes in the Huang-Huai-Hai River basin. *Hydrol. Earth System Sci.* 17 (7), 2859–2871, doi:10.5194/hess-17-2859-2013.
- Yevjevich, V., 1967. An objective approach to definition and investigations of continental hydrologic droughts. Hydrology papers 23, Colorado State University, Fort Collins, USA.
- Zaidman, M. D., Rees, H. G., 2000. Spatial patterns of streamflow drought in Western Europe 1960-1995. ARIDE Tech. Report no. 8, Centre for Ecology and Hydrology, Wallingford, UK.
- Zaidman, M. D., Rees, H. G., Young, A. R., 2002. Spatio-temporal development of streamflow droughts in north-west Europe. *Hydrol. Earth System Sci.* 6 (4), 733–751, doi:10.5194/hess-6-733-2002.
- Zarocostas, J., 2011. Famine and disease threaten millions in drought hit Horn of Africa. *BMJ* 343, d4696, doi:10.1136/bmj.d4696.
- Zeng, N., Yoon, J.-H., Marengo, J. A., Subramaniam, A., Nobre, C. A., Mariotti, A., Neelin, J. D., 2008. Causes and impacts of the 2005 Amazon drought. *Environ. Res. Lett.* 3 (1), 014002, doi:10.1088/1748-9326/3/1/014002.
- Zhai, J., Su, B., Krysanova, V., Vetter, T., Gao, C., Jiang, T., 2010. Spatial Variation and Trends in PDSI and SPI Indices and Their Relation to Streamflow in 10 Large Regions of China. *J. Clim.* 23 (3), 649–663, doi:10.1175/2009JCLI2968.1.

Summary

At the start of this research project, multi-model studies at the global scale for hydrological drought were missing both for the historic and future climate. To understand the space-time development of large-scale hydrological drought events and the relations between different types of drought, more research considering multiple models, was needed. Increased knowledge can lead to improved drought projections and can be used to safeguard global water availability in the future. The main objective of this research was to investigate the space-time development of large-scale hydrological drought for historic and future drought events through a multi-model analysis.

The identification of hydrological drought at the global scale has received considerable attention during the past decade. However, climate-induced variation in runoff across the world makes such analyses rather complicated. This especially holds for the drier regions of the world (both cold and warm), where for a considerable period of time, zero runoff can be observed. In this thesis, a method that enables drought identification at the global scale across climate regimes in a consistent manner is presented. The method combines the characteristics of the classical variable threshold level method, which is best applicable in regions with non-zero runoff most of the time, and the consecutive dry days (period) method, which is better suited for areas where zero runoff occurs. The method is demonstrated by identifying drought events from discharge observations of selected rivers, as well as from simulated runoff data at the global scale obtained from an ensemble of five different land surface models. The developed combined method especially shows its relevance in transitional areas, because in wetter regions, results are identical to the classical threshold level method. By combining both methods, the new method is able to identify single drought events that occur during positive and zero runoff periods, leading to a more consistent and realistic global drought characterisation, especially within drier environments.

During the past decades large-scale models have been developed to simulate the global and continental terrestrial water cycles. It is an open question whether these models are suitable to capture hydrological drought, in terms of runoff, on the global scale. It is important to know how well these large-scale models can reproduce major drought events in the past before projections for the 21st century can be made. A multi-model ensemble analysis was carried out to evaluate if ten of such large-scale models agree on major drought events during the second half of the 20th century. A comparison between a multi-model ensemble and reported drought events in the literature was made to assess the performance of large-scale models. Major drought events in the selected period (1963–2000) were reproduced by the model ensemble median, although the duration and spatial extent differed substantially from reported events. The major drought events are caused by precipitation deficits linked to oscillations in climatic patterns, such as El Niño-Southern Oscillation. This implies that major drought events were simulated if these were included in the forcing data.

Temporal development of area in drought for various regions across the globe was investigated more in detail. In this analysis, time series of monthly precipitation, monthly total runoff from ten global hydrological models, and their ensemble median have been used to identify drought. Model spread was largest in regions with low runoff and smallest in regions with high runoff. In vast regions, correlation between runoff drought derived from the models and meteorological drought was found to be low. This indicated that models add information to the signal derived from precipitation and that in global drought analyses runoff drought cannot directly be determined from precipitation data with a fixed aggregation period alone. However, duration and spatial extent of major drought events differed between models. Some models showed a fast runoff response to rainfall, which led to deviations from reported drought events in slowly responding hydrological systems. By using an ensemble of models, this fast runoff response was partly over-

come and delay in drought propagating from meteorological drought to drought in runoff was included. Finally, an ensemble of models also allowed to consider uncertainty associated with individual model structures.

Drought severity and related socio-economic impacts are expected to increase in multiple regions across the globe due to climate change. In this thesis, effects of climate change on drought events in several river basins across the globe were investigated. Downscaled and bias-corrected data from three General Circulation Models (GCMs) for the A2 emission scenario were used as forcing for large-scale hydrological models. Results from five large-scale hydrological models (GHMs) were used in this study to identify low flows and hydrological drought characteristics in the control period (1971–2000) and the future period (2071–2100). Low flows were defined by the monthly 20th percentile from discharge (Q_{20}). The variable threshold level method was applied to determine hydrological drought characteristics. The climatology of normalized Q_{20} from model results for the control period was compared with the climatology of normalized Q_{20} from observed discharge. An observation-constrained selection of model combinations (GHM and GCM) for the future analysis was made based on this comparison. In cold climates, model combinations projected a regime shift and increase in low flows between the control period and future period. Arid climates were found to become even drier in the future by all model combinations. Agreement between the model combinations on future low flows was low in humid climates. Changes in hydrological drought characteristics relative to the control period did not correspond to changes in low flows in all river basins. In most basins (around 65%), drought duration and deficit were projected to increase by the majority of the selected model combinations, while a decrease in low flows was projected in less basins (around 51%). This difference is partly caused by the use of the threshold of the control period to determine drought events in the future, which led to unintended drought events in terms of expected impacts. It is important to consider both low discharge and hydrological drought characteristics to anticipate changes in drought.

Storage processes in catchments have a large influence on river discharge regime. Hydrological drought events are therefore also affected by the amount of storage and storage dynamics in catchments. In this thesis, the influence of long-term storage variation on drought duration was analysed. Discharge time series were decomposed in three components with a Seasonal-Trend decomposition procedure based on Loess. The trend (slow-varying) component of the discharge characterises long term changes and is taken as a metric for storage processes. Discharge data from 1737 river catchments in Europe and the United States were used. In slowly-responding catchments the contribution of the trend component to total discharge variation (fraction of the trend component) was higher than in fast-responding catchments. Higher fractions of the trend component were associated with longer drought events. This means it is important to adequately include storage processes in (large-scale) hydrological models to determine drought events correctly. Without an adequate description of storage processes, drought duration will be underestimated and drought frequency will be overestimated. This will affect other characteristics (e.g., deficits) and predicted impacts.

Overall, large-scale hydrological models are an important tool to assess water availability at the global scale and can be employed to estimate current and future hydrological drought situations. However, some challenges for drought analysis still remain. The structure of large-scale hydrological models has to be improved to reduce uncertainties in the simulations and a common set of indicators suitable for historic and future drought analysis has to be agreed upon, including the way how to calculate the indices. The knowledge to be gained by evaluating the large-scale models results, in combination with increased hydrological process understanding derived from observed data, can play an important role in safeguarding water availability.

Samenvatting

Droogte kan grote ecologische en sociaal-economische gevolgen hebben. Daarom is er meer onderzoek nodig naar de ontwikkeling van grootschalige hydrologische droogte in tijd en ruimte en naar de relaties tussen verschillende droogtetypen. Meer kennis over dit onderwerp kan droogtevoorspellingen verbeteren en daardoor bijdragen aan een betere watervoorziening in de toekomst. In dit proefschrift wordt droogte gedefinieerd als een periode waarin minder water beschikbaar is dan normaal. Dit gebrek aan water kan zich voordoen in de neerslag (meteorologische droogte), bodemvocht (bodemvochtdroogte) of grondwater en/of afvoer (hydrologische droogte). Het belangrijkste doel van dit onderzoek was het bestuderen van de ontwikkeling van grootschalige droogte in tijd en ruimte voor zowel het verleden als de toekomst door gebruik te maken van meerdere grootschalige hydrologische modellen.

In het afgelopen decennium is er veel aandacht geweest voor methoden om hydrologische droogte op mondiale schaal te identificeren. Een dergelijke mondiale analyse wordt echter gecompliceerd door de grote variatie in afvoer, die wordt veroorzaakt door verschillen in klimaat. Vooral in droge gebieden (in koude en warme klimaten), waar een deel van de tijd geen afvoer voorkomt, is droogte-identificatie lastig. In dit proefschrift wordt een methode gepresenteerd die het mogelijk maakt om droogte op mondiale schaal op een consistente manier te identificeren. Deze methode combineert de bestaande variabele-drempelwaardemethode, die het beste gebruikt kan worden in gebieden waar altijd afvoer is, met de methode van de opeenvolgende droge dagen, die het beste toegepast kan worden in gebieden waar perioden zonder afvoer voorkomen. Door het combineren van deze twee methodes kan een droogte gedetecteerd worden die begint in een periode met te lage afvoer en zich voortzet in een periode zonder afvoer. Droogtes zijn geïdentificeerd in waargenomen afvoer van verschillende stroomgebieden en in gesimuleerde afvoer van een ensemble van vijf grootschalige hydrologische modellen. De gecombineerde methode is vooral relevant in overgangsgebieden tussen klimaatzones; in nattere gebieden is de gecombineerde methode gelijk aan de traditionele variabele-drempelwaardemethode.

Er worden steeds meer grootschalige modellen ontwikkeld voor het simuleren van de mondiale en continentale hydrologische kringloop. Het is nog onbekend in hoeverre deze modellen geschikt zijn voor het identificeren van hydrologische droogte. Voordat de modellen toegepast kunnen worden voor het voorspellen van droogte in de 21^{ste} eeuw, is het belangrijk te weten hoe goed de modellen historische droogte kunnen reproduceren. In dit proefschrift zijn uitkomsten van tien verschillende modellen gebruikt voor het identificeren van droogtes in de tweede helft van de 20^{ste} eeuw. De uitkomsten van de modellen zijn vergeleken met droogtes uit de literatuur. De mediaan van de uitkomsten van alle modellen reproduceerde wel het optreden van de meest extreme droogtes in de geselecteerde periode (1963–2000), maar de karakteristieken (duur en ruimtelijke verspreiding) van de gesimuleerde droogtes waren substantieel anders dan die van de gerapporteerde droogtes. De meest extreme droogtes worden veroorzaakt door tekorten in neerslag die gekoppeld zijn aan langjarige schommelingen in mondiale klimaatpatronen, zoals het fenomeen El Niño. Dit betekent dat de grootschalige modellen in staat zijn om droogtes te simuleren als deze neerslagtekorten zijn opgenomen in de invoerdata van de modellen.

De ontwikkeling van de oppervlakte in droogte is verder onderzocht voor verschillende regio's verspreid over de wereld. De spreiding in modelresultaten was het grootst in gebieden met weinig afvoer en het kleinst in gebieden met veel afvoer. De correlatie tussen hydrologische droogte en meteorologische droogte was in de meeste gebieden klein. Dit geeft aan dat de modellen informatie toevoegen aan het neerslagsignaal, hetgeen betekent dat in een mondiale analyse hydrologische droogtes niet vervangen kunnen worden door meteorologische droogtes. Er waren wel

grote verschillen in droogtekaracteristieken tussen de modellen. De afvoer reageerde niet in alle modellen op dezelfde manier op de neerslag; sommige modellen gaven een zeer snelle reactie van de afvoer op neerslag. Dit zorgde vooral in langzaam reagerende systemen voor grote verschillen tussen gesimuleerde en gerapporteerde droogtes. De gevolgen van een snelle reactie op neerslag in sommige modellen kunnen deels voorkomen worden door gebruik te maken van een ensemble van meerdere modellen. De voortplanting van meteorologische droogte naar hydrologische droogte wordt dan beter gesimuleerd. Het gebruik van meerdere modellen geeft ook informatie over de onzekerheid in de modelstructuren.

De verwachting is dat door klimaatverandering de intensiteit van droogte zal toenemen in verschillende gebieden op de wereld. Uitkomsten van vijf hydrologische modellen in combinatie met drie klimaatmodellen voor het A2 emissie scenario zijn gebruikt om effecten van klimaatverandering op hydrologische droogte te analyseren voor verschillende stroomgebieden. Droogtes en lage afvoeren (maandelijkse 20^{ste} percentiel waarden, Q_{20}) zijn geïdentificeerd uit de uitkomsten van de hydrologische modellen voor een historische periode (1971–2000) en een periode in de toekomst (2071–2100). De gesimuleerde lage afvoeren voor de historische periode zijn vergeleken met geobserveerde lage afvoeren van de verschillende stroomgebieden. De modelcombinaties (combinatie van een klimaatmodel en een hydrologisch model), die de beste resultaten gaven, zijn gebruikt voor verdere analyse. In koude klimaten werd een verschuiving in het hydrologische regime (de piek van sneeuwsmelt zal eerder optreden) waargenomen en een verhoging van de lage afvoeren tussen de historische periode en de periode in de toekomst. Voor aride klimaten gaven de modelcombinaties aan dat omstandigheden nog droger zullen worden in de toekomst. Voor vochtige klimaten werden zowel drogere als nattere situaties verwacht op basis van de modelcombinaties. Veranderingen in droogtekaracteristieken waren niet altijd gelijk aan veranderingen in lage afvoeren. In ongeveer 65% van de stroomgebieden werden droogteduur en -tekort hoger, terwijl maar in 51% van de stroomgebieden een afname van de lage afvoer werd gevonden. Dit verschil wordt voor een deel veroorzaakt door het gebruik van een in de historische periode bepaalde drempelwaarde voor droogte-identificatie in de toekomst. Dit leidde tot onverwachte droogtes, die beperkte of geen gevolgen hebben. Daarom is het belangrijk om zowel droogtekaracteristieken als lage afvoeren te analyseren voor het bepalen van veranderingen in droogte in de toekomst.

De bergingscapaciteit en -dynamiek binnen een stroomgebied hebben een grote invloed op het hydrologische regime van een rivier en dus ook op hydrologische droogte. In dit proefschrift is de invloed van langjarige bergingsveranderingen op de droogteduur geanalyseerd. Hiervoor zijn tijdreeksen van waargenomen afvoeren opgesplitst in drie componenten. De trendcomponent (langzaam variërende component) van de afvoer karakteriseert de langjarige veranderingen. Afvoerdata van 1737 stroomgebieden in Europa en de Verenigde Staten zijn gebruikt voor deze analyse. In langzaam reagerende gebieden was de bijdrage van de trendcomponent aan de totale afvoervariatie (de trendfractie), zoals verwacht, hoger dan in snel reagerende systemen. Hogere fracties van de trendcomponent waren gekoppeld aan langere droogtes. Voor het correct simuleren van droogtes is het daarom belangrijk om bergingsprocessen goed op te nemen in (grootschalige) hydrologische modellen. Zonder een goede weergave van de berging zal de droogteduur onderschat worden en het aantal droogtes overschat, wat ook de voorspelling van de gevolgen van droogte zal beïnvloeden.

Grootschalige hydrologische modellen zijn een belangrijk instrument om op mondiale schaal waterbeschikbaarheid te simuleren en om huidige en toekomstige droogtes te kwantificeren. Er resteren echter nog wel een aantal uitdagingen voor toekomstige droogte-analyses met deze modellen. De modelstructuur moet verbeterd worden om de onzekerheid in modeluitkomsten te verkleinen. Daarnaast moet er een reeks methoden vastgesteld worden voor droogte-identificatie geschikt voor historische en toekomstige droogtes, inclusief de manier waarop de methoden toegepast moeten worden. Kennis die verkregen wordt uit de uitkomsten van de grootschalige hydrologische modellen kan in combinatie met een beter begrip van hydrologische processen een belangrijke rol spelen bij het vaststellen van de toekomstige beschikbaarheid van water.

Dankwoord

Na bijna 5 jaar is het eindelijk zo ver, mijn proefschrift is afgerond. Bij het inleveren van de leesversie van je proefschrift denk je dat je er bent, de stress over, een enorme opluchting en blijdschap uiteraard. Maar dan komt nog het laatste en misschien wel belangrijkste deel (aangezien het toch zeker het eerste, wellicht het enige, stuk van het proefschrift is dat veel ontvangers zullen lezen), het dankwoord. Opnieuw slaat de stress toe, immers, wat als je iemand vergeet? Daarom wil ik om te beginnen iedereen die op enige wijze een bijdrage heeft geleverd aan mijn promotieonderzoek van harte bedanken. Een promotieonderzoek kan je namelijk nooit alleen. Zo, nu niemand zich meer benadeeld kan voelen, kom ik bij de meer persoonlijke dankbetuigingen.

Om te beginnen wil ik graag mijn dagelijkse begeleider en co-promotor Henny van Lanen noemen. Henny, bedankt voor al je goede begeleiding en je vertrouwen in mijn kunnen. Jouw gedetailleerde commentaar op alle teksten die ik produceerde was onmisbaar. Ik heb zeer goede herinneringen aan alle reizen die ik heb mogen maken naar onder andere de Ardennen, IJsland, Marokko en Noorwegen, zeker ook door alle goede gesprekken in de avonden met een wijntje of biertje erbij. Ook zal ik nooit vergeten dat je voor een overleg met jou altijd wat extra tijd moet inplannen voor alle familie verhalen. Bedankt voor alle kansen die je me hebt gegeven.

Daarnaast wil ik mijn promotor Remko Uijlenhoet bedanken. Jouw bijdrage aan de vele discussies die we over alle hoofdstukken van dit proefschrift hebben gevoerd en je grote betrokkenheid bij dit onderzoek waren cruciaal voor de uiteindelijke afronding. Jouw enorm enthousiasme voor resultaten van mijn promotieonderzoek, maar ook zeker voor de wetenschap in het algemeen, zorgde altijd voor extra motivatie. Bedankt voor alle tijd die je in mijn onderzoek hebt gestopt.

Hierna volgen traditioneel gezien in het dankwoord de paranimfen. Bram, dankjewel voor alle gezellige koffiepauzes, het samen biertjes drinken, de etentjes, en natuurlijk de vele spelletjesavonden (Sara, ook bedankt). Bij al deze gelegenheden was het goed om aan andere dingen te denken dan mijn onderzoek, maar ook zeker fijn om alle frustraties te kunnen uiten, dus bedankt voor je geduld. Anne, vanaf het begin van mijn promotieonderzoek heb ik ontzettend fijn met je samengewerkt. Ik heb hele goede herinneringen aan alle onze reizen, zeker aan de weekenden voor of na de officiële verplichtingen. Dat brengt mij bij mijn andere kamergenootje van de afgelopen 5 jaar, Claudia. Ik had me geen betere kamergenoten kunnen wensen dan jullie beiden. Bedankt voor alle inhoudelijke hulp en R-assistentie, maar ook zeker voor de nodige afleiding en gezelligheid.

Alle andere collega's van zowel HWM en de voormalige leerstoelgroep SEG, bedankt voor alle gezelligheid tijdens de koffiepauzes, lunches en vrijdagmiddagborrels. Dat ik mijn promotieonderzoek in een dergelijke hechte en prettige leerstoelgroep heb mogen uitvoeren, was geweldig. Specifiek wil ik Ryan Teuling bedanken voor alle hulp. Zeker in de laatste jaren van mijn onderzoek heb jij een grote bijdrage geleverd aan alle discussies en mijn proefschrift in het geheel. Het feit dat Henny, Remko en jij tijdens de vele inhoudelijke discussies altijd weer iets positiefs wisten te vinden in de resultaten op momenten dat ik het liefst alles in de prullenbak wilde gooien, heeft mij steeds weer verbaasd, maar ook ontzettend geholpen. Verder wil ik ook Pieter Hazenberg bedanken, dankzij jouw programmeerkunsten en de goede samenwerking is er nu een mondiale droogte-identificatiemethode.

Natuurlijk kan je tijdens al die jaren promotieonderzoek niet alleen maar werken en heb je ook zeker afleiding nodig om weer nieuwe energie op te doen. Julie, Lourain en Bianca, ik ben heel blij met onze jarenlange vriendschap en bedankt voor alle fijne strandbezoeken. Meike, Marcel en Timo, bedankt voor jullie steun en de ontspanning in de tuin. Alle leden van het GPG, bedankt voor de leuke verjaardagborrels en GPG-weekenden. Kirsten, Eveline, Jantiene, David,

Joost, Monique en alle andere Ibexers, bedankt voor de nodige afleiding elke donderdag (oké, misschien niet elke donderdag, maar toch regelmatig) en alle gezelligheid tijdens klimweekenden.

Oma, Saskia en Robert, bedankt voor jullie interesse in mijn onderzoek en alle gezellige familie-activiteiten. Niko, ik kan met volledige zekerheid zeggen dat dit proefschrift er zonder jou niet zou zijn geweest. Jouw enorme steun, zowel inhoudelijk als persoonlijk, heeft mij overeind gehouden tijdens de moeilijker momenten. Daarom ondanks alles, heel erg bedankt voor alles! Als allerlaatste wil ik mijn ouders bedanken. Zonder jullie onvoorwaardelijke vertrouwen en het besef dat ik altijd met alles bij jullie terecht kan, zou ik niet dezelfde persoon zijn. Pap en mam, bedankt voor alles wat jullie voor me hebben gedaan en nog steeds doen, en natuurlijk voor de ontelbare ritjes naar Wageningen.



Acknowledgements

This research has partly been financially supported by the EU-FP6 Project WATCH (036946) and by the EU-FP7 Project DROUGHT-R&SPI (282769). This research supports the work of the UNESCO-IHP EURO-FRIEND Water programme.

I would like to thank all colleagues related to these projects for their help and useful discussions. I especially remember all the good times during conferences and all the project meetings.

I want to thank all colleagues who provided the results of the large-scale models: Nathalie Bertrand (Laboratoire de Météorologie Dynamique, France), Douglas Clark (Centre for Ecology and Hydrology, United Kingdom), Sonja Folwell (Centre for Ecology and Hydrology, United Kingdom), Sandra Gomes (Centro de Geofísica da Universidade de Lisboa, Portugal), Simon Gosling (School of Geography, University of Nottingham, Nottingham, United Kingdom), Naota Hanasaki (National Institute for Environmental Studies, Tsukuba, Japan), Jens Heinke (Potsdam Institute for Climate Impact Research, Germany and International Livestock Research Institute, Nairobi, Kenya), Sujan Koirala (Institute of Engineering Innovation, University of Tokyo, Tokyo, Japan), Tobias Stacke (Max Planck Institute for Meteorology, Germany) and Frank Voss (University of Kassel, Germany). Furthermore, I would like to thank Graham Weedon (UK MetOffice) for supplying the WATCH forcing data. I wish to acknowledge all researchers involved in providing the downscaled and bias-corrected forcing data.

I also want to thank the Global Runoff Data Centre (56068 Koblenz, Germany) for providing the observed discharge data. I also acknowledge the National River Flow Archive (UK) for providing observed data from the Pang catchment, the Hydrological Service of the Walloon Region of Belgium (MET-SETHY) and the Royal Meteorological Institute of Belgium (KMI) for providing observed data from the Ourthe and Meuse catchments. Additional data from the Meuse catchment were provided by the Direction Régionale de l'Environnement (DIREN) de Lorraine, by Rijkswaterstaat / RIZA (Institute for Inland Water Management and Waste Water Treatment), and by Water Authority "de Dommel". I would like to thank my colleague Roel Dijkema for providing me with the data for the Noor catchment. All these sources are gratefully acknowledged.



List of publications

Peer-reviewed articles

- Van Huijgevoort, M.H.J., Van Lanen, H.A.J., Teuling, A.J., Uijlenhoet, R., 2014. Identification of changes in hydrological drought characteristics from a multi-GCM driven ensemble constrained by observed discharge. *Journal of Hydrology*, *Journal of Hydrology*, 512, 421–434, doi:10.1016/j.jhydrol.2014.02.060
- Van Huijgevoort, M.H.J., Hazenberg, P., Van Lanen, H.A.J., Teuling, A.J., Clark, D.B., Folwell, S., Gosling, S.N., Hanasaki, N., Heinke, J., Koirala, S., Stacke, T., Voss, F., Sheffield, J., Uijlenhoet, R., 2013. Global multi-model analysis of drought in runoff for the second half of the twentieth century. *Journal of Hydrometeorology*, 14, 1535–1552, doi:10.1175/JHM-D-12-0186.1
- Van Loon, A.F., Van Huijgevoort, M.H.J., Van Lanen, H.A.J., 2012. Evaluation of drought propagation in an ensemble mean of large-scale hydrological models. *Hydrology and Earth System Sciences*, 16, 4057–4078. doi:10.5194/hess-16-4057-2012
- Van Huijgevoort, M.H.J., Hazenberg, P., Van Lanen, H.A.J., Uijlenhoet, R., 2012. A generic method for hydrological drought identification across different climate regions. *Hydrology and Earth System Sciences*, 16, 2437–2451. doi:10.5194/hess-16-2437-2012
- Corzo Perez, G.A., Van Huijgevoort, M.H.J., Voss, F., Van Lanen, H.A.J., 2011. On the spatio-temporal analysis of hydrological droughts from global hydrological models. *Hydrology and Earth System Sciences*, 15, 2963–2978. doi:10.5194/hess-15-2963-2011

Extended abstracts

- Van Huijgevoort, M.H.J., Van Lanen, H.A.J., Teuling, A.J., Uijlenhoet, R., 2014. Do large-scale models capture reported drought events?, In: *Hydrology in a Changing World: Environmental and Human Dimensions*, Proc. of the FRIEND-Water Conference 2014 (IAHS Publ. 363, 66–71)
- Van Huijgevoort, M.H.J., Van Loon, A.F., Rakovec, O., Haddeland, I., Horacek, S., Van Lanen, H.A.J., 2010. Drought assessment using local and large-scale forcing data in small catchments, In: *Global Change: Facing Risks and Threats to Water Resources / Servat, E., Demuth, S., Dezetter, A., Daniell, T.*, Proc. of the Sixth World FRIEND Conference, Fez, Morocco. (IAHS Publ. 340, 77–85)

Cover design by Ivo Hofland (ivohofland.nl), photos by Niko Wanders

Financial support from Wageningen University for printing this thesis is gratefully acknowledged.



Netherlands Research School for the
Socio-Economic and Natural Sciences of the Environment

C E R T I F I C A T E

The Netherlands Research School for the
Socio-Economic and Natural Sciences of the Environment
(SENSE), declares that

***Marjolein Hubertina
Joanna van Huijgevoort***

born on 24 September 1984 in Waalwijk, The Netherlands

has successfully fulfilled all requirements of the
Educational Programme of SENSE.

Wageningen, 23 May 2014

the Chairman of the SENSE board

Prof.dr.ir. Huub Rijnaarts

the SENSE Director of Education

Dr. Ad van Dommelen

The SENSE Research School has been accredited by the Royal Netherlands Academy of Arts and Sciences (KNAW)



K O N I N K L I J K E N E D E R L A N D S E
A K A D E M I E V A N W E T E N S C H A P P E N



The SENSE Research School declares that **Ms. Marjolein van Huijgevoort** has successfully fulfilled all requirements of the Educational PhD Programme of SENSE with a work load of 60.2 EC, including the following activities:

SENSE PhD Courses

- o Understanding Global Environmental Change: Processes, Compartments and Interactions (2009)
- o Uncertainty Modelling and Analysis (2010)
- o Environmental Research in Context (2010)
- o Research Context Activity: Co-organizing WIMEK/ SENSE Symposium on: Modelling & Observing Earth Systems Compartments (22 February 2011, Wageningen)

Other PhD and Advanced MSc Courses

- o Techniques for writing and presenting a scientific paper (2012)
- o Voice Matters - Voice and Presentation Skills Training (2013)

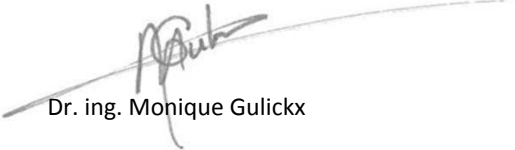
Management and Didactic Skills Training

- o Lecturing, developing and assisting in the courses *Integration Course Soil, Water and Atmosphere, Hydrogeology, and Hydrological Processes in Catchments* (2009-2013)
- o Supervision of two MSc theses, one BSc thesis and one internship (2010-2013)

Oral Presentations

- o *Space-time characteristics of global drought using model ensembles*. WATCH WB4 Meeting 'Large-scale data and analyses', 15-17 February 2010, Oslo, Norway
- o *Drought assessment using local and large-scale forcing data in small catchments*. Sixth World FRIEND conference, 25-29 October 2010, Fez, Morocco
- o *A generic hydrological drought identification method and its application at global scale*. SENSE symposium 'Water & Energy Cycles at Multiple Scales', 1 March 2012, Wageningen, The Netherlands
- o *Global multi-model hydrological drought analysis using a generic identification method*. FRIEND-Water Low flow and drought group, mid-term meeting, 3-5 October 2012, Payerbach, Austria
- o *Representation of drought propagation in large-scale models: a test on global scale and catchment scale*. EGU General Assembly, 8-12 April 2013, Vienna, Austria
- o *Identification of changes in hydrological drought characteristics from a multi-model ensemble*. AGU Fall Meeting, 8-13 December 2013, San Francisco, USA

SENSE Coordinator PhD Education


Dr. ing. Monique Gulickx

